5-2010

Delta like ligand 4 is a critical regulator of bone marrow cell differentiation into pericytes/vascular smooth muscle cells and is essential for the vasculogenesis that supports the growth of Ewing's sarcoma

Keri L. Stewart

Delta like ligand 4 is a critical regulator of bone marrow cell differentiation into pericytes/vascular smooth muscle cells and is essential for the vasculogenesis that supports the growth of Ewing's sarcoma

By
Keri Lynn Schadler Stewart, B.S.

APPROVED:

_____
Eugenie S. Kleinerman, MD, Supervisory Professor

_____
Michelle Barton, PhD

_____
Lee M. Ellis, MD

_____
Joseph H. McCarty, PhD

_____
Patrick A. Zweidler-McKay, MD, PhD

_____

APPROVED:

_____
George M. Stancel, PhD, Dean, The University of Texas
Graduate School of Biomedical Sciences at Houston

Delta like ligand 4 is a critical regulator of bone marrow cell differentiation into pericytes/vascular smooth muscle cells and is essential for the vasculogenesis that supports the growth of Ewing's sarcoma

A

DISSERTATION

Presented to the Faculty of
The University of Texas
Health Science Center at Houston
And
The University of Texas
M.D. Anderson Cancer Center
Graduate School of Biomedical Sciences

in Partial Fulfillment
of the Requirements
for the Degree of

DOCTOR of PHILOSOPHY

By

Keri Lynn Schadler Stewart

Houston,TX
May, 2010

DEDICATION

To my parents, who have supported me in every endeavor I've ever undertaken, and who love me unconditionally. To my mom, a woman whose strength, generosity, and kindness is an example for us all.

To my brother, Mark, and sister, Laura, who keep me honest.

To my husband, Morgan, for believing in me more than I could ever believe in myself, for being a safe haven in my life, and for selflessly supporting the pursuit of my career. Also, for running our home when I was too wrapped up in science to notice dishes and laundry.

ACKNOWLEDGEMENTS

I am eternally grateful to my advisor, Dr. Eugenie Kleinerman. Without her careful and diligent guidance, I would not have been successful in my pursuit of this degree. I thank Dr. Kleinerman for teaching me to think critically, interpret results carefully, and to fight fearlessly in defense of the story I have uncovered. Dr. Kleinerman's example of a woman who does it all has been irreplaceable in molding me into the scientist and woman that I am today.

I would also like to thank Dr. Patrick Zweidler-McKay, who served as co-mentor for my research. Dr. Zweidler-McKay's scientific knowledge has been essential to this research, and his mentorship was essential to my success. The other members of my supervisory committee, Dr. Shelley Barton, Dr. Lee Ellis, and Dr. Joseph McCarty offered support, advice, and motivation throughout my graduate school experience. In particular, I would like to thank Shelley for all of the extra pep talks.

None of this could have been accomplished without the help of all members of the Kleinerman laboratory. You have all been wonderful supporters in the quest for my PhD! Thank you for your scientific input and your friendship. I would especially like to thank Krishna, for his teaching when I first came to the lab, Randala, for being my companion from day one of this experience, and Nancy, for her loving friendship. I would also like to thank Mandy and Maya for their support through this process.

I am grateful to the T32 training program and all of the people who work hard to make it happen. Thank you Dr. Stancel and Pat Bruesch, for all of your effort! Thank you Dr. Pete Anderson and Maritza, for allowing me to learn from you in the big scary clinic.

Finally, thank you to my husband and all of my family and friends who make up the best support system in the world. You are a huge blessing in my life. If I've learned anything during my graduate school experience, it is that I am nothing without you. When my confidence, endurance, or dedication wavered, you carried me. I am grateful.

Delta like ligand 4 is a critical regulator of bone marrow cell differentiation into pericytes/vascular smooth muscle cells and is essential for the vasculogenesis that supports the growth of Ewing's sarcoma

Publication No. _____

Keri Schadler Stewart, B.S.

Supervisory Professor: Eugenie S. Kleinerman, M.D.

We have previously shown that vasculogenesis, the process by which bone marrow-derived cells are recruited to the tumor and organized to form a blood vessel network de novo, is essential for the growth of Ewing's sarcoma. We further demonstrated that these bone marrow cells differentiate into pericytes/vascular smooth muscle cells(vSMC) and contribute to the formation of the functional vascular network. The molecular mechanisms that control bone marrow cell differentiation into pericytes/vSMC in Ewing's sarcoma are poorly understood. Here, we demonstrate that the Notch ligand Delta like ligand 4 (DLL4) plays a critical role in this process. DLL4 is essential for the formation of mature blood vessels during development and in several tumor models. Inhibition of DLL4 causes increased vascular sprouting, decreased pericyte coverage, and decreased vessel functionality. We demonstrate for the first time that DLL4 is expressed by bone marrow-derived pericytes/vascular smooth muscle cells in two Ewing's sarcoma xenograft models and by perivascular cells in 12 out of 14 patient samples. Using dominant negative mastermind to inhibit Notch, we demonstrate that Notch signaling is essential for bone marrow cell participation in vasculogenesis. Further, inhibition of

DLL4 using either shRNA or the monoclonal DLL4 neutralizing antibody YW152F led to dramatic changes in blood vessel morphology and function. Vessels in tumors where DLL4 was inhibited were smaller, lacked lumens, had significantly reduced numbers of bone marrow-derived pericyte/vascular smooth muscle cells, and were less functional. Importantly, growth of TC71 and A4573 tumors was significantly inhibited by treatment with YW152F. Additionally, we provide in vitro evidence that DLL4-Notch signaling is involved in bone marrow-derived pericyte/vascular smooth muscle cell formation outside of the Ewing's sarcoma environment. Pericyte/vascular smooth muscle cell marker expression by whole bone marrow cells cultured with mouse embryonic stromal cells was reduced when DLL4 was inhibited by YW152F. For the first time, our findings demonstrate a role for DLL4 in bone marrow-derived pericyte/vascular smooth muscle differentiation as well as a critical role for DLL4 in Ewing's sarcoma tumor growth.

TABLE OF CONTENTS

List of Figures

List of Tables

Chapter 1.

Introduction

Ewing's Sarcoma

Ewing's sarcoma is the second most common pediatric bone cancer, and it accounts for about 2% of all pediatric malignancies [1]. The peak incidence is at age 15, and it is slightly more prevalent in males than females [2]. Although the most common sites of occurrence are the pelvic bone, the femur, and the ribs, Ewing's sarcoma can occur in any bone or soft tissue. The lungs, for example, are a common site for metastatic lesions. The site of the primary tumor weakly correlates with patient survival; patients with axially located tumors have a slightly worse prognosis than those with tumors in the appendicular skeleton [3].

Patients with Ewing's sarcoma often present initially with pain at the site of the tumor, or less frequently with swelling or a palpable mass. Although MRI, CT, and PET scans are used to determine the number and location of tumors present, these are not diagnostic. A biopsy is needed to diagnose Ewing's sarcoma by examination of the DNA. The molecular hallmark of Ewing's sarcoma is the t(11;22)(q24;q12) translocation, which creates an EWS-Fli1 fusion protein. This EWS-Fli1 fusion protein is present in 85% of Ewing's sarcomas, and the remaining 15% harbor a translocation that fuses the EWS gene to another member of the ETS family [2,3]. The presence of an EWS-ETS family fusion is a definitive indicator of Ewing's sarcoma.

The current standard of care for Ewing's sarcoma includes a combination of preoperative and adjuvant chemotherapy along with local control. Surgery is the preferred method of local control, but in cases where surgical resection is not possible, radiation therapy is used [1]. First line chemotherapy includes a combination of five drugs: vincristine, cyclophosphamide, doxorubicin, ifosfamide, and etoposide [4]. This

combination therapy achieves a nearly 70% survival rate for patients with non-metastatic disease [4]. However, the vast majority of patients with Ewing's sarcoma have metastatic disease at the time of diagnosis or develop metastases after the first round of therapy. Unfortunately, for these patients, 5 year survival remains around 25%, even with current combination therapies [1,4].

The need for new therapeutic options for patients with Ewing's sarcoma is clear. One possible way to inhibit tumor growth is by preventing the tumor from developing a vascular supply, essentially starving the tumor of nutrients and oxygen. Understanding the molecular mechanisms that direct blood vessel formation in Ewing's sarcoma is key to identifying therapeutic targets that might prevent vascular development. The research presented in this dissertation is intended to contribute to the understanding of the process of vascular development in Ewing's sarcoma in order to identify new molecular targets for inhibiting this process.

Blood Vessel Structure

Our goal is to understand the mechanisms by which tumors form blood vessels in order to target this process. Therefore, we must first have a basic understanding of the cellular organization of a blood vessel. In most blood vessels, the lumen, or inner tube through which blood flows, is surrounded by a single layer of endothelial cells. In arteries and veins, these endothelial cells are surrounded by one or several layers of mural cells. Mural cells include pericytes and vascular smooth muscle cells. Varying amounts of connective tissue, including collagen, elastic fibers, and other proteins and polysaccharides, are interspersed between and surround the cells of blood vessels.

Defining pericytes and vascular smooth muscle cells

Defining a pericyte separately from a vascular smooth muscle cell (vSMC) cell is challenging due to the continuum of phenotypes between the two cell types [5]. Generally, a pericyte is defined as a periendothelial cell within the basement membrane of a blood vessel which physically contacts endothelial cells, while a vSMC is outside of the basement membrane and does not directly contact endothelial cells [6]. The two cell types are sometimes differentiated on the basis of the type of vessel that they are a part of; pericytes typically surround capillaries and microvessels while vSMC surround larger vessels and arteries [5,6].

Although these definitions can be helpful, they are not finite and are not without controversy. Evidence for both mesodermal and neuroectodermal origin of both pericytes and vSMC supports the possibility that pericytes and vSMC may be phenotypic variations of the same cell type[5,7]. The identification of a pericyte versus a vSMC is further complicated by the fact that both can express several of the same proteins in vitro and *in vivo*. These markers include alpha-smooth muscle actin (α-SMA), desmin, regulator of g-protein signaling 5 (RGS5), neuron-glial 2 (NG2) and platelet-derived growth factor receptor-beta (PDGFR-β). No single marker is expressed by *all* pericytes or vSMC and no single marker is expressed *only* by pericytes or vSMC [6,8,9]. For the purpose of this thesis, the term 'pericyte/vSMC' will be used to refer to mural cells surrounding $CD31^+$ endothelial cells and expressing at least one of the following: α-SMA, desmin, RGS5, NG2, PDGFR-β.

Pericyte Morphology and Function

For an extensive review of historical and current knowledge about pericyte function, morphology, development, and relationship to endothelial cells, please see Diaz-Flores et al, 2009 [5].

Pericyte morphology can vary based on the tissue location and type of vessel that it is associated with [8]. Most often, the pericyte cell body (nuclear body) is small and oval (though it can be elongated) with several highly branched processes protruding outward. Primary processes are often oriented parallel to the vascular axis, with secondary protrusions wrapping around the endothelial tube. Partial overlap of processes from two or more pericytes is seen in some vessels, forming multiple layers of pericyte coverage [5].

Pericyte processes connect to multiple endothelial cells, often forming "umbrella-like structures that cover gaps between endothelial cells" [5]. The number of pericytes covering each vessel differs based on species, tissue, type and maturation stage of the vessel. Some vessels have few or no pericytes, while others, such as those found in the human retina, have a high pericyte density and a 1:1 pericyte to endothelial cell ratio [5].

Pericytes have several functions relating to vessel structural stability, regulation of blood flow, and vessel maturation [5,8,10]. Pericytes contribute to vessel structural stability both by secreting matrix proteins, which fortify the basement membrane, and by directly surrounding endothelial cells to form an outer cell layer [5]. During angiogenic growth, pericytes become activated and enter a period of rapid proliferation, dissociate from endothelial cells, and secrete basement membrane degrading proteins such as MMP-2 [5]. Additionally, pericytes function to protect vessels from regression [11]. During

retinopathy of prematurity, for example, the degree of vessel coverage with desmin^{+} pericytes/vSMC correlates with vessel protection[12].

Pericyte regulation of blood flow and perfusion is partially mediated by the adherens junctions formed between pericytes and endothelial cells. These adherens junctions allow mechanical contractile force to be transmitted from pericytes, which are contractile cells, to endothelial cells [13] .

In addition to adherens junctions, gap junctions between pericytes and endothelial cells foster cell-cell communication. Gap junctions allow direct sharing of cytoplasmic contents such as ions and small molecules to mediate endothelial cell quiescence or proliferation. Pericytes also communicate with endothelial cells by secreting factors including vascular endothelial growth factor (VEGF), and angiopoietin-1 (Ang1), which promote endothelial cell survival and/or proliferation. It is important to note that communication between endothelial cells and pericytes is bi-directional, and endothelial cells also provide pro-survival and maturation signals, such as platelet derived growth factor BB (PDGF-BB) and transforming growth factor beta (TGF-β), to pericytes [10,14].

<u>vSMC morphology and function</u>

Similar to pericytes, vSMC can display several different phenotypes. These phenotypes range from the synthetic phenotype, where cells are typically rhomboid shaped, to the contractile phenotype, where cells are elongated and spindle-shaped [7,8]. The synthetic phenotype is so named because during this stage, vSMC synthesize proteins and extracellular matrix at high rates. Generally, synthetic vSMC have qualities necessary during vascular remodeling such as high proliferation rates and migratory abilities. On the other end of the vSMC spectrum, contractile vSMC are senescent, with

low metabolic activity. Contractile vSMC are named for their contractile properties, partially due to the high expression of contractile filament proteins such as α-SMA and desmin [7].

The phenotypic state of vSMC is influenced by several factors, including shear stress, vicinity to endothelial cells, and molecular cues from the microenvironment. PDGF-B, for example, induces differentiation and maturation of mesenchymal precursors into vSMC, but induces a change from contractile to synthetic phenotype in mature vSMC [8].

The primary function of vSMC is the regulation of arterial tone and blood flow by providing contractile forces [15]. In addition to this, vSMC (like pericytes) secrete a number of extracellular matrix proteins including collagen, proteoglycans, and cadherins. Additionally, similar to pericyte regulation of endothelial cell proliferation and quiescence, vSMC can also form gap junctions with endothelial cells, allowing for direct communication between the two cell types [16].

Inhibiting pericyte/vSMC formation inhibits vessel function

In a simplified understanding, pericytes/vSMC can be viewed as the protectors of vascular integrity. Ultimately, defective pericyte/vSMC coverage induces poorly organized and leaky vasculature[5]. Using a model of postnatal retina remodeling, Benjamin et al. demonstrated that pericyte coverage protects blood vessels from the regression normally induced by hyperoxia. Further, they showed that disruption of endothelial-pericyte adhesion by intraocular injection of PDGF-BB resulted in excessive regression of vascular loops [17]. Therefore, inhibiting pericyte/vSMC formation is expected to make blood vessels more susceptible to death or regression. Considering anti-

vascular therapy in the tumor biology context, inhibiting pericytes/vSMC may lead to vessel regression, especially in combination with endothelial cell targeting agents, essentially starving the tumor of its blood supply.

Vasculogenesis

Angiogenesis versus Vasculogenesis

There are two main processes by which blood vessels are formed; angiogenesis and vasculogenesis. Angiogenesis is the sprouting of pre-existing vessels to form new ones. During angiogenesis, endothelial cells and pericytes proliferate and migrate, so that new blood vessels are formed by a locally derived cell population. Alternatively, vasculogenesis is the process by which bone marrow (BM)-derived precursor cells are recruited to sites of developing vasculature and organized to form a vessel network *de novo*. Vasculogenesis occurs during embryogenesis, and refers to the initial formation of the vasculature. Originally, it was believed that postnatal vascular development occurred only by angiogenesis, but several studies have highlighted the important role of vasculogenesis in postnatal processes such as the healing of cutaneous wounds, in response to ischemia, and more recently, in tumor growth. Angiogenesis and vasculogenesis both contribute to vascular growth in adults, and the level of contribution of each varies based on the tissue and stimulus[18].

Vasculogenesis

A simplified explanation of the series of events that occur during prenatal vasculogenesis is as follows: Splanchnic mesoderm cells arise from the cells of the lateral plate mesoderm, and from these, hemangioblasts are formed. Hemangioblasts are the common progenitor to both endothelial and hematopoietic cells. Hemangioblasts cluster

to form blood islands, which then form a network of tubules known as the capillary plexus. After the initial formation of a capillary plexus, pericytes and vSMC are required for remodeling into a functional circulatory network [19]. Recent evidence suggests that the hemangioblasts in blood islands can be subdivided into two progenitor groups: those that become either endothelial cells or hematopoietic cells, and those that become pericytes/vSMC [20]. Traditionally, pericyte/vSMC ontogeny is thought to depend on the location of the blood vessel, but most pericytes/vSMC are believed to be derived from the mesoderm or neural crest [18,19].

The process of postnatal vasculogenesis is less fully understood. In postnatal vasculogenesis, the vascular progenitor cells originate from a pool of pluripotent stem-like cells in the BM. The presence of BM-derived endothelial cells and pericytes/vSMC has been documented in several physiologic and pathologic situations. For example, a series of BM transplant studies by Asahara et al. provided early evidence for the incorporation of BM-derived precursors as endothelial cells during vasculogenesis after ovulation, during wound healing, in response to ischemia, and finally during tumor growth in mice [21-23]. The contribution of BM-derived endothelial precursor cells to vasculogenesis in several postnatal models, including tumors, has now been extensively documented [24].

BM-derived pericytes/vSMC have also been shown to participate in postnatal vasculogenesis. Recently, using a mouse BM transplant model, BM-derived vSMC were found in the healed femoral artery of a mouse after wire induced injury [25]. BM-derived pericytes/vSMC have also been identified in tumors. Rajantie et al identified $NG2^+$ BM-derived perivascular cells in B16 melanomas in mice [26]. Additionally, Du et al

demonstrated that BM-derived cells become desmin$^+$ and α-SMA$^+$ cells and incorporate into the vasculature of glioblastomas in mice [27].

Vasculogenesis in Ewing's sarcoma

We have previously shown that bone marrow(BM)-derived cells participate in vascular formation in Ewing's sarcoma by differentiating into both endothelial cells and pericytes [28,29]. The contribution of BM cells to the endothelial cell population within the tumor is relatively small; about 10% of vessels have at least one BM derived endothelial cell [28]. However, a much larger portion of vessels contain BM-derived pericytes/vSMC.

The pericytes/vSMC component of the majority of the blood vessels in Ewing's sarcoma is a mosaic of BM-derived and locally derived cells, indicating a combination of angiogenesis and vasculogenesis [29-31]. This was demonstrated using a GFP BM transplant model. Nude mice recipients were lethally irradiated to eradicate endogenous BM and then rescued with GFP$^+$ BM from GFP transgenic mice. After engraftment of the GFP$^+$ BM cells, TC71 Ewing's sarcoma cells were injected subcutaneously and allowed to form tumors. Tumors were then removed and immunohistochemistry was performed. Analysis of these tumors revealed thick layers of GFP$^+$ BM-derived cells surrounding CD31$^+$ endothelial cells. Co-staining for GFP and the pericyte/vSMC markers desmin, α-SMA, and PDGFR-β demonstrated that many of the GFP$^+$ BM-derived cells also expressed pericyte/vSMC markers, indicating that BM cells differentiate into pericyte/vSMC in Ewing's sarcoma *in vivo* [29].

BM cell participation in vasculogenesis is a complex, multi-step process. BM progenitors must be recruited to the tumor, retained at sites of developing vasculature, and then differentiate into endothelial cells and pericytes/vSMC. Understanding the

molecular signals in each step of the vasculogenesis process may lead to the identification of new targets for the inhibition of vasculogenesis, ultimately identifying possible therapeutic agents for the treatment of Ewing's sarcoma.

We have previously demonstrated that $VEGF_{165}$ is the major chemotactic stimulant for the recruitment of BM-derived cells to the tumor [32]. shRNA was used to specifically inhibit the expression of $VEGF_{165}$ by TC71 Ewing's sarcoma cells, creating a stable TC/si$VEGF_{165}$ clone. TC/si$VEGF_{165}$ cells were injected subcutaneously into mice and allowed to form tumors. Fluorescently labeled BM cells were then injected intravenously into tumor bearing mice. TC/si$VEGF_{165}$ cells formed smaller, slower growing tumors in vivo than parental TC71 cells or TC/si control. Importantly, TC/si$VEGF_{165}$ had decreased microvessel density and reduced numbers of BM-derived cells. This experiment demonstrates the essential role of $VEGF_{165}$ in recruiting and retaining BM-derived cells in the tumor [32].

To further confirm the importance of vasculogenesis in Ewing's sarcoma growth, the chemokine stromal cell derived factor-1 alpha (SDF-1α) was used [33]. SDF-1α is a chemoattractant for BM progenitor cells, but has little or no effect on local angiogenesis and does not stimulate tumor cell proliferation. Bilateral TC/si$VEGF_{165}$ were implanted into both flanks of nude mice. Tumors were then treated with intratumor injections of adenoviral SDF-1α (Ad-SDF-1, right side tumors) or adenoviral control (Ad-control, left side tumors). Ad-SDF-1α tumors had more infiltrated GFP^+ BM-derived cells that contributed to larger, more organized blood vessels than Ad-control treated tumors. Importantly, the increased influx of BM cells and subsequent increased vascularity caused by SDF-1α was able to partially rescue tumor growth even in the absence of

$VEGF_{165}$; Ad-SDF1α treated tumors were larger than their Ad-control counterparts. The increased participation of BM-derived cells in vascular formation in Ad-SDF-1α treated tumors and the subsequent increase in tumor growth suggests that the formation of BM-derived vascular cells is important for Ewing's sarcoma tumor growth [33].

BM-cell participation in vasculogenesis in Ewing's sarcoma and the important contribution of this process to tumor growth is well established [28,29,34]. $VEGF_{165}$ is a key chemoattractant recruiting BM progenitor cells to Ewing's sarcoma tumors. Once BM cells reach the tumor, however, they must adhere to sites of developing vasculature and differentiate into endothelial cells and/or pericytes/vSMC. The majority of vessels within Ewing's sarcoma tumors have perivascular BM-derived cells. Several of the vessels that have perivascular BM-derived cells are only partially surrounded by these cells, as shown in figure 1. This phenotype implies that a combination of angiogenesis and vasculogenesis occurs in Ewing's sarcoma. It further implies that molecular signals on some developing vessels direct incoming BM cells to adhere and participate in vascular formation, while other vessels do not have these signals. The molecular mechanisms that direct BM progenitor cells to adhere to certain vessels but not others and to differentiate into pericytes/vSMC are unknown. One family of signaling molecules known to be important in vascular formation during embryonic development as well as in adult angiogenesis and vasculogenesis is the Notch family of ligands and receptors. As explained in the next section, the Notch signaling pathway, in particular the Notch ligand DLL4, is likely plays to play an important role in directing BM-derived cells to participate in vasculogenesis in Ewing's sarcoma by controlling their differentiation into pericytes/vSMC.

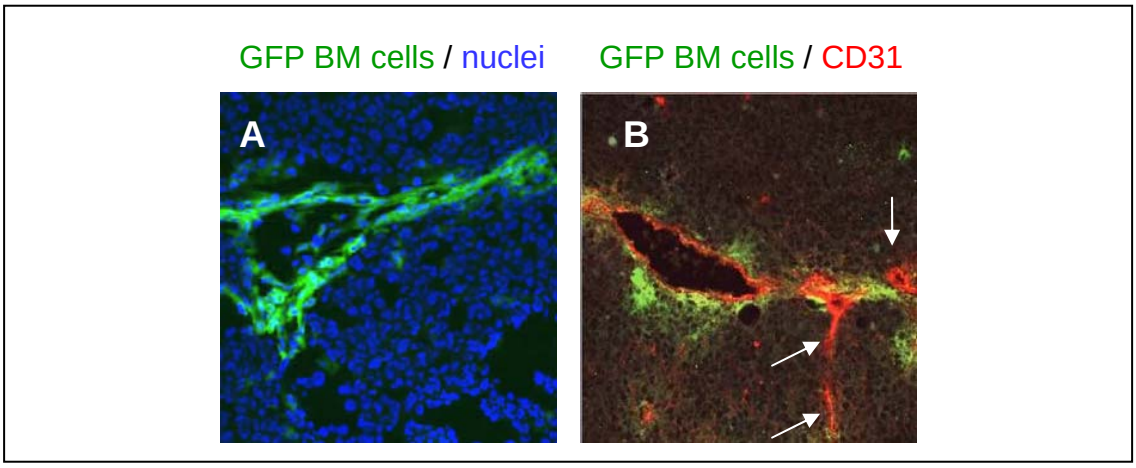

Figure 1. BM-derived cells surround the majority, but not all, blood vessels in Ewing's sarcoma. TC71 cells were implanted subcutaneously into nude mice that had previously received GFP BM transplants and allowed to form tumors. 3 weeks later, tumors were harvested, frozen and cryosectioned for immunohistochemical evaluation. **A)** Immunohistochemistry was performed to identify GFP^+ BM-derived cells (green) and nuclei (blue). **B)** Immunohistochemistry was performed to identify GFP^+ BM-derived cells (green) and $CD31^+$ endothelial cells (red). White arrows indicate blood vessels that do not have perivascular BM-derived cells.

Notch

The Notch family is an evolutionarily conserved group of ligands and receptors that regulate diverse biologic processes including cell fate assignment, stem cell maintenance, and boundary formation during development [35]. The mammalian Notch family includes four heterodimeric transmembrane receptors, Notch 1-4, and five transmembrane ligands, Jagged 1,2 and Delta like ligand 1,3,4 (DLL1-4).

The canonical Notch signaling pathway has been well described. Ligand binding activates Notch receptors, which induces two cleavage events. The first cleavage, mediated by an ADAM-type protease, leads to a conformational change in the receptor that exposes the second cleavage site. The Notch Intracellular Domain (NICD) is released by a second cleavage, performed by the proteolytic γ-secretase/presenilin complex. After NICD is cleaved from the transmembrane and extracellular domains, it translocates to the nucleus, where it complexes first with Recombination Signal Binding Protein 1 for J-κ (RBP-Jκ, also known as CSL) and then with one of three Mastermind like proteins (MAML1-3). This RBP-Jk/MAML complex recruits other co-activators, including p300, and releases co-repressors to induce transcription of downstream Notch effectors. The Notch effectors are themselves basic Helix-loop-Helix transcription factors, including Hairy Enhancer of Split (Hes) and Hairy-related (Hey) family members [36,37].

Non-canonical Notch signaling has also been reported, but is beyond the scope of this thesis [37].

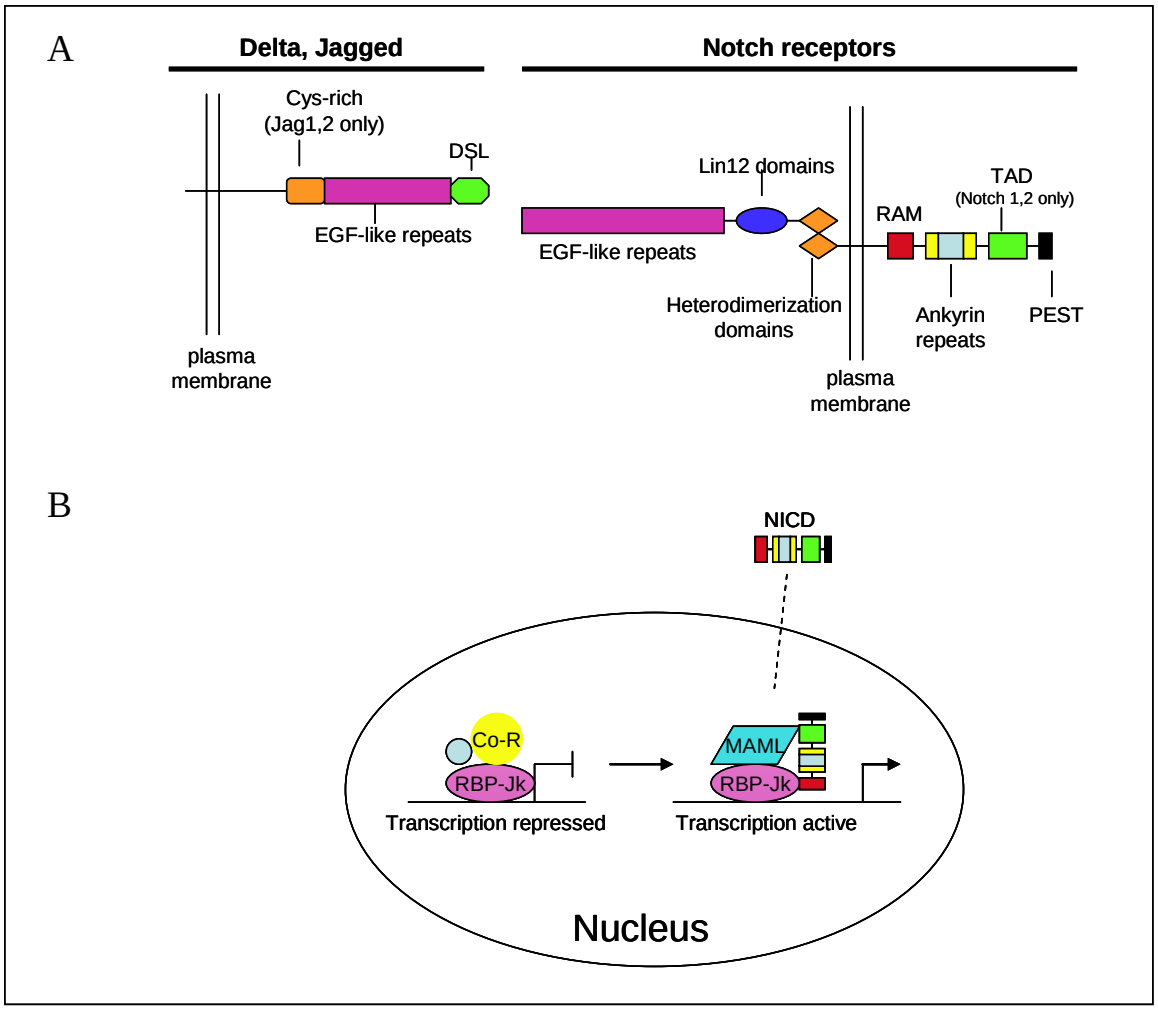

Figure 2. The Notch Signaling Pathway. A) Structural domains of Notch ligands and receptors. The five Notch ligands, Delta like ligand 1 (DLL1), DLL3, DLL4, Jagged 1 (Jag1) and Jag2 each have a small intracellular region, a transmembrane region, and an extracellular portion that can bind to Notch receptors on an adjacent cell. Jag1 and Jag2 contain cysteine-rich domains. All of the ligands contain EGF-like repeats (Jag1 and Jag2 have 18, DLL3 has 6, and DLL1 and DLL4 have 8) and a DSL (delta-serrate-lag) domain. The Notch receptors are heterodimers. The external subunits contain varying numbers of EGF-like repeats (Notch1 has 36, Notch4 has 29) and a Lin12 domain. The subunit containing the intracellular domain (NICD) is a made up of a transmembrane region (with a γ-secretase cleavage site), an internal RAM (RBP-Jκ associated molecule) domain, ankyrin repeats flanked by nuclear localization sequences, a transactivation domain (TAD, in Notch1 and Notch2 only), and a proline-glutamate-serine-threonine (PEST) rich domain. **B) Canonical Notch pathway regulation of transcription.** After cleavage by the γ-secretase complex, NICD translocates to the nucleus where it associates with RPBP-Jκ. The RBP-Jκ-NICD complex then associates with mastermind-like protein (MAML), causing the release of transcriptional repressors and the recruitment of co-activators, leading to active transcription of Notch effectors, including Hes and Hey family members. Hes and Hey family members are basic helix-loop-helix transcription factors which then regulate expression of downstream Notch targets.

Notch in the vascular system

Notch signaling contributes to several processes during vascular development including early differentiation between blood cell/endothelial cell progenitors and vSMC progenitors, control of blood vessel sprouting, and arteriovenous fate specification [38,39]. The important role for Notch in differentiating between blood cell/endothelial cell progenitors and vSMC progenitors during early extraembryonic mesoderm differentiation was demonstrated by a series of elegant experiments in chick and quail embryos. Extraembryonic mesodermal cells electroporated with NICD1 differentiated exclusively into smooth muscle progenitor cells, and conversely, Notch inhibition by γ-secretase inhibitors significantly reduced the number of smooth muscle progenitor cells, indicating that Notch pushes the pluripotent progenitors towards a smooth muscle cell fate[20].

The essential roles of Notch signaling during vascular formation are most apparent in Notch knockout mouse models. For example, Notch $1^{-/-}$ is embryonically lethal. A primary vascular plexus is formed in the mutants, but fails to remodel into large and small blood vessels. The abnormal vascular phenotype includes a reduction in arterial marker expression by endothelial cells, indicating a role for Notch1 in arterial fate specification [40]. Notch 1 and Notch 4 appear to have some redundant function; deletion of Notch 4 alone produces viable, normal adult mice and Notch $1^{-/-}$ Notch $4^{-/-}$ double knockout mice have only slightly more severe defects than Notch$1^{-/-}$ mutants. Phenotypic variations indicative of impaired vascular remodeling were apparent in both Notch$1^{-/-}$ and Notch$1^{-/-}$Notch$4^{-/-}$ mutants. Malformed large blood vessels in the anterior of the embryo are apparent in both mutants [40]. Jagged 1 null mutants are also embryonic lethal due to vascular remodeling defects. Jag$1^{-/-}$ mice display severe hemorrhaging and a lack of large

blood vessels by day E10.5 and are either completely resorbed or necrotic by day E11.5 [41].

Several groups have demonstrated an essential role for Notch during pericyte/vSMC development. However, much of the data is conflicting and difficult to interpret. In vitro, Notch has been shown to both promote and inhibit pericyte/vSMC differentiation. The variation in reports may be due to the fact that individual studies stimulated or mimicked Notch signaling differently (some used NICD transfection while others used ligand stimulation), used different cell types as pericyte/vSMC models, and defined vSMC differentiation using different markers [42-45]. More recent studies using *in vivo* manipulations of Notch indicate a necessity for Notch during pericyte/vSMC differentiation. For example, when the Notch inhibitor dominant negative Mastermind (DNMAM) was genetically introduced into neural crest cells (the pericyte/vSMC progenitor of the cardiac outflow tract), mice displayed defective aortic arch patterning due to an inability of neural crest cells to differentiate into vSMC [46]. Additionally, $DLL4^{+/-}$ mice and mice with endothelial cell specific deletion of Jagged 1 display reduced numbers of α-SMA^{+} cells [47,48].

The role for Notch in vasculogenesis during development indicates that Notch may also be involved in vascular formation in adults. DLL1, for example, plays an important role during postnatal blood vessel formation. $DLL1^{+/-}$ mice subjected to hindlimb ischemia had severely impaired artery formation, indicating a necessity for DLL1 in artery regrowth in adults [49]. Several Notch ligands and receptors are present in the adult vascular system. To date, endothelial cell expression of Notch 1 and Notch 4 as well as Jagged 1,2 and DLL1,4 has been demonstrated. Pericytes/vSMC are known to

express Jagged 1, Notch 2 and Notch 3 [39]. We have shown that pericytes/vSMC also express DLL4 in Ewing's sarcoma [31]. Expression of the other Notch receptors and ligands by endothelial cells and pericytes/vSMC is probable; further exploration of Notch in these cell types is needed.

The dramatic vascular defects observed in the above described Notch mutant mice provide evidence for the key role of Notch in vascular development, and the presence of Notch family members on cells of mature blood vessels indicates that Notch may be important for vascular maintenance in adults. Our interest is in the role of Notch signaling during blood vessel formation in tumors, specifically Ewing's sarcoma. In regard to tumor vascular development, perhaps the most well studied and critical Notch family member is DLL4, described in detail below.

DLL4 plays a critical role in blood vessel development

DLL4 is essential for proper vessel formation. Vascular development is so exquisitely sensitive to DLL4 dosage that even DLL4 heterozygosity causes embryonic lethality in most mouse genetic backgrounds due to "profound vascular defects" [50,51]. DLL4 is highly expressed by the endothelium of large arteries during embryogenesis and is expressed at low levels by smaller arteries and microvessels in adult mice, particularly in tissues with active angiogenesis. DLL4 expression is increased, for example, in the vasculature of maturing follicles of ovaries in sexually mature mice during ovulation [50].

While VEGF stimulates vessel branching and endothelial cell proliferation, DLL4-Notch signaling inhibits these processes. Specifically, DLL4-Notch1 signaling regulates endothelial tip vs stalk cell identity [52,53]. Tip cells are specialized endothelial cells at the leading front of growing vessels with increased migratory capacity. Tip cells

extend filopodia and determine the direction of vessel growth. Stalk cells make up the length of the vessel and generally do not extend filipodia. In normal mouse retinas, DLL4 is expressed by tip cells while Notch1 is expressed by stalk cells, and cells with active Notch1 preferentially assume a stalk cell phenotype. Genetic or pharmacologic inhibition of either DLL4 or Notch1 causes increased numbers of tip cells throughout the blood vessels of mouse retinas and hindbrains. Endothelial cells in all parts of the vessel, including the stalk, begin to extend filopodia and proliferate, leading to excessive vessel branching and disorganization [52,53]. DLL4 is therefore important for the formation of a mature blood vessel network.

In addition to being expressed by endothelial cells during active vascular growth or remodeling in physiologic conditions, DLL4 is highly expressed in the vasculature of solid tumors, a hallmark of which is angiogenic growth [54]. Increased expression of DLL4 by tumor endothelium compared to the endothelium of surrounding normal tissue has been reported in several tumor xenograft models, including lymphoma, breast, colon, and lung cancer [55,56]. High DLL4 expression has also been identified in human patient samples, including renal clear cell carcinoma and colon cancer [55,57].

Similar to the effect of DLL4 inhibition on mouse retinal blood vessel development, DLL4 inhibition in tumors leads to increased microvessel proliferation, but a paradoxical decrease in vessel functionality as assessed by vessel perfusion and hypoxia within the tumor [56,58]. Gliomas, for example, in mice treated with DLL4-Fc, a soluble and therefore dominant negative form of DLL4, had increased endothelial cell density but unorganized, non-perfuse vessels [58].

A possible role of DLL4 in pericyte/vSMC formation during vascular maturation is supported by the observation that in either mouse retinas or xenograft tumor models where DLL4 is inhibited, there is a decrease in number of α-SMA$^+$ cells surrounding endothelial cells [59]. Additionally, in human bladder cancer, DLL4 expression correlates with vessel maturation. In a study of 60 human bladder cancer samples, Patel et al. found that 98.7% of DLL4-positive tumor vessels co-expressed α-SMA, while only 64.5% of DLL4-negative tumor vessels were associated with α-SMA$^+$ cells [60].

The correlation between DLL4 expression and α-SMA expression implies that DLL4 may be important for the formation of pericytes/vSMC. Also, DLL4 is highly expressed by growing tumor vessels but is expressed at low levels on quiescent vessels. Further, VEGF, which is highly expressed in Ewing's sarcoma, positively regulates DLL4 expression. When stimulated by VEGF, VEGF Receptor 2 induces increased expression of DLL4 in a cell autonomous manner [61]. We would therefore expect Ewing's sarcoma vessels, which are rapidly growing in a VEGF rich environment, to express DLL4. Taken together, this makes DLL4 an attractive candidate as a key molecular regulator of tumor vascular formation in Ewing's sarcoma.

Studies of the role of DLL4 during blood vessel formation have thus far focused on DLL4-Notch regulation of endothelial cell sprouting, an angiogenic process. Whether DLL4-Notch signaling is also important in vasculogenesis, specifically in the differentiation of BM-derived progenitor cells into pericytes/vSMC, is still unknown. We have demonstrated that the blood vessels in Ewing's sarcoma are formed by a combination of vasculogenesis and angiogenesis, that vasculogenesis is essential for tumor growth, and that BM cells contribute to the pericyte/vSMC population of most

vessels in Ewing's sarcoma tumors [62,63]. Ewing's sarcoma is therefore a unique model for the study of the role of DLL4 in vasculogenesis.

Hypothesis

Considering the following:

- Notch receptors are expressed by BM cells and Notch signaling is necessary for vSMC differentiation from neural crest progenitors
- DLL4 is expressed by growing vessels, including tumor blood vessels
- DLL4 is essential for the formation of mature, functional blood vessels
- DLL4 expression correlates with α-SMA^{+} cell coverage of the endothelial layer in several tumor models

The research presented in this dissertation was guided by the hypothesis that **DLL4-Notch signaling plays an important role in the formation of BM-derived pericytes/vSMC in Ewing's sarcoma. Specifically, we hypothesized that DLL4 stimulates Notch on incoming BM cells and activates pericyte/vSMC maturation pathways.**

Chapter 2.

DLL4 is expressed by bone marrow derived pericytes/vascular smooth muscle cells in Ewing's sarcoma

RATIONALE

We have previously demonstrated that a large portion of the pericytes/vSMC in Ewing's sarcoma are BM-derived [29,30]. Additionally, we have demonstrated that while most Ewing's sarcoma tumor vessels have BM-derived perivascular cells, some do not. The molecular mechanisms directing incoming BM progenitor cells to participate in vascular formation and differentiate into pericytes/vSMC in some vessels but not others are unknown. Understanding how BM-derived pericytes/vSMC are formed in Ewing's sarcoma may identify new targets to inhibit vasculogenesis and ultimately inhibit tumor growth.

DLL4 plays an important role in tumor vessel development in several types of solid tumors, including melanoma, breast, and colon cancer. It is selectively expressed by endothelial cells of growing vessels as opposed to established, quiescent vessels. DLL4 expression by endothelial cells in tumors has functional significance; when DLL4 is inhibited, tumor vessels are less organized with reduced perfusion and decreased pericyte coverage [47,64,65]. The high expression of DLL4 by growing vessels together with loss of pericyte coverage after DLL4 inhibition indicates that DLL4 may play a role in the formation of BM-derived pericytes/vSMC.

Prior to this dissertation research, DLL4/Notch signaling had not yet been studied in Ewing's sarcoma. We therefore examined DLL4 expression in Ewing's sarcoma patient samples and xenograft models. Based on reports of DLL4 expression by endothelial cells in other tumor types, we expected to see $CD31^{+}DLL4^{+}$ endothelial cells surrounded by GFP^{+} BM-derived pericytes/vSMC. We initially hypothesized that that

DLL4 expressed by endothelial cells signals incoming BM cells to adhere and participate in vascular formation.

In this chapter, immunohistochemical analysis was used to confirm the BM origin of pericytes/vSMC and determine which cell types, if any, express DLL4 in Ewing's sarcoma.

RESULTS

12 out of 14 patient samples are DLL4$^+$

To determine whether DLL4 is present in Ewing's sarcoma, we first obtained fourteen patient samples and performed immunohistochemistry to evaluate DLL4 expression. These included both primary and metastatic tumor samples from a total of ten patients. Tumors were scored in a qualitative manner; 12 of 14 had DLL4$^+$ regions (Figure 3). The majority of DLL4$^+$ cells in the patient samples were in thick layers surrounding the vasculature. The perivascular location of these DLL4$^+$ cells suggests that they may be pericytes/vSMC. We were unable to confirm the pericyte/vSMC identity of the DLL4$^+$ cells because these samples are paraffin embedded and therefore multi-color fluorescence immunohistochemistry could not be performed. A few DLL4$^+$ cells were also dispersed in the mass of the tumor.

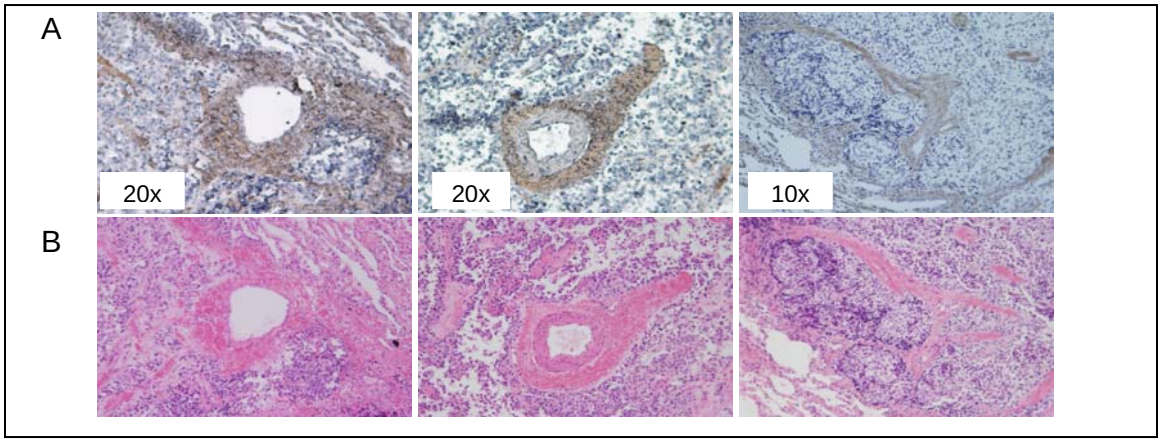

Figure 3. DLL4 is expressed by perivascular cells in human Ewing's sarcoma samples. A) Immunohistochemistry was performed on 14 patient samples to examine DLL4 expression. Brown cells are DLL4$^+$.B) Hematoxylin and Eosin staining was performed to examine the histology of the tumor sections and to identify blood vessels. Magnification is indicated in white boxes. *This figure was originally published in Clinical Cancer Research, February 2010*[66].

TC71 and A4573 Ewing's sarcoma xenograft models mimic the DLL4 expression pattern of patient tumors

To confirm that our xenograft models effectively recapitulate the DLL4 expression pattern observed in the patient tumor specimens, we performed immunohistochemistry for DLL4 on TC71 and A4573 tumor sections. Nude mice received GFP BM transplants. Engraftment was confirmed one month later. Mice were then injected subcutaneously with either TC71 or A4573 human Ewing's sarcoma cells. Tumors were allowed to grow to 2 cm^3 before mice were sacrificed and tumors were harvested and frozen for immunohistochemical evaluation. Tumor sections were co-stained for DLL4 and the endothelial cell marker CD31.

Similar to our findings using patient samples, several thick layers of $DLL4^+$ cells surrounded $CD31^+$ endothelial cells (Figure 4). A few $CD31^+DLL4^+$ endothelial cells were also observed in a small portion of the vessels.

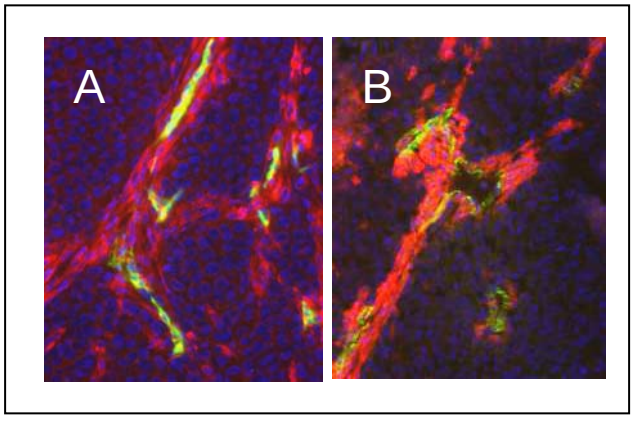

Figure 4. DLL4 is expressed by perivascular cells in TC71 and A4573 Ewing's sarcoma tumors. (A) TC71 or **(B)** A4573 cells were implanted subcutaneously in nude mice that had received a GFP BM transplant one month prior to tumor cell injection. Three weeks later, tumors were removed and examined by immunohistochemistry for CD31, to identify endothelial cells (green) and DLL4 (red). CD31 and DLL4 double positive cells are yellow. 20x magnification.

DLL4 expression by perivascular cells is confirmed by a second antibody

Prior to our work, DLL4 expression by non-endothelial cells had not been previously reported. We therefore wished to confirm that the observed DLL4 expression by perivascular cells in Ewing's sarcoma was not an artifact of non-specific antibody binding during immunohistochemistry. We again performed immunohistochemistry against DLL4, using both the original antibody and a second anti-DLL4 antibody. With both antibodies, a thick layer of perivascular cells expressing DLL4 was observed (Figure 5).

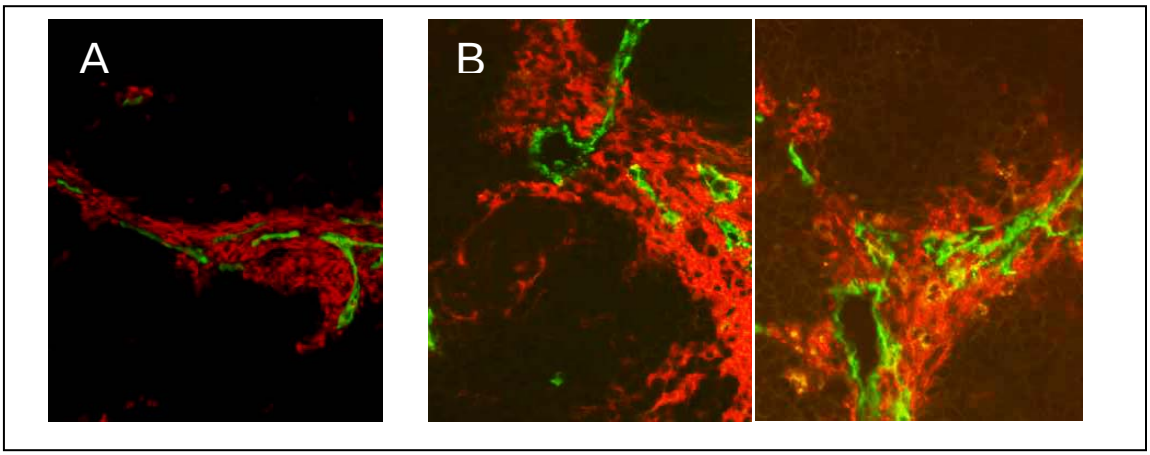

Figure 5. DLL4 expression by perivascular cells is confirmed by two antibodies. TC71 cells were implanted subcutaneously in nude mice and allowed to form tumors. Tumors were then examined by immunohistochemistry for endothelial cells using anti-CD31 (green) and **(A)** Abcam anti-DLL4 (red) or **(B)** Cell Signaling Technology Anti-DLL4 (red). 20x magnification.

DLL4 co-localizes with pericyte/vSMC markers

The peri-endothelial location of $DLL4^{+}$ cells suggests that they may be pericytes/vSMC. We performed immunohistochemistry for DLL4 in combination with the pericyte/vSMC markers desmin and α-SMA on TC71 and A4573 tumors. DLL4 co-

localizes extensively with desmin and with α-SMA (Figure 6), suggesting that the majority of perivascular DLL4^{+} cells are pericytes/vSMC. In the DLL4 and desmin double stained tumors, several desmin^{+}DLL4^{-} were also present. Additionally, in the DLL4/α-SMA double stained tumors, several DLL4^{+}/α-SMA^{-} cells were present, as well as α-SMA^{+}/DLL4^{-}. This indicates that not all pericytes/vSMC within the tumor express DLL4.

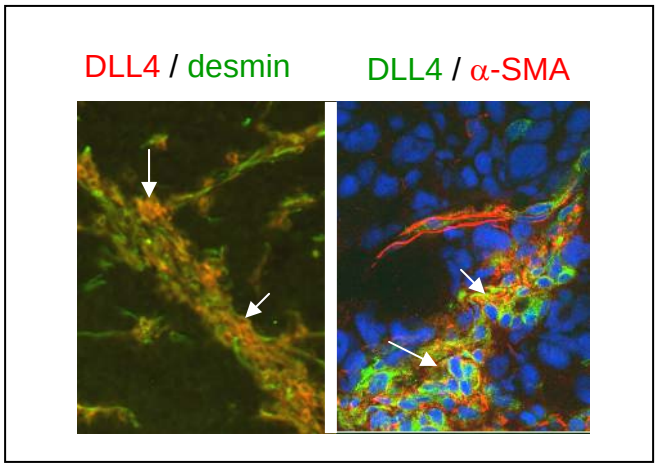

Figure 6. DLL4 co-localizes with the pericyte/vSMC markers desmin and α-SMA. Immunohistochemistry was performed on TC71 xenograft tumor sections to examine expression of **A)** DLL4 (red) and the pericyte/vSMC marker desmin (green) or **B)** DLL4 (green) and α-SMA (red). In both panels, double positive cells are orange or yellow (arrows indicate double positive cells).

DLL4^{+} pericytes/vSMC are BM-derived

The large network of perivascular DLL4^{+} cells was strikingly similar to the pattern of GFP^{+} BM-derived pericytes/vSMC previously described [29]. We first confirmed our earlier finding that many of the pericytes/vSMC in Ewing's sarcoma are BM-derived by co-staining for GFP and desmin or α-SMA (Figure 7).

To determine whether the DLL4^{+} pericytes/vSMC were themselves BM-derived, we performed co-staining for DLL4 and GFP. The majority of DLL4^{+} perivascular cells were also GFP^{+} (greater than 90%, Figure 8). Taken together with the finding that GFP and DLL4 both co-localize with pericyte markers, we conclude that DLL4 is expressed by BM-derived pericytes/vSMCs.

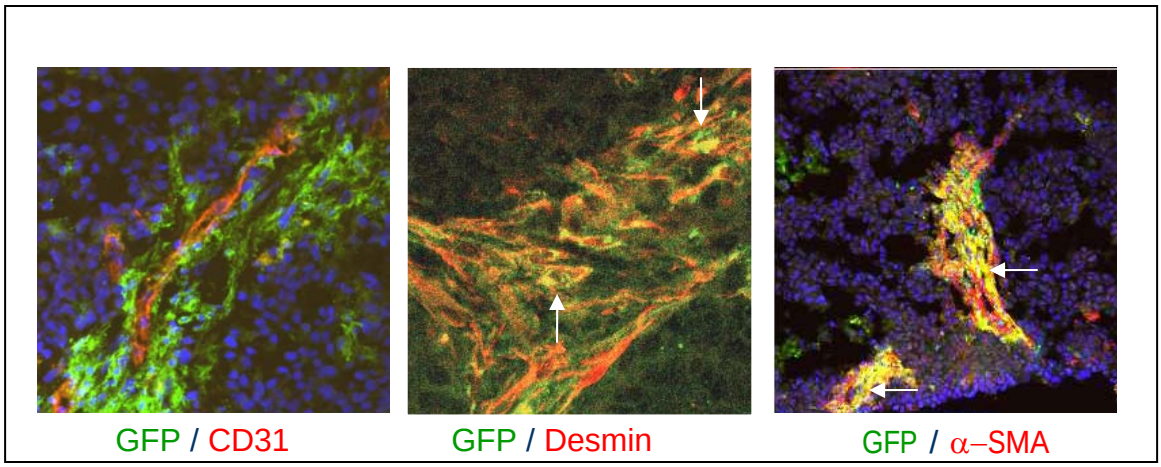

Figure 7. GFP^{+} BM-derived cells express desmin and α-SMA. TC71 cells were subcutaneously implanted in nude mice that had previously received a GFP BM transplant. When tumors reached 2cm^{3}, they were harvested, frozen and sectioned for immunohistochemistry. Immunohistochemistry was performed using antibodies against **A)** GFP (green), to identify BM-derived cells, and CD31 (red), to identify endothelial cells, **B)** GFP (green), to identify BM-derived cells and desmin (red), to identify pericytes/vSMC, and **C)** GFP (green), to identify BM-derived cells and α-SMA (red) to identify pericytes/vSMC. Double positive cells are yellow or orange (arrows show double positive cells).

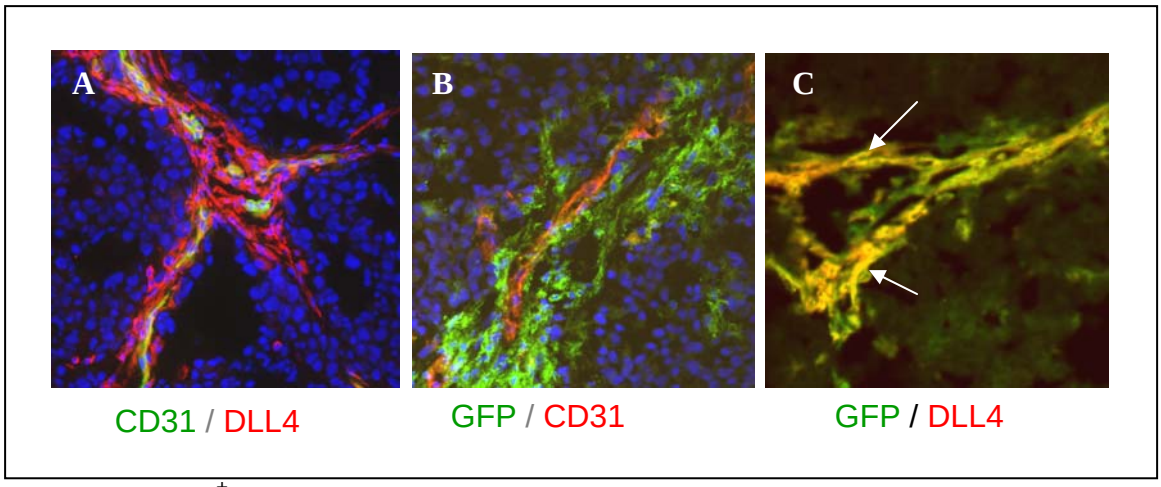

Figure 8. DLL4$^+$ cells in Ewing's sarcoma are BM-derived. TC71 cells were subcutaneously implanted in nude mice that had previously received a GFP BM transplant. When tumors reached 2cm^3, they were harvested, frozen and sectioned for immunohistochemistry. Immunohistochemistry was performed using antibodies against **A)** DLL4 (red) and CD31 (green), to identify endothelial cells, **B)** GFP (green), to identify BM-derived cells and CD31 (red), to identify endothelial cells, and **C)** GFP (green) to identify BM-derived cells and DLL4 (red). Double positive cells are yellow or orange (arrows show double positive cells). 20x magnification.

RT-PCR confirms DLL4 expression by BM-derived cells

To determine whether DLL4 is expressed by BM-derived cells before they reach the tumor, we used RT-PCR to examine DLL4 expression. Whole mouse BM was isolated from mouse femurs and fluorescent activated cell sorting (FACS) was used to collect Flk1$^+$Sca1$^+$ and Sca1$^+$Gr1$^+$ BM cell subpopulations. These subpopulations were chosen because they were previously shown to differentiate into pericytes/vSMC in Ewing's sarcoma [63]. RNA was collected from the whole BM as well as the two subpopulations and RT-PCR for DLL4 was performed. DLL4 mRNA was present in whole BM as well as both sub-populations, indicating DLL4 expression by each of the three BM populations prior to migration to the tumor and participation in vasculogenesis (Figure 9).

We next confirmed our finding of DLL4 expression by GFP^+ BM-derived cells within the tumor. To this end, we again implanted TC71 cells subcutaneously in nude mice that had previously received a GFP BM transplant and allowed tumors to grow until they reached $2cm^3$. Tumors were then harvested and homogenized to obtain a single cell suspension, and GFP^+ BM-derived cells from within TC71 tumors were collected by FACS. RNA was isolated, and RT-PCR was performed to look at DLL4 expression. In agreement with previous immunohistochemical findings, DLL4 mRNA is present in GFP^+ BM-derived cells isolated from TC71 tumors (Figure 10).

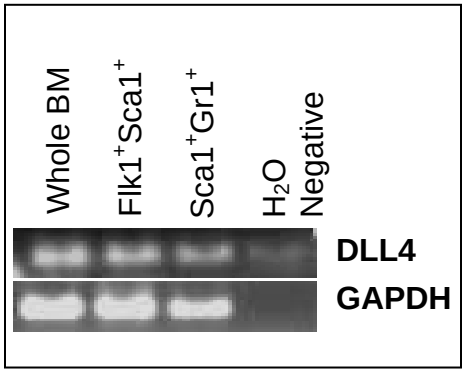

Figure 9. Whole BM, $Flk1^+Sca1^+$, and $Sca1^+Gr1^+$ BM subpopulations express DLL4. Whole BM was collected from nude mice, and $Flk1^+Sca1^+$ or $Sca1^+Gr1^+$ subpopulations were isolated by FACS. RNA was collected from whole BM and both subpopulations, and RT-PCR for DLL4 was performed.

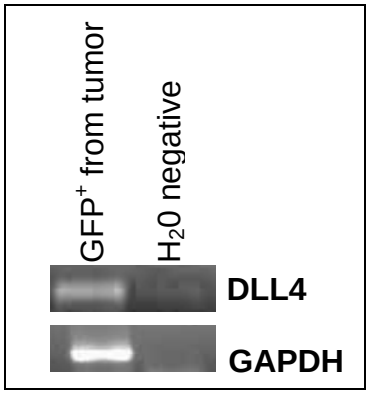

Figure 10. GFP^+ BM-derived cells isolated from TC71 tumors express DLL4 mRNA. TC71 cells were subcutaneously implanted in nude mice that had previously received GFP BM transplants and tumors were allowed to form. Tumors were homogenized and GFP^+ BM-derived cells were collected by FACS. RNA was collected from GFP^+ BM-derived cells, and RT-PCR for DLL4 was performed.

The majority of BM-derived cells are not fibroblasts

Due to the extensive number of GFP^+ BM-derived perivascular cells, it seemed likely that some of the BM-derived cells were a cell type other than pericytes/vSMC. Fibroblasts are non-tumor derived infiltrating cells within tumors and can express desmin and PDGFR-β[67]. We therefore considered the possibility that a portion of the perivascular BM-derived cells within the tumor are fibroblasts. To this end, we performed immunohistochemistry for the fibroblast marker S100A4 in conjunction with CD31 or GFP. $S100A4^+$ cells were observed in small regions throughout the tumor, including in some perivascular locations adjacent to CD31 (Figure 11a). However, only a small portion of vessels had $S100A4^+$ cells in the perivascular region and the majority of GFP^+ BM-derived cells were did not express S100A4 (Figure 11b,c).

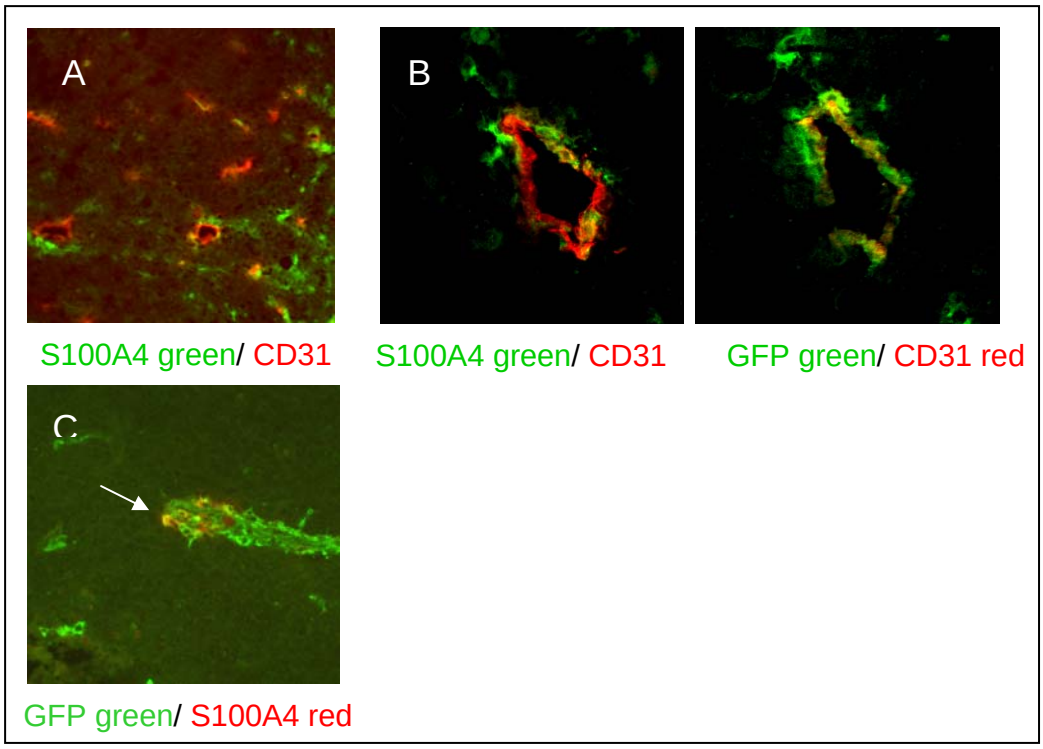

Figure 11. The majority of BM-derived cells are not fibroblasts. TC71 cells were implanted subcutaneously in nude mice that had previously received GFP BM transplants. Tumors were harvested and examined by immunohistochemistry for **A)** S100A4, to identify fibroblasts (green) and CD31, to identify endothelial cells (red), 10x magnification. **B)** Immunohistochemistry was performed for either S100A4 (green) and CD31 (red) or GFP, to identify BM-derived cells (green), and CD31 (red). The same vessel was located and photographed on adjacent tumor sections. 20x magnification. **C)** Co-staining for GFP (green), to identify BM-derived cells, and S100A4 (red), to identify fibroblasts, was performed. BM-derived fibroblasts are double positive and are orange (arrow indicates BM-derived fibroblast). 10x magnification.

SUMMARY

Contrary to our initial hypothesis, DLL4 is highly expressed by the perivascular cells and only rarely by endothelial cells in Ewing's sarcoma. This was demonstrated in both patient samples and xenograft models. It is unlikely that the observed DLL4 expression by perivascular cells is an artifact of a nonspecific antibody used for immunohistochemistry, because it was further confirmed using a second anti-DLL4 antibody. The majority of $DLL4^+$ cells in Ewing's sarcoma vasculature are pericytes/vSMC. This was shown by immunohistochemistry, which was used to demonstrate co-localization of DLL4 with the pericyte/vSMC markers desmin and α-SMA.

We are the first to report DLL4 expression by predominantly pericytes/vSMC in a tumor model. Recent reports of DLL4 expression by non-endothelial cells corroborate our initial findings. Indracollo et el. have reported the presence of $DLL4^+/CD31^-$ cells within MICOL-14 T-ALL xenograft tumors. Our findings are unique in that we show that the $DLL4^+$ cells are pericytes/vSMC in Ewing's sarcoma and are BM-derived. A GFP BM transplant model was used to confirm our previous finding that the pericytes/vSMC in Ewing's sarcoma tumors are a mosaic of locally and BM-derived cells. The similar perivascular pattern of GFP^+ BM-derived cells and $DLL4^+$ cells, together with the fact that both GFP and DLL4 are expressed by $desmin^+$ and $\alpha\text{-}SMA^+$ pericytes/vSMC, suggested that the $DLL4^+$ cells are themselves BM-derived. This was confirmed by co-staining for GFP and DLL4, which revealed greater than 90% co-localization.

RT-PCR for DLL4 demonstrated that DLL4 mRNA is present in whole BM from the mouse femur as well as the $Flk1^+Sca1^+$ and $Sca1^+Gr1^+$ subpopulations. Additionally, DLL4 mRNA was present in GFP^+ BM-derived cells isolated directly from TC71 tumors.

This confirms our immunohistochemical data indicating that BM-derived perivascular cells are $DLL4^+$.

In light of the findings presented in this chapter, our initial hypothesis, that DLL4 expressed by endothelial cells signals to incoming BM cells and directs them to adhere and/or differentiate into pericytes/vSMC, was modified. While this may be true to a small extent (a few $DLL4^+$ endothelial cells were observed in the Ewing's sarcoma xenograft models), we concluded that the majority of $DLL4^+$ cells are BM-derived pericytes/vSMC. With this in mind, we **hypothesized that DLL4 expressed by one perivascular BM-derived cell activates Notch receptors on neighboring BM cells and vice versa. We further hypothesized that this DLL4-Notch signaling plays an important role in BM cell participation in vasculogenesis and differentiation into pericytes/vSMC**.

Chapter 3.

Notch signaling is required for bone marrow cell participation in vascular formation

RATIONALE

The surprising discovery that DLL4 is expressed by BM-derived pericytes/vSMC in Ewing's sarcoma led to the hypothesis that DLL4 on perivascular BM-derived cells activates Notch signaling in surrounding BM cells, and that this DLL4-Notch signaling is critical for maturation of BM-derived progenitor cells into pericytes/vSMC. If this hypothesis is correct, and DLL4-Notch signaling plays an important role in the formation of BM-derived pericytes/vSMC, then active Notch signaling in BM-derived cells within the tumor should be evident. Additionally, if Notch signaling is essential for the BM-derived cells to become pericytes/vSMC within the tumor, then inhibition of Notch signaling within incoming BM cells should prevent them from becoming a part of the perivascular layer in tumor vasculature. Since we demonstrated that the majority of the pericytes were BM-derived, the inhibition of Notch signal should result in a significant decrease in the number of pericytes/vSMC.

In this chapter, we first looked for evidence of active Notch signaling within BM-derived cells of Ewing's tumor vasculature. Immunohistochemistry was used to examine the localization of cleaved Notch 1, an indicator of activated Notch. As a second indicator of Notch signaling activity, GFP^+ BM-derived cells were isolated directly from TC71 tumors and RT-PCR was performed to look at the expression of downstream Notch effectors.

To determine whether active Notch in BM cells has functional significance during vasculogenesis, Dominant Negative Mastermind (DNMAM) was used to inhibit the ability of BM cells to receive the Notch signal. BM cells with inhibited Notch function were then assessed for their ability to participate in tumor vascular formation.

RESULTS

Cleaved Notch1 is in a similar perivascular location to GFP and DLL4

When Notch receptors are activated, the intracellular domain is cleaved and translocates to the nucleus. We therefore used an antibody specific for the Notch1 intracellular domain (NICD1) to look for evidence of Notch receptor activation by immunohistochemistry. Sequential sections of TC71 tumors from mice that had previously received GFP BM transplants were examined by immunohistochemistry for CD31 in combination with GFP, NICD1, or DLL4. The same vessel on each slide was located and photographed. GFP^+ BM-derived cells, $NICD1^+$ cells, and $DLL4^+$ cells all form perivascular layers surrounding $CD31^+$ cells. As shown in figure 12, the pattern of GFP, NICD1, and DLL4 expression is similar, implying that Notch 1 is activated in GFP^+DLL4^+ BM-derived perivascular cells. Triple color staining could not be performed due to the limitations of our microscope equipment.

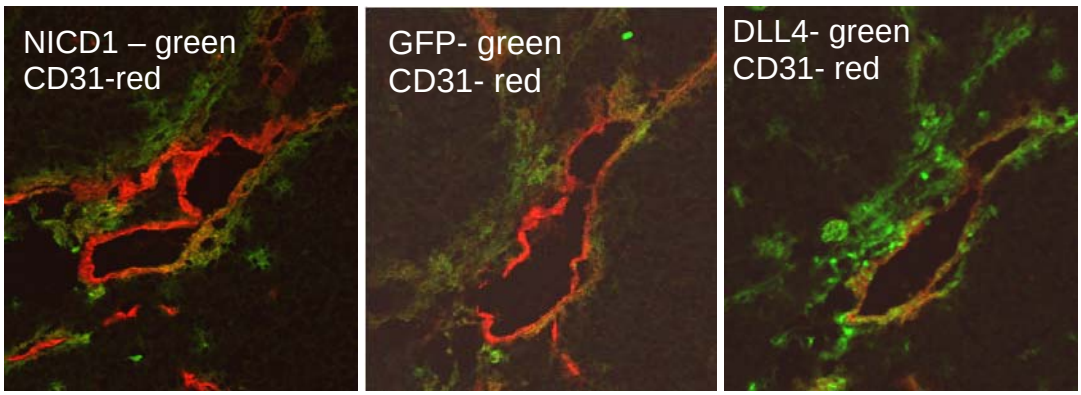

Figure 12. NICD1, GFP, and DLL4 are expressed in a similar pattern by perivascular cells in TC71 tumors. TC71 cells were implanted in GFP BM-transplanted nude mice and allowed to form tumors. Tumors were then harvested and immunohistochemistry was performed on adjacent frozen sections to examine CD31 (red), to identify endothelial cells, in combination with **A)** NICD1 (green), to identify active Notch 1 **B)** GFP (green), to identify BM-derived cells **C)** DLL4 (green). 20x magnification.

Notch signaling is active in BM-derived cells within the tumor

To gain further evidence that Notch signaling is active in GFP^+ BM-derived cells within the tumor, we again harvested TC71 tumors from nude mice that had previously received a GFP BM transplant. Tumors were homogenized until single cell suspension was achieved. GFP^+ cells were collected by FACS, and RNA was collected from these GFP^+ BM-derived cells. RT-PCR was performed to look at expression of the Notch effector Hes1 as a surrogate marker of active Notch signaling. Hes1 was expressed in GFP^+ cells collected from TC71 tumors (Figure 13). Real time PCR was then used to confirm the presence of the Notch effectors Hey1 and Hey2 in the GFP^+ BM-derived cells (data not shown). Hes1, Hey1, and Hey2 were each present, indicating that the Notch pathway is active in BM-derived cells within the tumor.

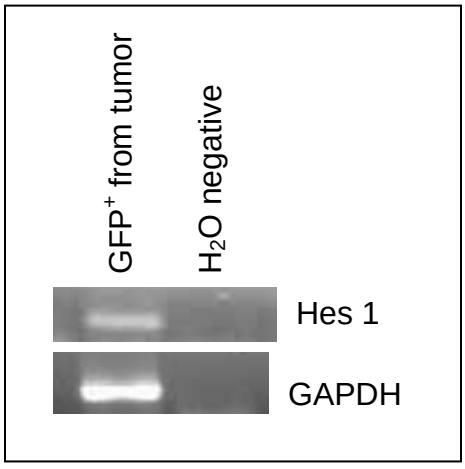

Figure 13. Notch effector Hes1 is expressed in BM-derived cells within Ewing's sarcoma tumors. TC71 cells were subcutaneously implanted in GFP BM-transplanted nude mice and allowed to form tumors. When tumors reached $2cm^3$, they were harvested and digested into a single cell suspension. GFP^+ BM-derived cells from within the tumor were collected by FACS, and RNA was isolated, and RT-PCR was performed for the Notch effector Hes1.

Notch signaling is necessary for BM cells to become pericytes/vSMC in Ewing's sarcoma

After confirming that Notch is active in BM-derived cells within Ewing's sarcoma tumors, we wished to determine whether Notch signaling is necessary for BM cell participation in vasculogenesis in Ewing's sarcoma. As depicted in figure 14, nude mouse BM cells were transduced with retroviral MigR1 containing dominant negative mastermind (MigR1-GFP/DNMAM) or MigR1-GFP control. DNMAM inhibits canonical Notch signaling by preventing the formation of the NICD/RBP-Jk/MAML transcriptional activating complex. MigR1-GFP/DNMAM induces expression of a DNMAM-GFP fusion protein; transduced cells can be tracked by GFP expression. 48 hours after transduction of BM cells, GFP^+ cells from both groups (MigR1-GFP/DNMAM and MigR1-GFP control) were collected and BM transplants were performed on nude mice. Recipients were given either MigR1-GFP/DNMAM BM or MigR1-GFP. One month after transplant, TC71 cells were injected subcutaneously. Tumor growth was followed for 2 weeks before mice were sacrificed and tumors were harvested for immunohistochemical analysis. While several perivascular GFP^+ cells were observed in tumors from MigR1-GFP control mice, there were very few perivascular GFP^+ cells in tumors from MigR1-GFP/DNMAM transplanted mice (Figure 15).

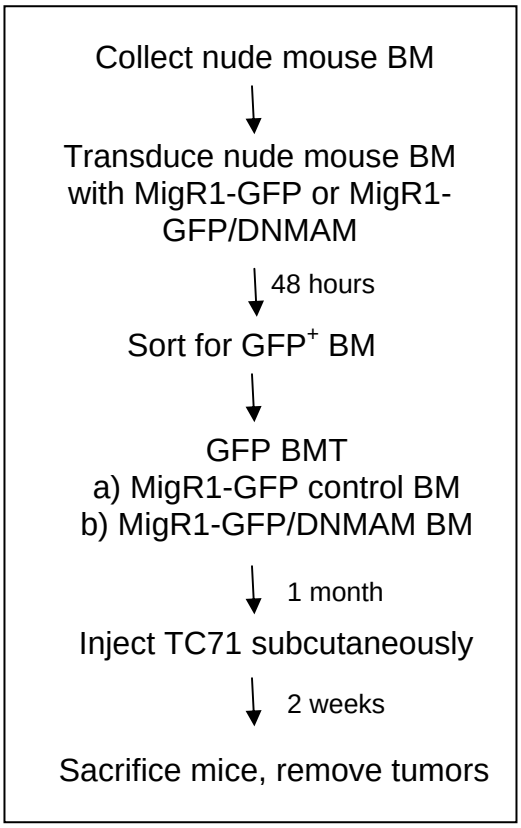

Figure 14. Schematic diagram of MigR1-GFP/DNMAM experimental design. Nude mouse BM was be collected from femurs and immediately transduced with MigR1-GFP or MigR1-GFP/DNMAM. Transduced BM was cultured in vitro for 48 hours, and then GFP^+ (transduced) cells were collected by FACS. BM transplants were then performed on nude mice, where recipients were given either MigR1-GFP or MigR1-GFP/DNMAM BM. After BM engraftment, mice were injected subcutaneously with TC71 cells. Tumors were allowed to grow for two weeks before mice were sacrificed and tumors were harvested.

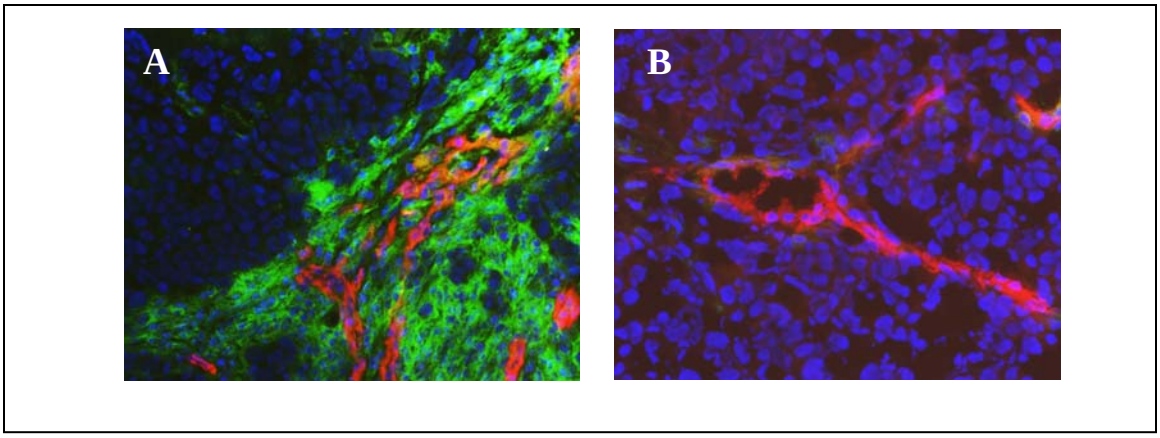

Figure 15. GFP$^+$ BM-derived cells are reduced in tumors in mice that received MigR1-GFP/DNMAM BM transplants compared to control. Nude mouse BM cells were transduced with **A)** MigR1-GFP or **B)** MigR1-GFP/DNMAM and transplanted into recipient mice. TC71 cells were injected subcutaneously and allowed to form tumors. Two weeks later, tumors were harvested and examined by immunohistochemistry for the presence of GFP$^+$ BM-derived cells (green) and CD31$^+$ endothelial cells (red). Nuclei are blue. 20x magnification.

Additionally, there was a trend towards smaller tumors in mice that had received MigR1-GFP/DNMAM transplants compared to control (data not shown). The trend towards smaller tumors in the MigR1-GFP/DNMAM mice compared to MigR1-GFP implies that tumors in MigR1-GFP/DNMAM mice may have regions undergoing apoptosis. To determine whether this was in fact the case, immunohistochemistry for TUNEL was performed to identify apoptotic cells. TUNEL$^+$ regions were larger and more frequent in the tumors from MigR1-GFP/DNMAM transplanted mice compared to control (Figure 16).

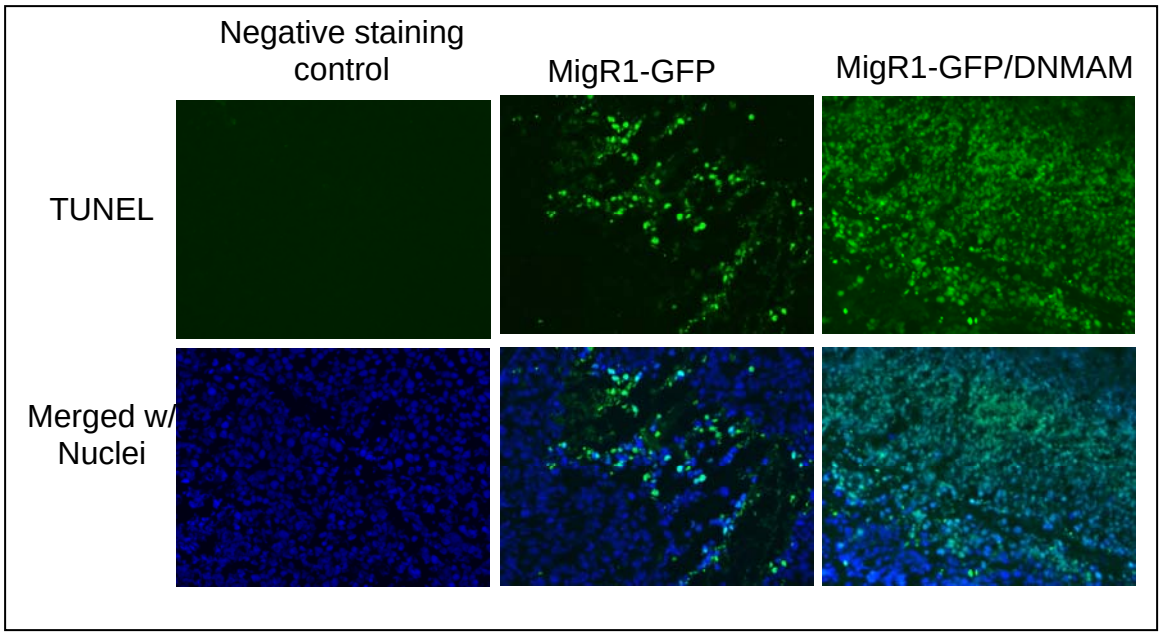

Figure 16. Apoptosis is increased in tumors from MigR1-GFP/DNMAM BM-transplanted mice compared to tumors in MigR1-GFP control BM-transplanted mice. Nude mouse BM cells were transduced with MigR1-GFP or MigR1-GFP/DNMAM and transplanted into recipient mice. TC71 cells were injected subcutaneously and allowed to form tumors. Two weeks later, tumors were harvested and examined by immunohistochemistry for the presence of TUNEL to identify apoptotic cells (green). Nuclei are blue. 20x magnification.

SUMMARY

In support of our hypothesis that Notch signaling is activated in incoming BM-derived cells, NICD1 (cleaved Notch1) was detected by immunohistochemistry in the perivascular cells surrounding $CD31^+$ endothelial cells. This pattern of NICD1 was consistent with the pattern of GFP^+ BM-derived cells and $DLL4^+$ cells surrounding the same $CD31^+$ vessel on serial tumor sections. However, because we are unable at this time to use triple color immunohistochemistry, a definitive demonstration of NICD1 in perivascular GFP^+ BM-derived cells cannot be obtained. Therefore, to validate these findings, RT-PCR was used.

GFP^+ BM-derived cells were isolated from TC71 tumors, RNA was collected, and RT-PCR performed. RT-PCR and real time PCR for the Notch effectors Hes1, Hey1, and Hey2 revealed expression of all three. This indicates active Notch signaling within BM-derived cells after the cells reach the tumor and participate in vascular formation.

After demonstrating that Notch signaling is active in BM-derived cells within the tumor, we used DNMAM to demonstrate that Notch signaling in these cells is necessary for their participation in vascular formation. TC71 tumor cells were subcutaneously injected in mice that had received BM transplants of either MigR1-GFP control BM or MigR1-GFP/DNMAM BM. As expected, thick layers of perivascular GFP^+ BM-derived cells were observed in tumors from mice transplanted with MigR1-GFP control BM. However, in tumors from mice that had received MigR1-GFP/DNMAM BM transplants, very few GFP^+ BM-derived cells surrounded the vasculature. This indicates that Notch signaling is critical for BM-derived cells to participate in formation of the perivascular layer of blood vessels in Ewing's sarcoma.

Additionally, tumors from MigR1-GFP/DNMAM mice were smaller than their control counterparts. We confirmed that large regions of the MigR1-GFP/DNMAM tumors were undergoing apoptosis using TUNEL staining. This reduced tumor growth is likely due to a decrease in blood vessel functionality caused by the loss of perivascular BM-derived cells. However, to definitively attribute this decreased tumor growth and increased tumor cell apoptosis to a change in vascular function, vessel perfusion and hypoxia studies would need to be performed.

Chapter 4.

DLL4 is critical for pericyte/vSMC formation in Ewing's sarcoma *in vivo*

RATIONALE

Having established that DLL4 is expressed by BM-derived pericytes/vSMC and that Notch signaling is activated and necessary in these BM-derived cells for their participation in pericyte/vSMC formation, we next wished to determine whether DLL4 is the Notch ligand responsible for activating Notch receptors on incoming BM cells. We hypothesized that inhibition of DLL4 will inhibit the formation of BM-derived pericytes/vSMC in Ewing's sarcoma.

To determine whether DLL4 is necessary for BM-derived cells to contribute to the pericyte/vSMC pool in tumor vasculature, we first wanted to inhibit DLL4 locally within the tumor, but not systemically. When this research was initially begun, very little was understood about the role of DLL4, if any, in immature BM-derived pericyte progenitor cell maintenance. Systemic inhibition of DLL4 could potentially negatively impact BM progenitor cell viability while they were still in the BM or in circulation, before the cells ever reached tumor vasculature. A reduction in BM-derived perivascular cells after systemic DLL4 inhibition would therefore be difficult to interpret because it could be the result of two different possibilities. While the reduction might be due to blocking DLL4-Notch signaling during BM maturation into pericyte/vSMCs, it may also be due to BM progenitor cell death before the cells reached the tumor.

Therefore, to circumvent this obstacle, shRNA to inhibit DLL4 expression was delivered directly to the tumor via intratumor injection. In this model, bilateral tumors in the same mouse were injected with shDLL4 in the right side tumor and non-targeting sh^- control in the left side tumor. Since both tumors are in the same host, both tumors share an identical BM progenitor pool. DLL4 expression is locally inhibited within the tumor

but not in the BM. Any difference in the GFP^+ BM-derived cell population seen within the tumor can be attributed only to the inhibition of DLL4-Notch in BM cells after migration to the tumor. We used shDLL4 to determine whether DLL4 is important for the formation of BM-derived pericytes/vSMC.

RESULTS

Intratumor PEI/shDLL4 inhibits expression of DLL4 on tumor vessels

We used intratumor injections of the nonviral vector polyethylenimine (PEI) carrying shRNA against DLL4 (shDLL4) or a non-targeting shRNA control (sh^- control) to inhibit expression of DLL4 on tumor vasculature. As illustrated by the schematic in figure 16, one month after GFP BM transplantation, nude mice were subcutaneously injected with TC71 Ewing's sarcoma cells on both the left and right flanks. When tumors were palpable (day 4) intratumor injections of shDLL4 (right side) or sh^- control (left side) were begun, continuing every other day for 24 days. The final tumor volumes were measured, mice were sacrificed, and tumors were harvested for evaluation by immunohistochemistry.

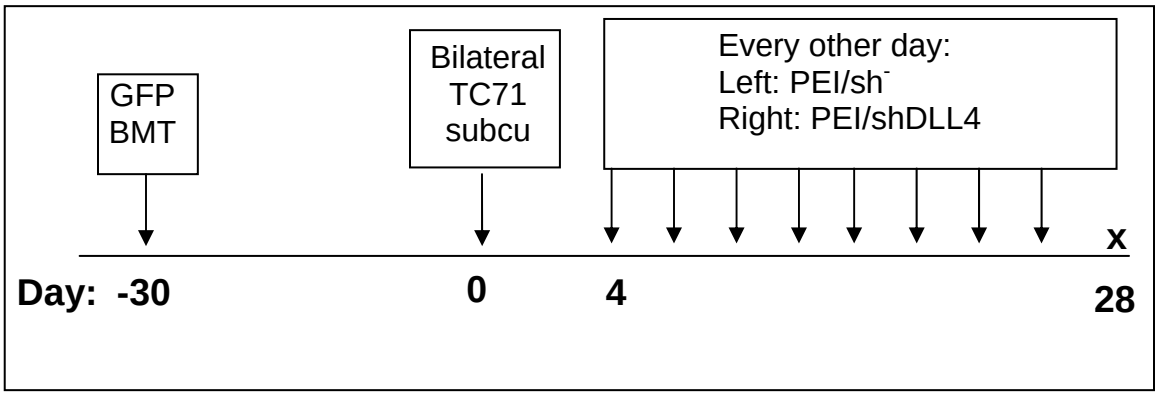

Figure 17. Experimental schema for intratumor injections of PEI/shDLL4 or PEI/sh^-control. Nude mice received GFP BM transplants and 30 days were allowed for BM cell engraftment. TC71 cells were then injected bilaterally. When tumors became palpable four days later, every other day intratumor injections were begun. Right side tumors received PEI/shDLL4 and left side tumors received PEI/ sh^- control. Mice were sacrificed 28 days after injection of TC71 cells and tumors were harvested for immunohistochemical evaluation.

We first confirmed that DLL4 was inhibited following injection of PEI/shDLL4. In tumors treated with PEI/shDLL4, DLL4 was dramatically reduced compared to control (Figure 18a). In the PEI/shDLL4 treated tumors, very few $DLL4^+$ cells were observed surrounding the vessels.

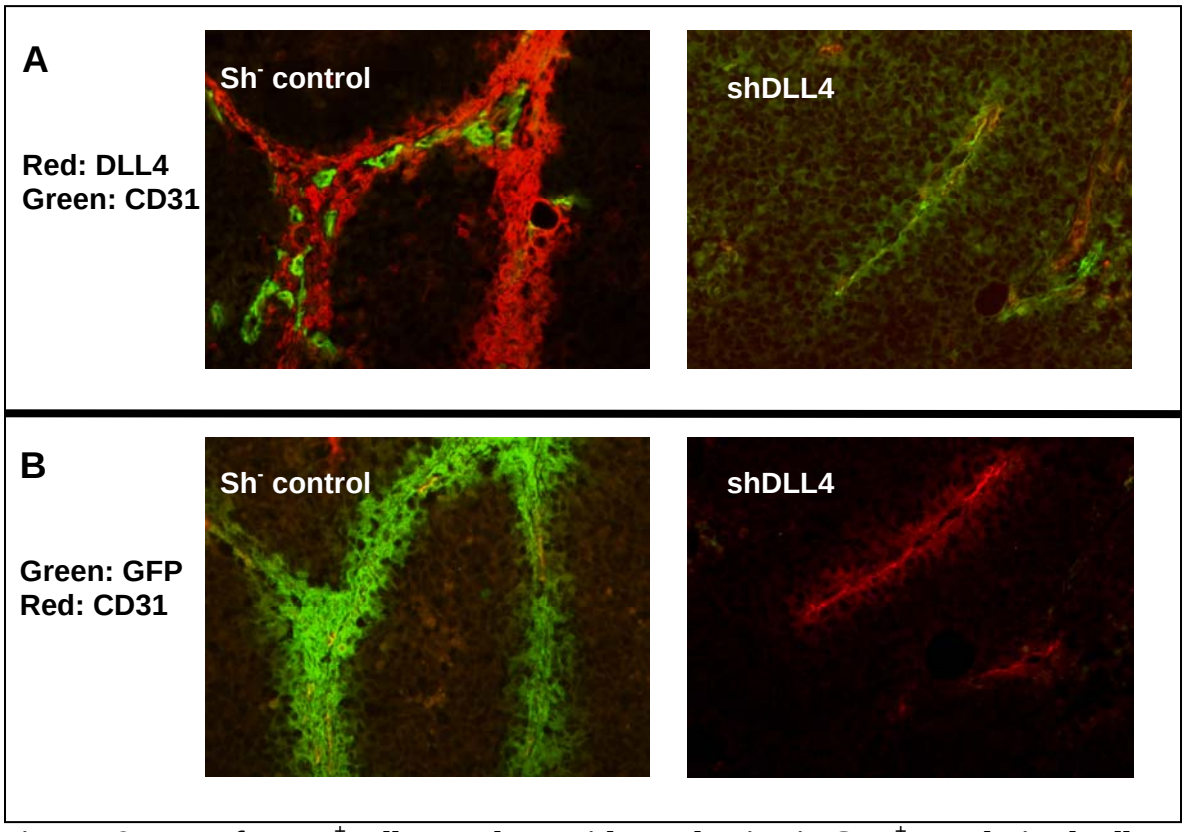

Figure 18. Loss of $DLL4^+$ cells correlates with a reduction in GFP^+ BM-derived cells in TC71 tumors after treatment with PEI/shDLL4. TC71 cells were implanted bilaterally in mice that had previously received a GFP BM transplant. When tumors were palpable, every other day intratumor injections of PEI/shDLL4 (right side tumors) or PEI/sh- control (left side tumors) were begun. 28 days after tumor inoculation, tumors were harvested and examined by immunohistochemistry for **A)** DLL4 (red) and CD31 (green), to identify endothelial cells or **B)** GFP (green) to identify BM-derived cells and CD31 (red) to identify endothelial cells. PEI/sh- control or PEI/shDLL4 treatment is indicated in the top left of each photo. 20x magnification.

Loss of DLL4 correlates with a loss of GFP^+ BM-derived perivascular cells

After confirming loss of DLL4 in PEI/shDLL4 treated tumors, we next used immunohistochemistry to determine whether the number of GFP^+ BM-derived cells was reduced. Similar to the reduction in $DLL4^+$ cells, few or no GFP^+ cells were observed surrounding $CD31^+$ endothelial cells in PEI/shDLL4 treated tumors compared to PEI/sh^- control (Figure 18b).

Loss of DLL4 correlates with a reduction in α-SMA^+, $NG2^+$, and $desmin^+$ perivascular cells

To determine whether the loss of DLL4 and GFP^+ BM-derived cells correlates with an overall reduction in the number of pericytes/vSMC, we examined the expression of α-SMA, desmin, and NG2. α-SMA expression was reduced by 91% ($p < 0.0001$), desmin by 57% ($p < 0.001$), and NG2 by 43% (p: 0.08). Representative fields and quantification data are shown in figure 19.

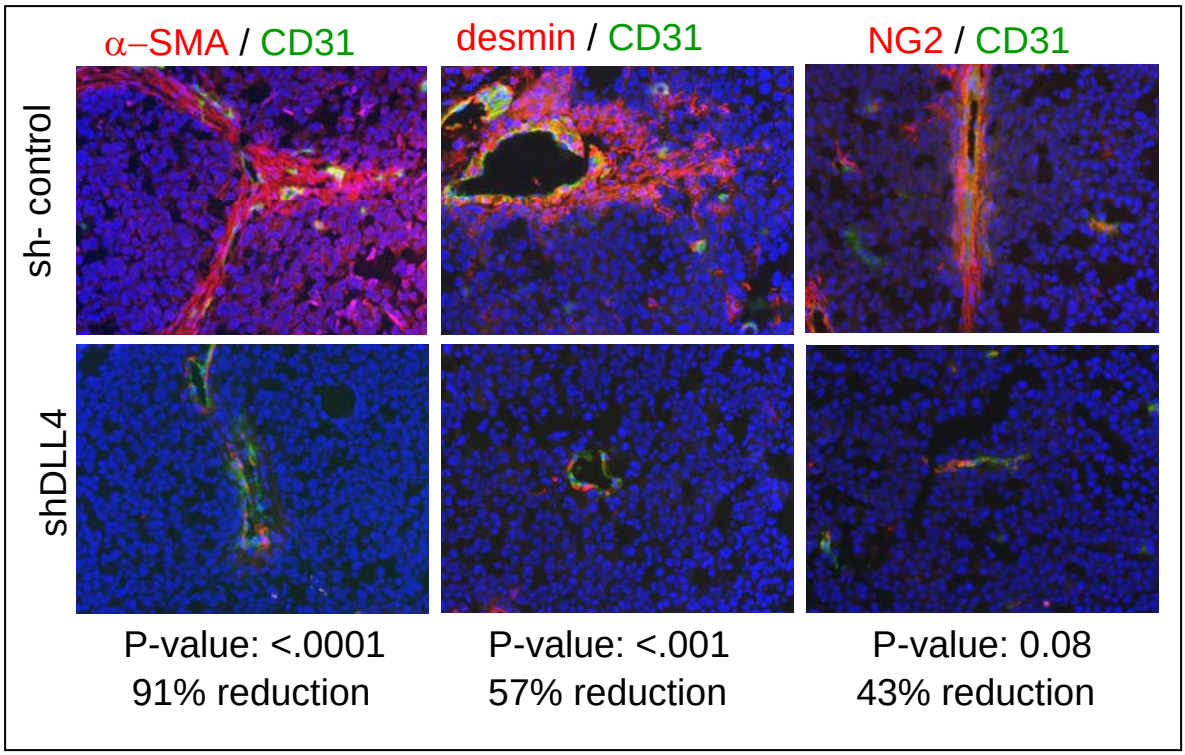

Figure 19. The pericyte/vSMC markers α-SMA, desmin and NG2 are reduced in shDLL4 treated tumors. TC71 cells were implanted bilaterally in GFP BM-transplanted nude mice. Tumors were treated with intratumor injections of PEI/shDLL4 (right side tumors) or PEI/sh- control (left side tumors) for 23 days. Tumors were then harvested and examined for the presence of CD31 (green) to identify endothelial cells in combination with α-SMA, desmin, or NG2 (red, indicated above each panel) to identify pericytes/vSMC. The total positive pixels for each pericyte/vSMC marker was quantified and the reduction in PEI/shDLL4 treated tumors compared to PEI/sh- control was determined. Percent reduction and p-values are reported below each panel.

PEI/shDLL4 treated tumors have increased hypoxia

Without pericytes, vessel functionality may be compromised. To determine whether the near complete loss of pericytes/vSMC in PEI/shDLL4 treated tumors correlated with a reduction in vessel functionality, we examined hypoxia. Increased hypoxia is a surrogate marker for reduced vessel function. Nude mice were again injected with bilateral subcutaneous TC71 cells. As before, left side tumors were treated every other day with intratumor injections of PEI/sh$^-$ control and right side tumors were treated with PEI/shDLL4. Prior to sacrifice, mice were injected with Hypoxyprobe-1.

Hypoxyprobe-1 forms pimonidazole adducts in hypoxic cells and can be recognized by immunohistochemistry. Tumors were then harvested and evaluated for hypoxia. Hypoxia was significantly increased in tumors treated with PEI/shDLL4 compared to control (p = 0.03, Figure 20), implying reduced supply of oxygenated blood to these tumors most likely secondary to reduced vessel functionality.

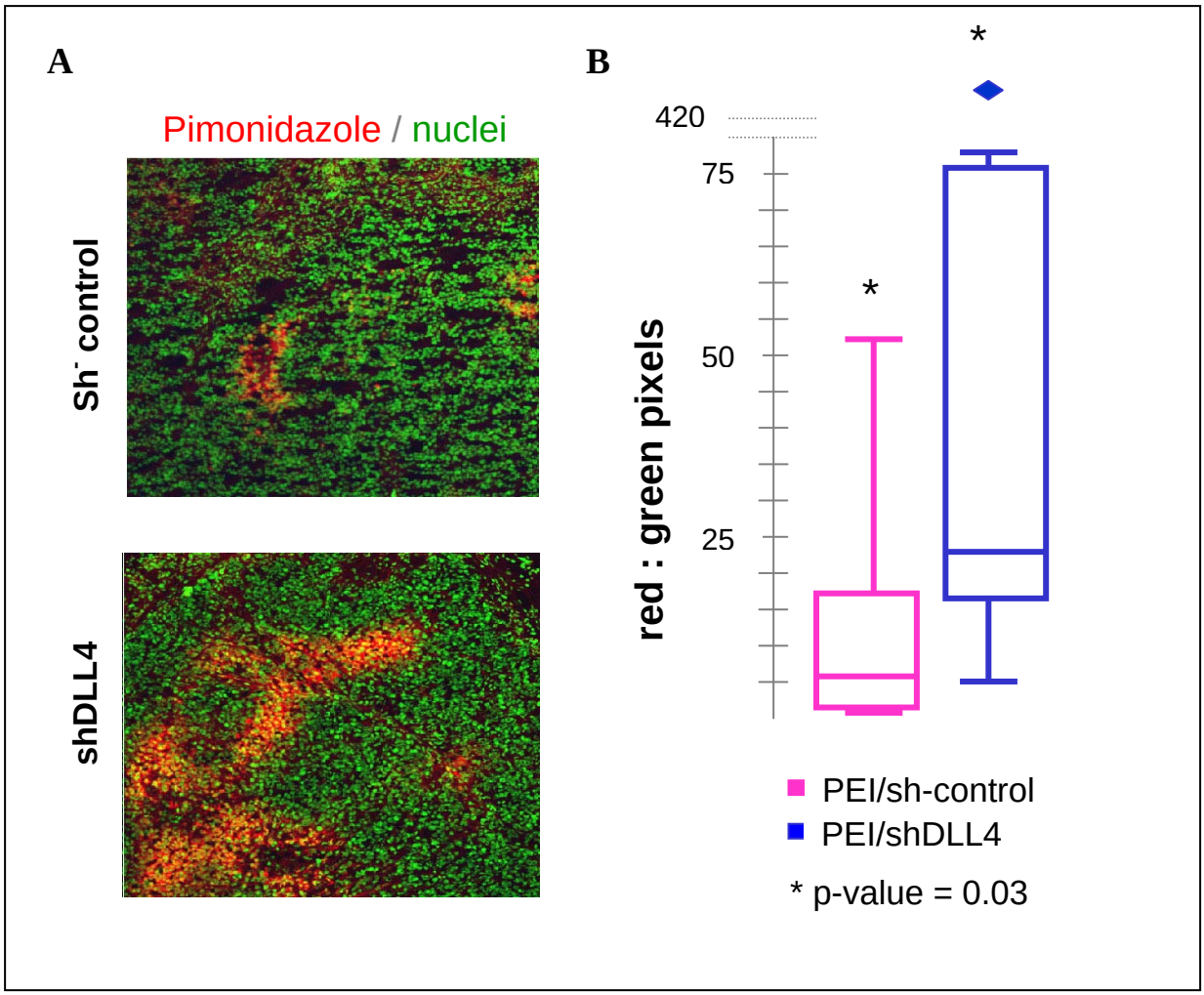

Figure 20. Hypoxia is increased in tumors treated with shDLL4 compared to sh- control. TC71 cells were injected subcutaneously on both flanks of nude mice. Mice were treated with intratumor injections of PEI/shDLL4 (right side tumors) or PEI/sh-control (left side tumors). Prior to sacrifice, mice were injected i.v. with hypoxyprobe-1 (pimonidazole hydrochloride). Tumors were then removed and examined by immunohistochemistry. **A)** Hypoxic cells were identified using an anti-hypoxyprobe-1 antibody (red/orange) and nuclei by sytox green (green). **B)** The hypoxia to nuclei ratio was quantified for five 10x fields per tumor using SimplePCI software.

Hoescht 33342 was an ineffective measure of vessel perfusion

To further explore the functionality of tumor blood vessels, we wished to measure the number of vessels with blood flow compared to the total number of vessels present. To do this, we used tail vein injections of Hoescht33342 dye immediately prior to sacrifice. Hoescht33342 dyes the nuclei of any cell that it contacts blue; thus it can be used to track the pattern of blood flow. Extensive blue labeling of cells distant from blood vessels in tumors in both shDLL4 and sh^- control groups made experimental results from Hoescht33342 nuclei labeling difficult to interpret. We were unable to determine which vessel the dye had leaked from, and therefore unable to distinguish perfused from non-perfused vessels. Hoescht 33342 studies were therefore inconclusive (data shown in appendix).

shDLL4 inhibits tumor growth *in vivo*

The impaired vessel functionality in tumors treated with PEI/shDLL4 suggested that tumor growth might also be inhibited. Tumor volume was measured immediately before mice were sacrificed. As shown in figure 21, tumors treated with PEI/shDLL4 were significantly smaller (120 mm^3) than those treated with PEI/sh^- control (299 mm^3, $p = 0.03$). In mice where right side tumors were not smaller than left side tumors, immunohistochemistry demonstrated that DLL4 expression was not significantly inhibited (data not shown).

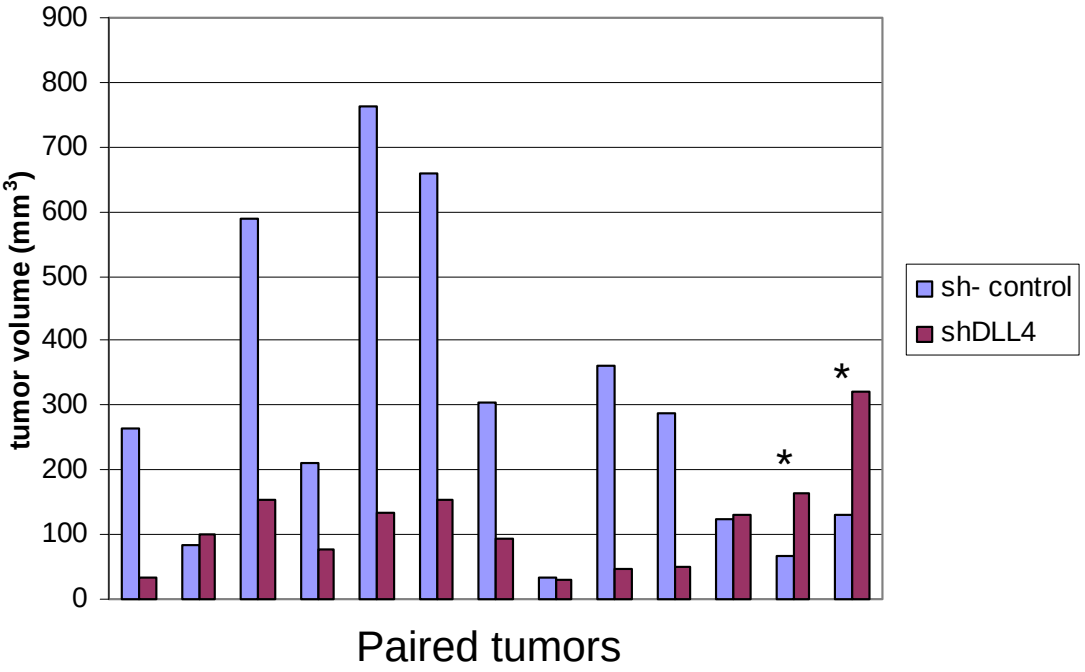

Figure 21. shDLL4 inhibits TC71 tumor growth in vivo. Mice were injected with bilateral subcutaneous TC71 cells. When tumors were palpable, every other day intratumor injections of PEI/shDLL4 (right side tumors) or PEI/sh$^-$ control (left side tumors) were begun. Two weeks later, final tumor volumes were measured and mice were sacrificed. Tumor volumes are displayed as matched pairs of right and left side tumors from the same mouse. Student's paired t-test p-value = 0.03, * represents tumors where DLL4 was not significantly inhibited after treatment with PEI/shDLL4

SUMMARY

In this chapter, evidence of a critical role for DLL4 in BM-derived cell participation in vasculogenesis in Ewing's sarcoma is provided. The hypothesis that inhibition of DLL4 will inhibit the formation of BM-derived pericytes/vSMC was confirmed.

Intratumor injections of shDLL4 caused a dramatic reduction of DLL4 expression by perivascular cells compared to sh^- control tumors. Loss of DLL4 correlated with a near complete loss of GFP^+ BM-derived perivascular cells. This was shown by immunohistochemistry for DLL4 or GFP together with CD31 (to identify endothelial cells). The reduction in BM-derived perivascular cells after loss of DLL4 can be attributed to an important role for DLL4-Notch signaling once BM cells reach the tumor. This was confirmed by the use of a bilateral tumor model. In this model, sh^- control treated tumors and their shDLL4 treated counterparts shared the same BM progenitor cell pool. Sh-control tumors displayed the expected thick layers of perivascular GFP^+ BM-derived cells, while shDLL4 treated tumors had almost no GFP^+ BM-derived cells present.

After identifying a role for DLL4 in the formation of the GFP^+ BM-derived perivascular cell layer, we next demonstrated that loss of DLL4 correlates with a significant reduction in pericytes/vSMC within the tumor. α-SMA, desmin, and NG2 were all significantly reduced in tumors treated with shDLL4 compared to sh-control treated tumors, as assessed by immunohistochemistry. This reduction in cells positive for three pericyte/vSMC markers indicates an overall reduction in pericytes/vSMC after DLL4 expression is inhibited.

The striking change in vascular phenotype after DLL4 inhibition is indicative of a potential change in vessel functionality. Hypoxia was measured as a surrogate marker for vessel functionality; increased hypoxia correlates with reduced vessel functionality. Tumor hypoxia was increased in tumors treated with shDLL4 compared to control. This increased hypoxia correlates with decreased pericyte coverage and agrees with previous studies by Noguera-Troise et al. demonstrating increased tumor hypoxia in C6 gliomas in mice after DLL4 inhibition [58].

Reduced pericyte coverage of blood vessels and subsequent reduced vessel functionality in tumors treated with shDLL4 was expected to have a negative impact on tumor growth. In agreement with this, tumors treated with shDLL4 were significantly smaller than their sh^- control treated counterparts.

These studies are the first to show the critical role of DLL4 in BM-derived pericyte/vSMC differentiation and formation, and to demonstrate Ewing's sarcoma tumor growth inhibition caused by loss of DLL4. Inhibition of DLL4 resulted in fewer BM-derived cells within the tumor. The tumor vessels had decreased pericyte/vSMC coverage, were smaller, and less functional. Tumor growth was also inhibited. To further confirm and expand these novel findings, we used a second, more elegant tool, the DLL4 neutralizing antibody YW152F, described in the next chapter.

Chapter 5.

DLL4 blockade inhibits tumor growth by disrupting the formation of functional vasculature

RATIONALE

Previous DLL4 inhibition studies using shDLL4 demonstrated that DLL4 is necessary for the formation of BM-derived pericytes/vSMC in Ewing's sarcoma. However, there are some limitations associated with using intratumor injections of shRNA. First, equal distribution of shRNA (and therefore uniform DLL4 knockdown) throughout the entire tumor is highly unlikely. Although immunohistochemical analysis confirmed knockdown of DLL4 in the majority of vessels in tumors treated with PEI/shDLL4, some DLL4 expression was still observed in small regions of treated tumors and there were a small number of tumors where DLL4 expression was not inhibited by shDLL4. Another limitation of the intratumor injection model is the lack of clinical application. In general, shRNA is not stable enough to be delivered systemically to patients and intratumor injections are not feasible.

Therefore, to confirm our findings, we elected to use a second approach to demonstrate the essential role of DLL4 in pericyte/vSMC formation in Ewing's sarcoma. YW152F is a humanized DLL4-neutralizing antibody that binds to and inhibits the function of both human and mouse DLL4 with similar efficiency and efficacy. It is an attractive inhibitor of DLL4 because it can be delivered systemically via i.v. injection and is highly specific for DLL4 but not the other Notch ligands. In addition to using YW152F as a second tool to confirm our initial finding that DLL4 is essential for BM-derived pericyte/vSMC formation, we also wished to determine whether DLL4 is a viable therapeutic target for inhibiting the growth of Ewing's sarcoma *in vivo.* For these investigations, the two models discussed previously, TC71 and A4573, were used.

Studies in this chapter confirmed our previous findings and expanded our understanding of DLL4 inhibition as a way to inhibit Ewing's sarcoma tumor growth.

RESULTS

YW152F inhibits the growth of Ewing's sarcoma *in vivo*

To confirm our previous finding that DLL4 is essential for vasculogenesis and tumor growth in Ewing's sarcoma, we used the DLL4-neutralizing antibody YW152F (Figure 22). One month after GFP BM transplant, mice were injected subcutaneously with either TC71 or A4573 cells. Five days later, twice weekly tail vein injections of either YW152F, IgG control, or PBS were begun. Twenty-one or 24 days after tumor inoculation, final tumor volumes were measured before mice were sacrificed and tumors were harvested for immunohistochemical analysis. TC71 tumors from mice treated with YW152F were significantly smaller than tumors from mice treated with IgG or PBS controls ($p = 0.03$, Figure 23). A4573 tumors from mice treated with YW152F were also significantly smaller than those in mice treated with IgG control ($p = 0.015$, Figure 24).

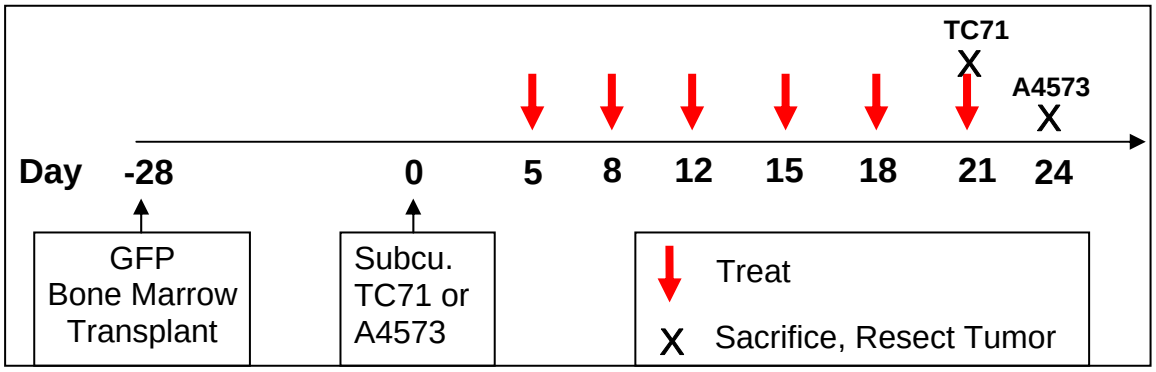

Figure 22. Experimental schema using YW152F, IgG or PBS. Twenty eight days after GFP BM transplants were performed on nude mice, TC71 or A4573 cells were injected subcutaneously. Five days later, twice weekly i.v. injections of either YW152F, IgG or PBS were begun. Mice with TC71 tumors received a total of 5 treatments and mice with A4573 tumors received a total of 6 treatments. 3 days after the last treatment, tumors were measured, mice were sacrificed, and tumors were harvested.

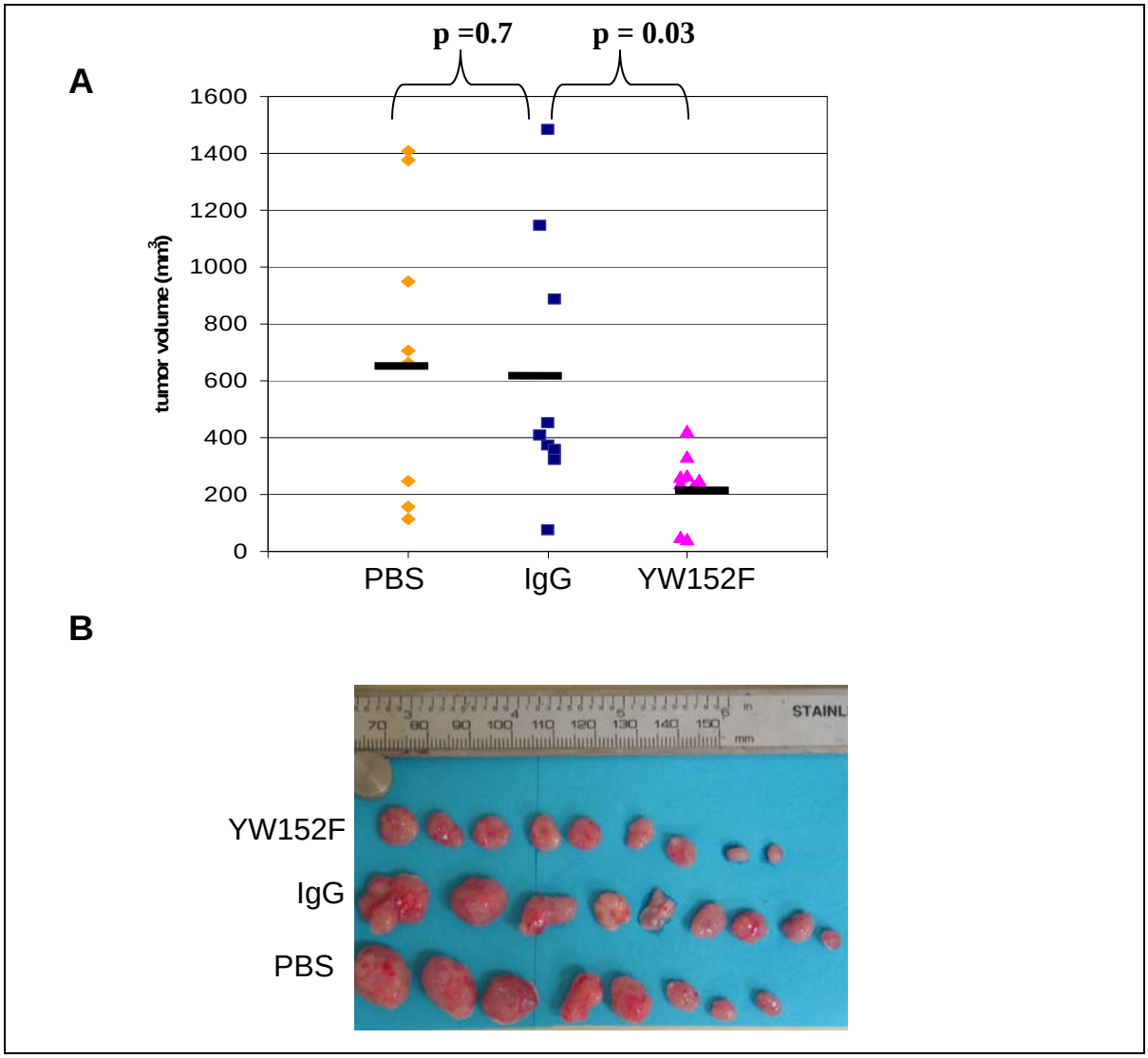

Figure 23. YW152F inhibits TC71 tumor growth *in vivo*. TC71 cells were subcutaneously injected in nude mice that had previously received GFP BM transplants. Mice were treated with either YW152F, IgG, or PBS. Final tumor volumes were measured prior to sacrifice of mice, and statistical significance for the difference in size was calculated using the student's t-test. Tumors were then harvested for immunohistochemical evaluation. **A)** Final tumor volumes. Orange diamonds represent tumors from PBS treated mice, blue squares represent tumors from IgG treated mice, and pink triangles represent tumors from YW152F treated mice. **B)** Resected tumors before being frozen for immunohistochemistry. Treatment group is indicated to the left of the photo.

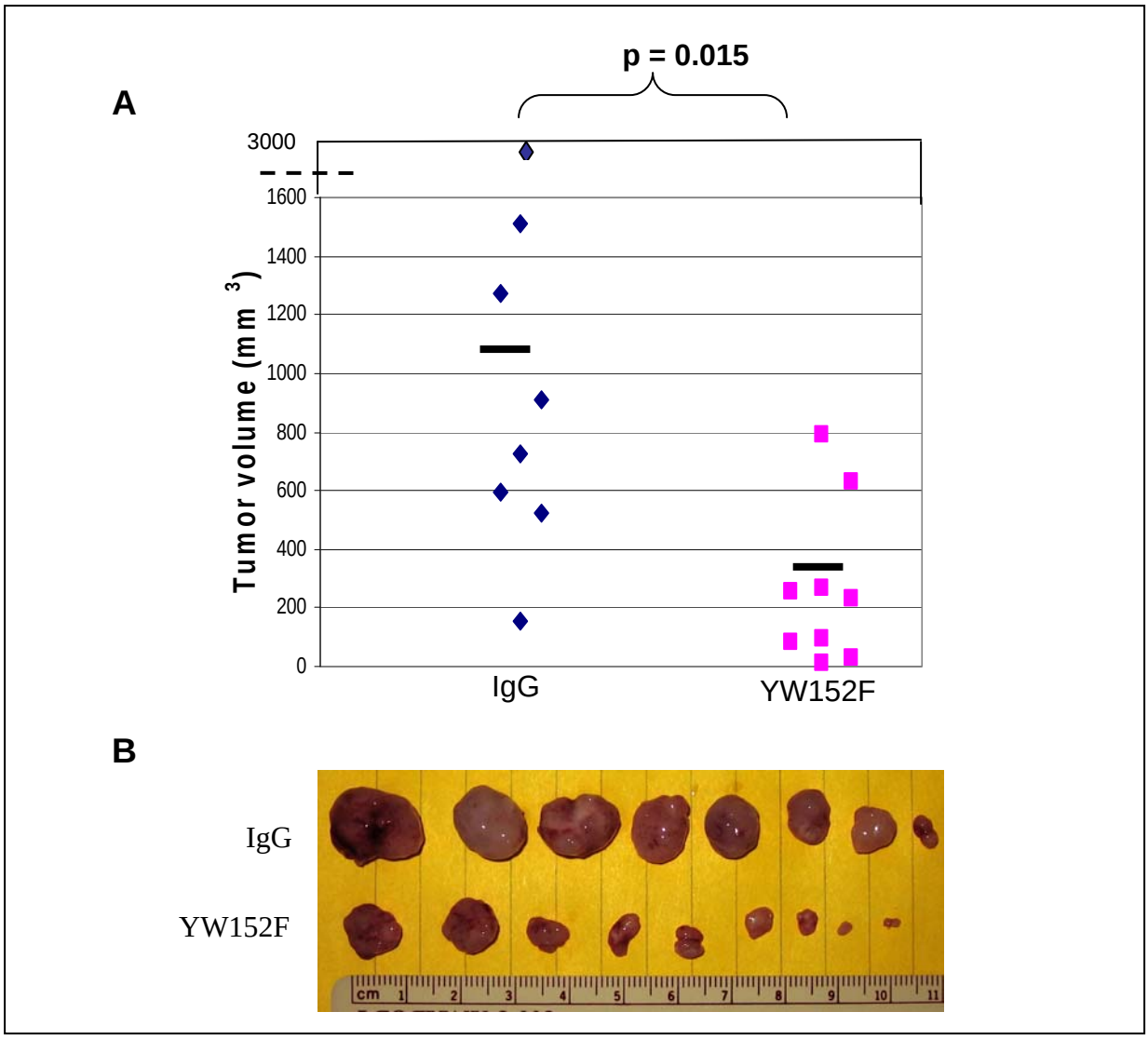

Figure 24. YW152F inhibits the growth of A4573 tumors *in vivo*. A4573 cells were subcutaneously injected in nude mice that had previously received GFP BM transplants. Mice were treated with YW152F or IgG. Final tumor volumes were measured prior to sacrificing mice. **A)** Final tumor volumes. Blue diamonds represent tumors from IgG treated mice and pink squares represent tumors from YW152F treated mice. **B)** Resected tumors before being frozen for immunohistochemistry. Treatment group is indicated to the left of the photo.

YW152F does not effect cell proliferation *in vitro*

To determine whether the inhibition of tumor growth by YW152F was due to a direct effect of the antibody on tumor cell proliferation, we treated TC71 and A4573 cells with either YW152F or IgG control (5μg/ml, refreshed daily) in vitro. Total number of viable cells was assessed using the trypan blue assay by a ViCell automated cell counter at 48 and 72 hours. There was no significant difference between the number of viable cells in YW152F treated wells compared to control at either dose or time point (Figure 25).

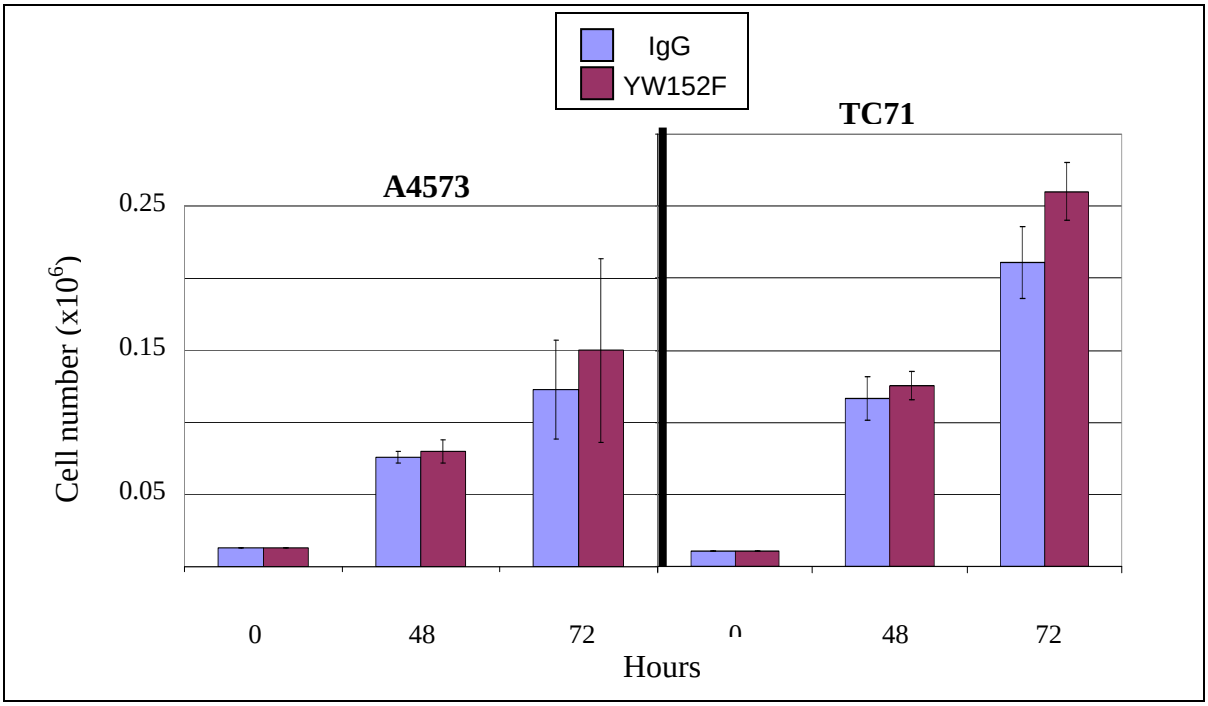

Figure 25. YW152F does not inhibit tumor cell proliferation in vitro. A4573 or TC71 cells were treated with 5μg/ml YW152F or IgG, refreshed daily. Total number of viable cells was measured using the trypan blue assay and automated ViCell counter at 48 and 72 hours. Blue bars represent IgG control treated cells, maroon represent YW152F treated cells.

GFP$^+$, α-SMA$^+$, NG2$^+$, and desmin$^+$ cells are reduced after YW152F treatment

After demonstrating that tumor growth inhibition by YW152F was not due to a direct effect on tumor cell proliferation, we examined the vasculature for changes in the number of BM-derived pericytes/vSMC. We first used immunohistochemistry to evaluate TC71 tumors for the presence of GFP$^+$ BM-derived cells. Similar to our findings using shDLL4, the number of GFP$^+$ BM cells was reduced in tumors from YW152F treated mice compared to control (85% reduction, p= 0.001). We next examined the α-SMA$^+$, NG2$^+$, and desmin$^+$ populations of pericytes/vSMC by immunohistochemistry. As shown in figure 26, the number of α-SMA$^+$, NG2$^+$, and desmin$^+$ cells was significantly reduced in YW152F treated tumors compared to control (α-SMA reduced 87%, p: 0.005; NG2 61%, p:0.007; desmin 70%, p:0.002).

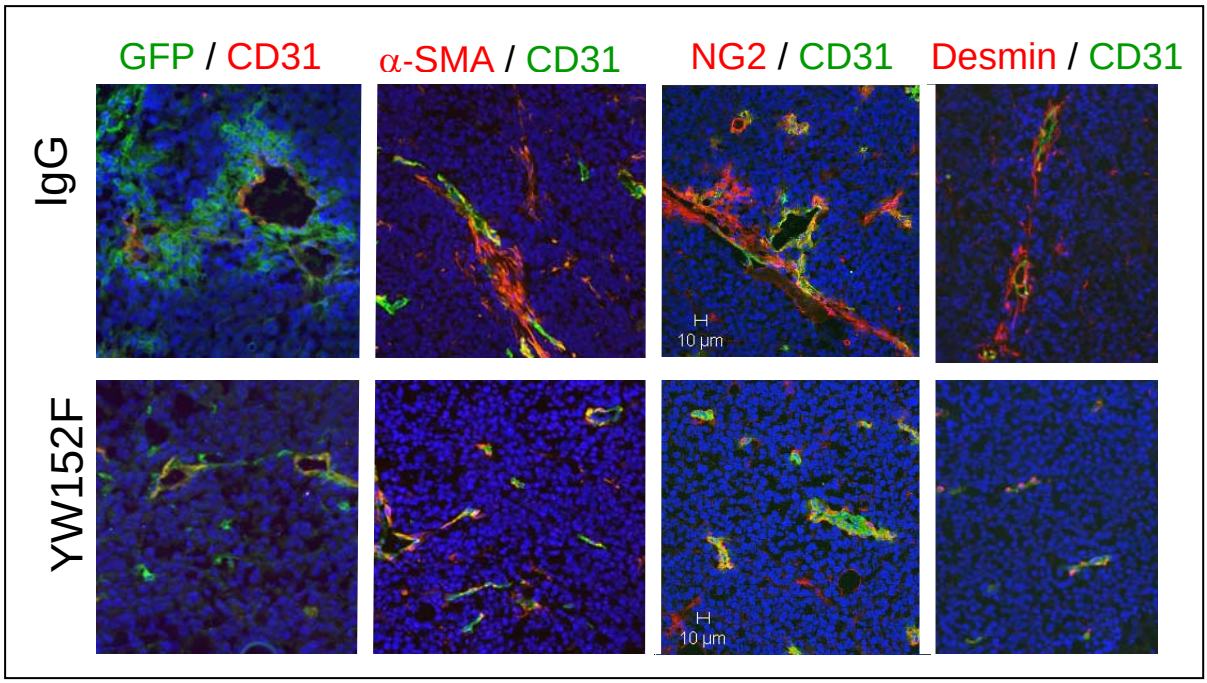

Figure 26. GFP, α-SMA, NG2 and desmin are significantly reduced in tumors after YW152F treatment. TC71 cells were subcutaneously injected in nude mice that had previously received GFP BM transplants. Mice were treated with either YW152F or IgG. After mice were sacrificed and tumors were harvested, immunohistochemistry was performed for CD31 to identify endothelial cells in combination with GFP (green, to identify BM-derived cells), or α-SMA, NG2, or desmin (red, to identify pericytes/vSMC). The top panels show IgG treated tumors and the bottom panels show YW152F treated tumors. In all photos, nuclei are blue and 20x magnification was used.

protein	% reduced in YW152F (positive pixels: total nuclei ratio)	Mann-Whitney p-value
GFP	**85%**	**0.001**
α-SMA	**87%**	**0.005**
Desmin	**70%**	**0.002**
NG2	**61%**	**0.007**

Table 1. GFP, α-SMA, desmin, and NG2 were reduced in YW152F treated mice. Five 10x fields were randomly photographed from each tumor. Simple PCI software was used to determine the average ratio of positive pixels for the marker being evaluated (for example, GFP) compared to nuclei present. Mean values for each marker from the YW152F treated group were then compared to mean values for the same marker in the IgG treatment group, and a percent reduction in YW152F group compared to IgG was calculated (column 1). Mann-Whitney p-values for the difference in means were calculated (column 2).

YW152F treatment did not affect total number of $CD31^+$ cells but did reduce the number of open vessel lumens

To further characterize the effect of DLL4 inhibition on the tumor vascular phenotype, we used immunohistochemistry against CD31 to identify endothelial cells. We compared both the total $CD31^+$ cells present in each tumor, using quantification software, and the average number of visible vessel lumens. The average number of vessel lumens per slide for each tumor was manually counted. There was no difference in total $CD31^+$ cells present in YW152F treated tumors compared to IgG control (data not shown). There was, however, a trend towards fewer open lumens in YW152F treated tumors compared to control (0.8 vs 2.1 lumens per 10x field, $p = 0.06$). The difference between endothelial cell vascular structures in tumors of YW152F treated mice and IgG control is visually striking. Long, lumen bearing vessels were plentiful in control tumors. By contrast, most $CD31^+$ structures in YW152F treated tumors were small, punctate and non-lumen bearing (Figure 27).

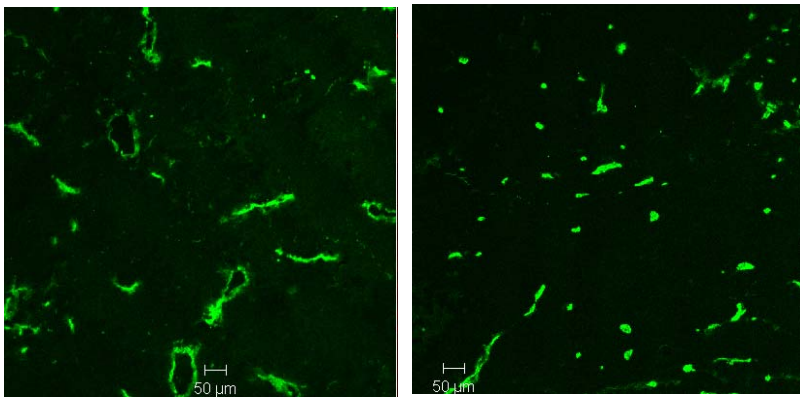

Figure 27. The number of vessel lumens is reduced in TC71 tumors from mice treated with YW152F compared to IgG control. Immunohistochemistry was performed on TC71 tumor sections from mice treated with YW152F or IgG to identify $CD31^{+}$ endothelial cells. The number of open lumens in five 10x fields was manually counted for each tumor. Average lumen number was 2.1 per 10x field in IgG treated tumors, and 0.8 in YW152F treated tumors. $p = 0.059$.

Hypoxia is increased in YW152F treated tumors

The dramatic change in tumor vessel phenotype after treatment with YW152F *in vivo*, together with the lack of effect on cell proliferation *in vitro* on TC71 and A4573 cells implied that the observed inhibition of tumor growth might be attributable to reduced blood vessel functionality. As a measure of vessel functionality, we examined hypoxia within the tumors. GFP^+ BM transplanted nude mice were injected subcutaneously with TC71 cells as described previously. Beginning five days after tumor cell injection, mice were treated twice weekly for 23 days with YW152F or IgG in the same experimental schema used previously. Prior to sacrifice, mice were injected with hypoxyprobe-1. Tumors were then harvested and analyzed by immunohistochemistry to identify hypoxic regions. As shown in figure 28, the size of the hypoxic regions in YW152F treated tumors was significantly increased compared to control (5.3 fold increase, $p = 0.003$).

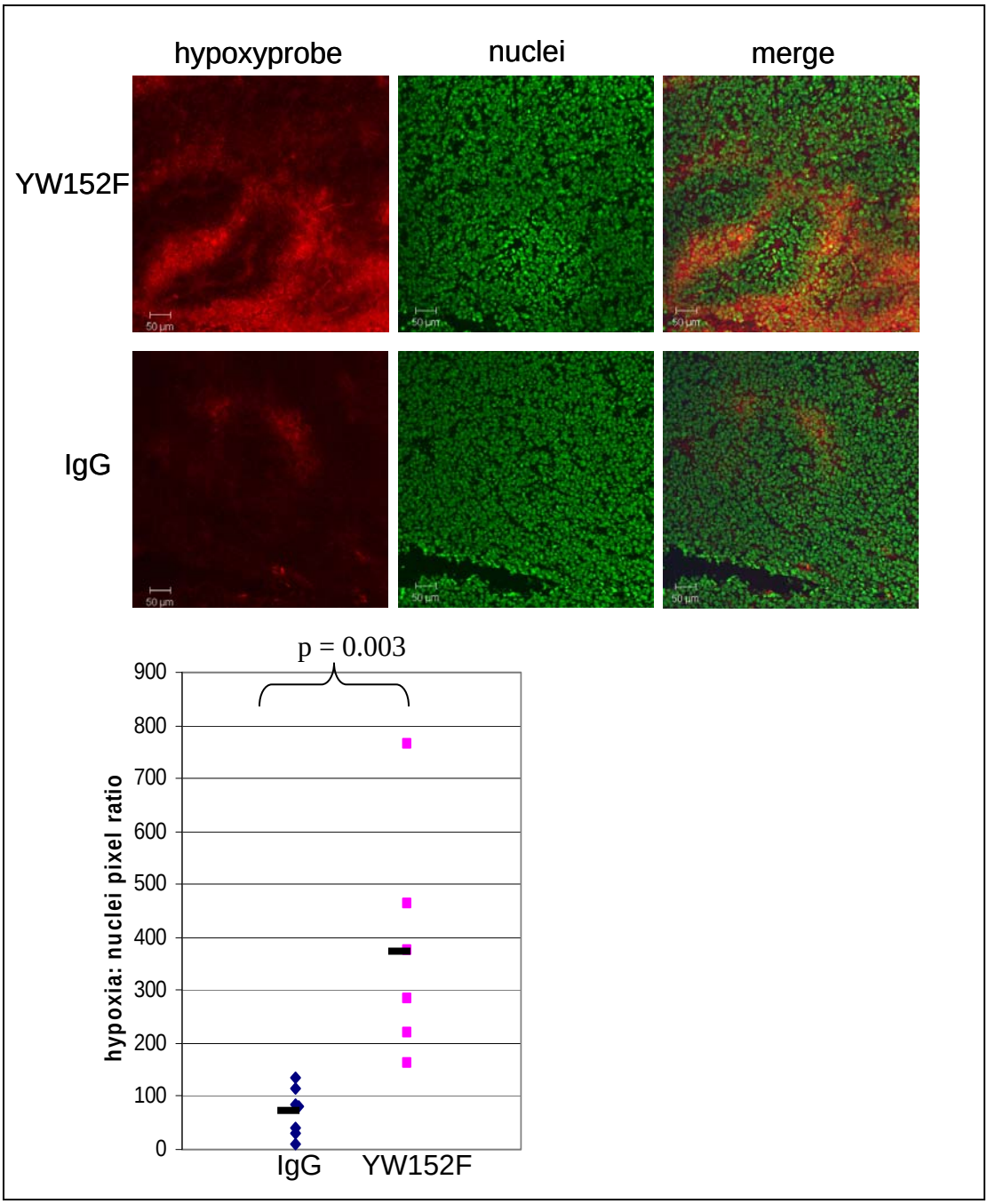

Figure 28. Hypoxia is increased in YW152F treated tumors compared to control. TC71 tumor bearing mice were treated with YW152F or IgG. Prior to sacrifice, mice were injected with hypoxyprobe-1 (pimonidazole hydrochloride) by tail vein injection. Tumors were then harvested and **A)** evaluated by immunohistochemistry to identify hypoxic regions using anti-hypoxyprobe-1 (red). Nuclei were identified using sytox green (green). In the merged images, hypoxic regions appear red or orange. **B)** The ratio of positive pixels for hypoxia (red) to nuclei (green) was determined for five 10x fields per tumor using Simple PCI software and averaged to obtain one value for each tumor. Blue diamonds represent IgG treated tumors, and pink squares represent YW152F. Black bars show mean values.

Biotin perfusion studies were inconclusive

To compliment our demonstration of increased hypoxia and thus reduced vessel functionality, we performed biotin perfusion studies to identify vessels with blood flow. TC71 tumors were again implanted in nude mice that had previously received GFP BM transplants and treated twice weekly with either YW152F or IgG control. Immediately after sacrifice, biotin in PBS was perfused through the mouse circulation by direct injection into the heart. Tumors were then evaluated by immunohistochemistry for biotin and CD31. The regions of the tumor that were positive for biotin did not co-localize with CD31, therefore they are not blood vessels. It is unclear whether this unlikely finding is due to extensive leakage of the biotin away from vessels and into the tumor, or whether it is due to non-specific binding of the fluorescently labeled streptavidin, which was used during immunohistochemistry to identify biotin.

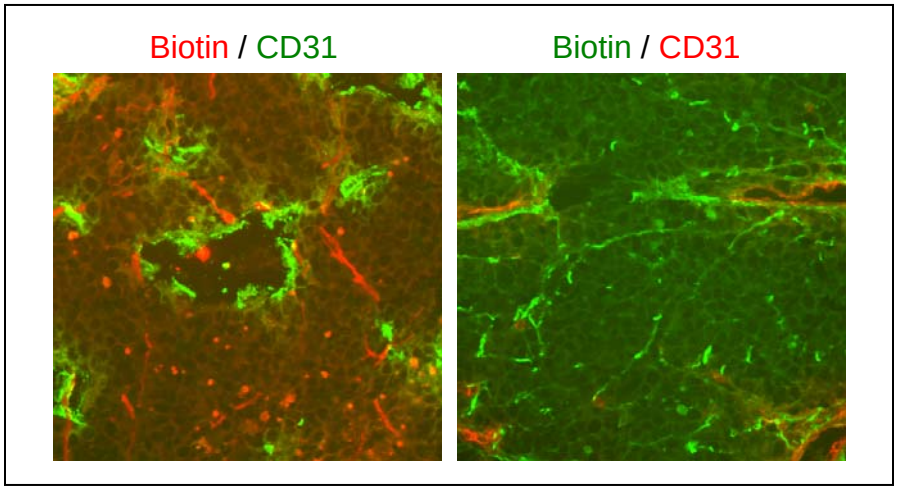

Figure 29. Biotin and CD31 do not co-localize in Ewing's sarcoma. TC71 tumor bearing mice were treated with YW152F or IgG. Immediately after sacrifice, the circulation was perfused with biotin by direct injection into the heart. Immunohistochemistry was performed with **A)** AlexaFlour 594-Streptavidin (red) to identify biotin, and anti-CD31 (green) to identify endothelial cells, or **B)** AlexaFlour 488-Streptavidin (green), to identify biotin and anti-CD31 (red), to identify endothelial cells.

SUMMARY

Experiments presented in this chapter validate and expand upon our previous findings using shDLL4 by using YW152F to inhibit DLL4 expression. Immunohistochemical analysis demonstrated that YW152F treated tumors had significantly reduced numbers of perivascular GFP^+ BM-derived cells as well as significantly reduced numbers of α-SMA^+, $desmin^+$, and $NG2^+$ pericytes/vSMC. This confirms the critical role of DLL4 in pericyte/vSMC formation in Ewing's sarcoma.

The reduction in all three pericyte markers achieved by YW152F treatment was more significant than that achieved by shDLL4 treatment. This is most likely a reflection of more complete and more uniform inhibition of DLL4 by YW152F than by intratumor injection of shDLL4. Interestingly, several of the blood vessels in tumors treated with YW152F maintained a very thin layer of GFP^+, pericyte/vSMC $marker^+$ cells surrounding the endothelial cells. This indicates that even when DLL4 is inhibited, a small number of BM cells are able to adhere to the tumor vasculature, but they do not expand into the thick layers of pericytes/vSMC observed in control tumors during the three weeks that was allowed for tumor growth. The implications of this observation in relation to the mechanistic function of DLL4 in vasculogenesis are discussed in further detail in the Discussion portion of this thesis. It is also possible that the systemic inhibition of DLL4 with YW152F caused BM cell death before the cells reached the tumor site. However, the thin layer of BM-derived perivascular cells in YW152F treated tumors indicates that BM cells were viable when they reached the tumor. An in depth analysis of BM cell viability after treatment with YW152F would be needed to definitely demonstrated that BM cells were not killed in circulation prior to reaching the tumor. Previous experiments using shDLL4 confirmed that even when

DLL4 is only inhibited on BM cells after they have reached the tumor, the participation of BM-derived cells in vasculogenesis is significantly reduced.

In addition to the reduction in BM-derived pericytes/vSMC in YW152F treated tumors, there was a change in the morphology of the endothelial cell portion of vessels. Large, lumen bearing $CD31^+$ vessels were apparent in IgG control treated tumors. In contrast, $CD31^+$ endothelial cells in YW152F treated tumors formed small, punctate structures with few obvious lumens. This change in endothelial cell organization and vessel structure is in agreement with previous reports of increased proliferation of unorganized, non-functional microvessels after DLL4 inhibition [47,58].

The relationship between changed blood vessel morphology and decreased vessel functionality was confirmed by examining hypoxia and blood vessel perfusion. Hypoxia was increased in YW152F treated tumors compared to control, indicating reduced blood vessel functionality.

As was expected, the reduction in blood vessel functionality negatively impacted on tumor growth. The growth of two different Ewing's sarcoma xenograft models, A4573 and TC71, was significantly inhibited *in vivo* after treatment with YW152F compared to IgG control. This indicates that DLL4 may be a novel therapeutic target for the treatment of Ewing's sarcoma.

Chapter 6.

DLL4-Notch signaling plays a role in pericyte/vSMC differentiation: In vitro support

RATIONALE

We have shown that DLL4 is important for BM-derived pericyte/vSMC formation and tumor growth in Ewing's sarcoma using both shDLL4 and YW152F. However, while immunohistochemical analysis provides excellent evidence that when DLL4 is inhibited, the number of BM-derived pericytes/vSMC is reduced, it provides little insight into which part of the vasculogenesis process is controlled by DLL4-Notch signaling.

The process of BM participation in vasculogenesis is complex. BM cells must first migrate to the tumor. We have previously shown that this process is largely mediated by tumor cell secretion of $VEGF_{165}$ [32]. Once BM cells reach the tumor, they must adhere to the vasculature, proliferate, and differentiate. Little is known about which of these processes DLL4-Notch signaling is involved in, particularly in Ewing's sarcoma. To determine whether DLL4-Notch signaling is critical for BM cell differentiation into pericytes/vSMC, in vitro model systems were utilized. In this chapter, co-culture systems with $DLL4^{+}$ feeder layers and whole BM cells were established and DLL4-Notch signaling was manipulated to determine whether the differentiation pathway of BM cells would be altered. Additionally, 10T1/2 mesenchymal cells were used to examine the effects of active Notch signaling on pericyte/vSMC marker expression during the pericyte/vSMC maturation process.

RESULTS

BM cell expression of pericyte markers in vitro is partially DLL4 dependent

We first determined whether DLL4 signaling is necessary for immature BM cells to begin expressing markers of differentiated pericytes/vSMC. SC9-19 embryonic mouse stromal cells, which express DLL4, were used as a feeder layer. Whole BM was collected from the femurs of GFP transgenic mice (thus BM cells were GFP^+) and plated on top of a monolayer of SC9-19 cells. Co-cultured cells were treated with either IgG control or YW152F for one week (5μg/ml, refreshed daily). BM cells were then collected by FACS for GFP^+ cells, and RNA was analyzed by RT-PCR. The pericyte/vSMC markers RGS5 and desmin were reduced (46% and 40%, respectively) in YW152F treated BM cells compared to IgG control (Figure 30a).

We next wished to determine whether DAPT, a γ-secretase inhibitor, which inhibits all Notch receptor signaling, would have an even more profound effect on BM cell differentiation into pericyte-like cells. The co-culture experiment described above was repeated, but this time co-cultured cells were treated daily with either γ-secretase inhibitor (100μM) or YW152F (2.8μg/mL). As expected, treatment with γ secretase inhibitor further reduced the expression of desmin and RGS5 compared to YW152F treated or untreated cells (Figure 30b). RT-PCR for the downstream Notch effector Hey2 showed that while YW152F treatment only partially reduced Hey2 expression (53%), γ-secretase inhibition more completely inhibited Hey2 mRNA expression (97%), implying more complete blockage of the Notch pathway.

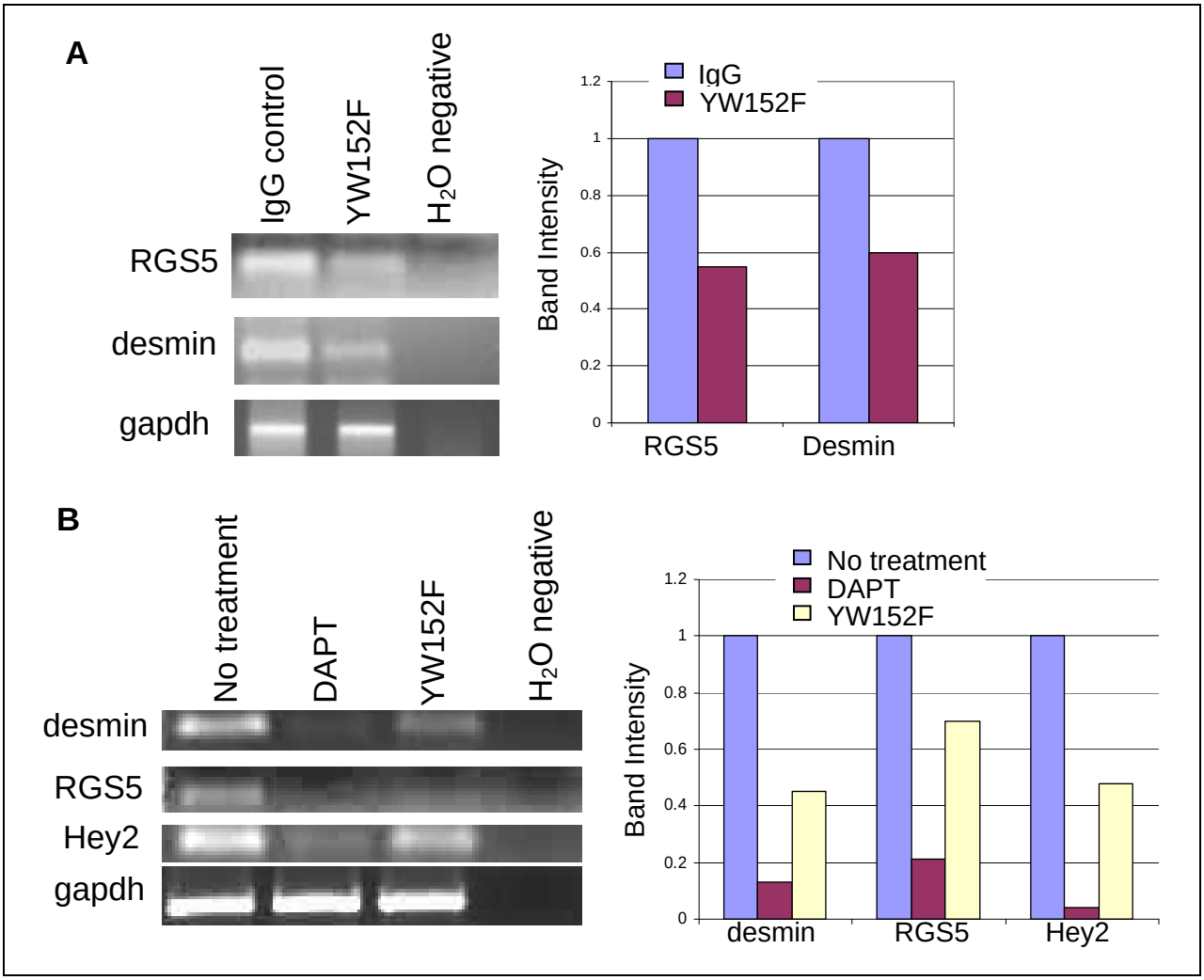

Figure 30. Inhibition of DLL4 or Notch reduces the expression of pericyte markers RGS5 and desmin by BM cells in co-culture. Whole BM was collected from GFP transgenic mice femurs and co-cultured with SC9-19 cells for one week. **A)** Co-cultured cells were treated daily with YW152F or IgG. GFP^+ BM cells were collected by FACS and RT-PCR was performed for RGS5 and desmin. Densitometry quantification was performed. **B)** Co-cultured cells were treated daily with DAPT or YW152F. GFP+ BM cells were collected by FACS and RT-PCR was performed for desmin, RGS5, and Hey2. Densitometry quantification was performed. Experiments were performed three times with similar results; data shown is representative.

Notch regulates expression of pericyte/vSMC markers in 10T1/2 cells

After demonstrating that inhibition of either DLL4 or Notch impairs BM cell expression of pericyte/vSMC markers, we wished to determine whether active Notch

signaling can induce upregulation of pericyte/vSMC markers. 10T1/2 cells, pluripotent mesenchymal cells that can differentiate into pericyte-like cells in culture, were utilized [68].

MigR1-GFP plasmids containing DNMAM (to inhibit Notch signaling), the intracellular domain of Notch 1 (NICD1, to mimic active Notch 1), and Hes1 (a downstream mediator of Notch signaling), were transfected into 10T1/2 cells. Forty eight hours after transfection, RNA was collected and RT-PCR was performed. DNMAM reduced RGS5 mRNA compared to 10T1/2 control (Figure 31a, column 2). Conversely, NICD1 increased expression of all three pericyte/vSMC markers measured: desmin, RGS5, and PDGFR-β (Figure 31a, column 3). Transfection with MigR1-GFP/Hes1 increased expression of desmin, but not RGS5 or PDGFRβ (Figure 31a, column4). The lack of induction of RGS5 or PDGFRβ by Hes1 indicates that another mediator of the Notch pathway, possibly another member of the Hes or Hey family, is responsible for the induction of RGS5 and PDGFRβ mRNA expression. We therefore examined Hes1, Hey1, and Hey2 expression in 10T1/2 cells transfected with MigR1 control, DNMAM, NICD1, DLL4, or Hes1 to determine whether these Notch effectors may be candidates for the regulation of RGS5 and PDGFR-β. Hes1 was constitutively expressed in 10T1/2 cells, even in the presence of DNMAM, and was not increased by NICD1 or DLL4 (Figure 31b). This indicates that Hes1 expression in 10T1/2 cells is regulated by a pathway other than Notch. Hey1 mRNA, and to a lesser extent Hey2 mRNA, was increased in 10T1/2 cells transfected with either NICD1 or DLL4 compared to non-transfected or control transfected cells. Hey1 and Hey2 may be intermediates in the regulation of RGS5 and PDGFRβ by Notch.

To determine whether the induction of pericyte/vSMC marker expression is unique to Notch 1 or can be achieved by the other Notch receptors, MigR1-GFP plasmids containing the intracellular domains of each of the four mammalian Notch receptors (NICD1-4) were transfected into 10T1/2 cells. Forty eight hours after transfection, RNA was collected, RT-PCR and real time PCR was performed. Transfection with each of the four NICDs led to increased RGS5 and desmin expression compared to control MigR1-GFP (Figure 31c). This indicates that active Notch signaling, by either direct or indirect mechanisms, stimulates the expression of pericyte/vSMC markers during the progression from an immature progenitor cell towards a mature pericyte/vSMC.

In addition to the reduction of RGS5 expression described above, MigR1-GFP/DNMAM transfected 10T1/2 cells underwent a dramatic change in phenotype compared to MigR1-GFP control transfected cells. Control cells maintained the parental culture phenotype of elongated, spindle shaped cells while MigR1-GFP/DNMAM transfected cells become rounded and formed clumps on the culture dish (Figure 32). Together with the reduction in expression of RGS5, this rounded morphology indicates a less differentiated state following Notch inhibition.

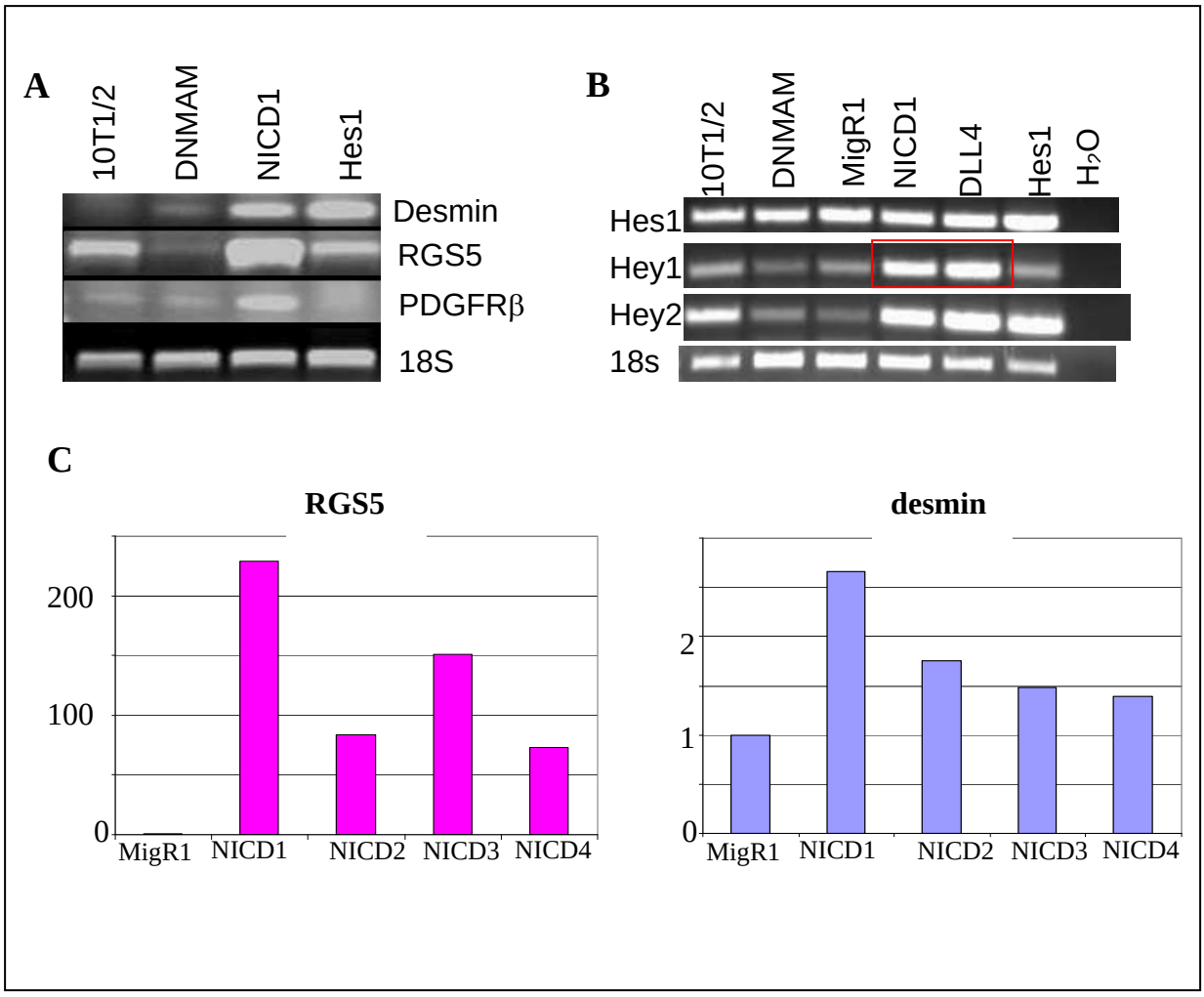

Figure 31. Notch induces pericyte/vSMC marker expression in 10T1/2 cells. 10T1/2 cells were transfected with various MigR1 plasmids. Forty eight hours later, RNA was collected and RT-PCR or real time PCR was performed. **A)** RT-PCR for desmin, RGS5, and PDGFRβ was performed on RNA from 10T1/2 cells transfected with MigR1-GFP/DNMAM, NICD1, or Hes1. **B)** RT-PCR for Hes1, Hey1, and Hey2 was performed on RNA from 10T1/2 cells transfected with MigR1-GFP control, MigR1-GFP/DNMAM, NICD1, DLL4, or Hes1. **C)** Real time PCR for RGS and desmin was performed on RNA from 10T1/2 cells transfected with MigR1-GFP control, MigR1-GFP/NICD1,2,3, or 4. Relative mRNA levels compared to MigR1-GFP control was calculated. Experiments were repeated at least twice with similar results.

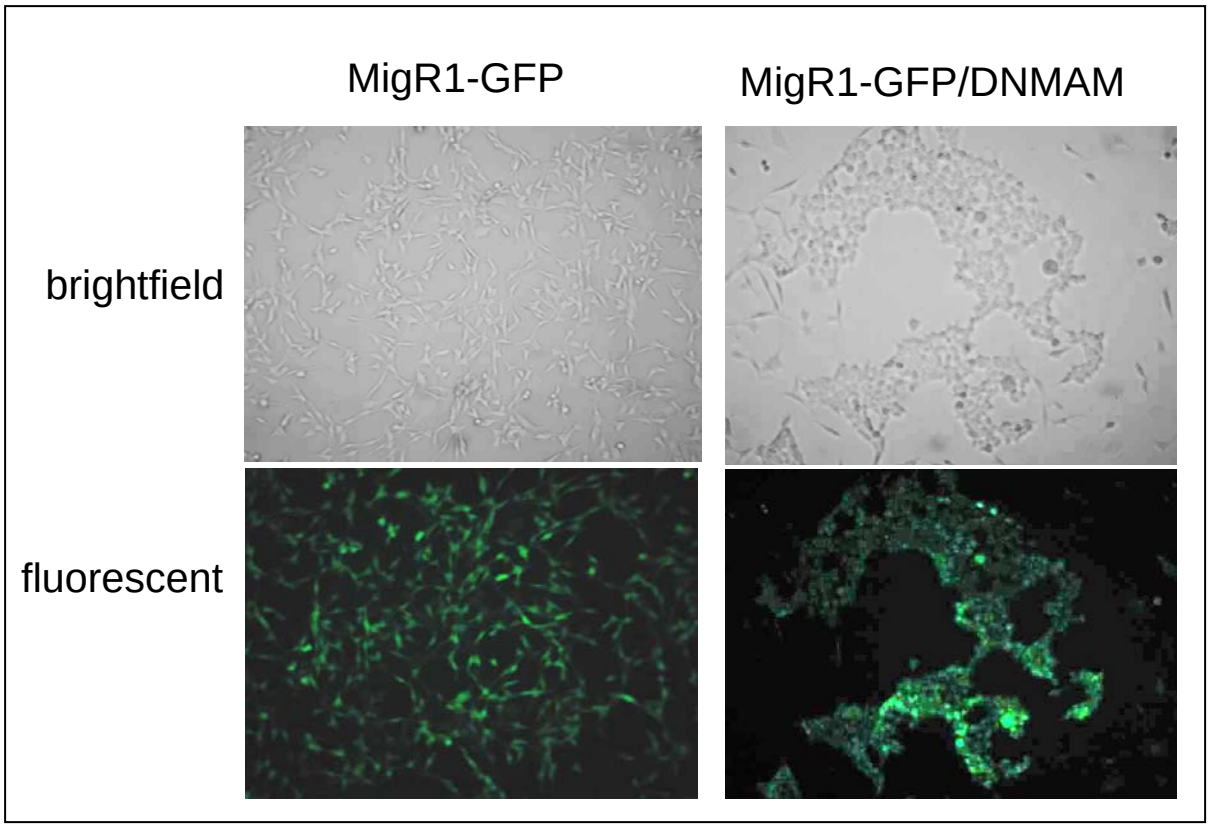

Figure 32. DNMAM changes the morphology of 10T1/2 cells in culture. 10T1/2 cells were transfected with MigR1-GFP or MigR1-GFP/DNMAM. Forty-eight hours later, brightfield and fluorescent microscopy was performed. 10x maginification.

SUMMARY

Co-culture experiments presented here confirm that a portion of whole BM cells cultured on a $DLL4^+$ feeder layer will begin to express the pericyte/vSMC markers RGS5 and desmin, indicating a progression towards pericyte/vSMC maturation. Further, this co-culture system was used to demonstrate that inhibition of DLL4 by YW152F leads to a reduction in expression of RGS5 and desmin by BM cells. This demonstrates that DLL4 is important for the maturation and/or differentiation process as BM-derived cells become pericytes/vSMC.

A second series of co-culture experiments using γ secretase inhibitors and YW152F, demonstrated that DAPT, a γ secretase inhibitor, more effectively reduces the expression of RGS5 and desmin than YW152F. The Notch effector Hey2, which is directly induced by activated Notch receptors, was also more significantly reduced by treatment with the γ secretase inhibitor. One possible explanation for this is that at the doses used the γ secretase inhibitor is more efficient than YW152F, and equal reduction in Notch effector expression as well as equal reduction in RGS5 and desmin might be achieved with increased concentrations of YW152F. A more likely explanation is that in addition to DLL4, other Notch ligands are also involved in the differentiation of BM cells into pericytes/vSMC, and inhibition of DLL4 only inhibits a portion of the Notch signaling needed for the process. This possibility is supported by studies by Doi et al., demonstrating that the Notch ligand Jagged 1 plays an important role in vSMC formation [69].

Experiments performed using 10T1/2 mesenchymal precursor cells further support the finding that DLL4-Notch signaling plays a role in the regulation of

expression of pericyte markers. The active domain of each Notch receptor as well as the Notch inhibitor DNMAM was transfected into 10T1/2 cells. Each NICD increased RGS5 and desmin mRNA, indicating progression towards pericytes/vSMC. Conversely, when Notch was inhibited in 10T1/2 cells by DNMAM, RGS5 mRNA was reduced, and the cells changed from an elongated, spindle shaped morphology to a rounded, clumped morphology. Together, the reduction in RGS5 with the rounded morphology is indicative of a reversion to a less differentiated state when Notch signal is inhibited.

Taken together, our findings using a co-culture system and 10T1/2 cells demonstrate a role for Notch signaling in the regulation of expression of the pericyte markers RGS5 and desmin at the mRNA level. This indicates that Notch signaling is involved in the maturation of pericyte progenitor cells into pericytes/vSMC, and supports our *in vivo* finding of reduced numbers of pericytes/vSMC when DLL4 is inhibited.

In the canonical Notch signaling pathway, NICD translocates to the nucleus where it becomes part of a transcriptional activating complex. The complex then induces expression of Notch effector proteins, such as Hes and Hey family members, which are themselves transcription factors. These Notch effectors then regulate the expression of downstream Notch targets. We demonstrated that when 10T1/2 cells are transfected with MigR1-GFP/Hes1, the Notch effector Hes1 induces increased mRNA levels of desmin but not RGS5 or PDGFR-β, indicating that other Notch effectors may also be involved in transducing the Notch signal to induce expression of pericyte/vSMC markers. We demonstrated upregulation of Hey1 and Hey2 by NICD1 and DLL4 in 10T1/2 cells. This indicates that these Notch effectors may be involved in pericyte/vSMC differentiation

and/or maturation. Further study of the individual roles of Hey1, Hey2 and other Notch effectors during pericyte/vSMC maturation is warranted.

Interestingly, the above experiments were performed *in vitro* without Ewing's sarcoma cells present. This demonstrates that Notch partially regulates BM cell maturation into pericyte/vSMC maturation even outside of the Ewing's sarcoma environment. These studies may therefore have more broad implications regarding the role of Notch signaling in pericyte/vSMC formation and differentiation in other tumors or in vasculogenesis in normal tissue.

It is important to note that DLL4-Notch signaling may be involved in more than one step of BM cell participation in vasculogenesis. While the findings presented here support a role for Notch signaling in BM cell to pericyte/vSMC differentiation and/or maturation, they do not support nor refute a role for DLL4-Notch signaling in BM-derived cell adhesion to vessels or in pericyte/vSMC proliferation.

Chapter 7.

Discussion

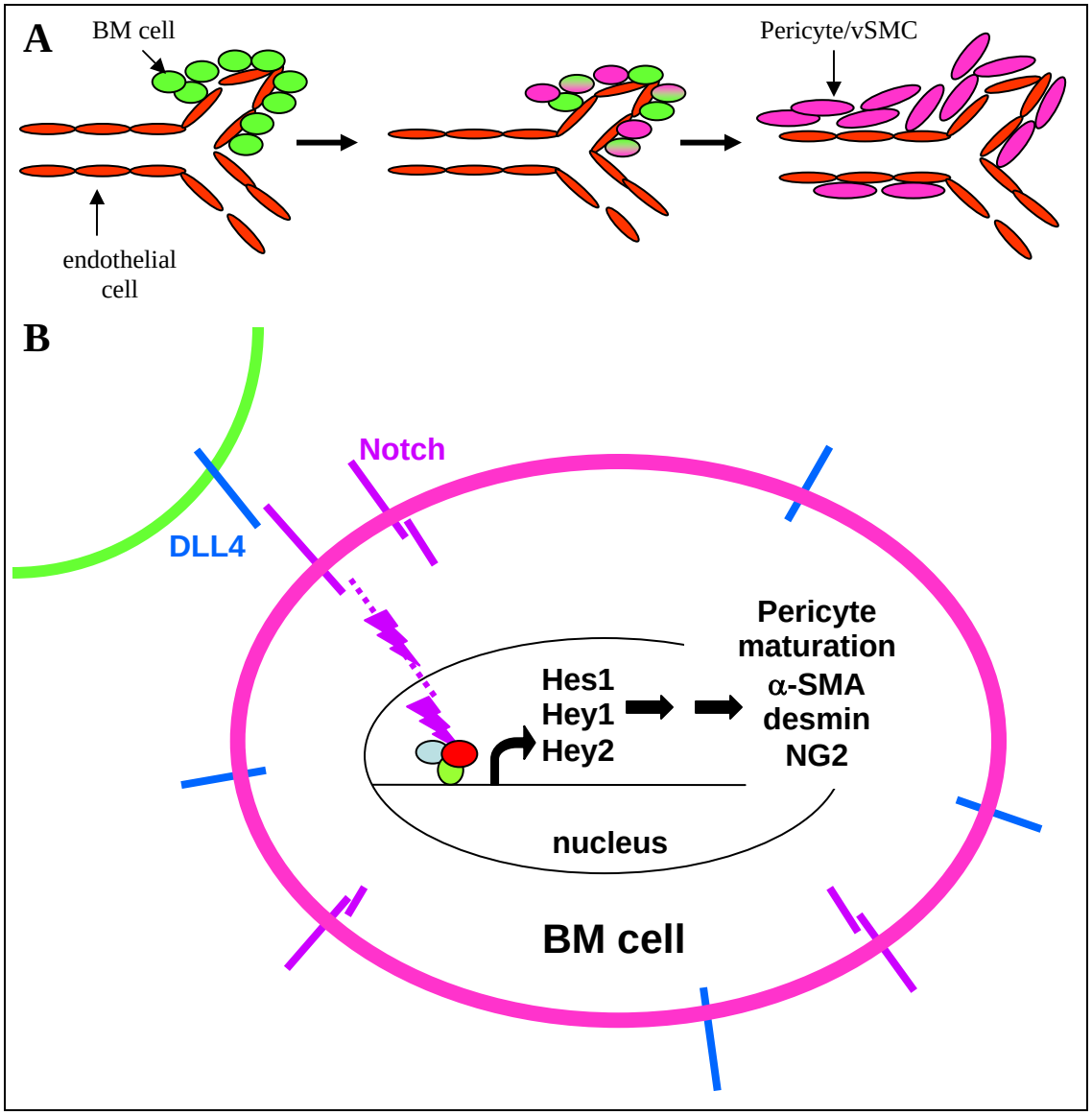

Figure 33. Proposed model of DLL4-Notch signaling during BM cell maturation into pericytes/vSMC. A) Schematic diagram of BM cell participation in vasculogenesis. Immature BM cells (green) migrate to the tumor and adhere to sites of developing blood vessels. After a BM cell has reached the vessel wall, DLL4 on one BM cell activates Notch receptors on neighboring BM cells, signaling the immature BM cells to activate pericyte/vSMC maturation pathways and differentiate into pericytes/vSMC (pink cells). **B)** Intracellular signaling. When DLL4 binds to Notch receptor on a neighboring BM cell, the receptor is cleaved and NICD (purple lightning bolt) translocates to the nucleus where it forms a transcriptional activating complex including MAML, RBP-Jk, and CBP/300. The complex induces transcription of Notch effectors of the Hes and Hey family, which are themselves transcription factors. The Notch effectors then either directly or indirectly induce expression of pericyte/vSMC markers α-SMA, desmin, RGS5, NG2 and PDGFRβ during the pericyte maturation process.

We have previously used various mouse BM transplant models to demonstrate that BM-derived cells contribute to vascular development in Ewing's sarcoma by differentiating into both endothelial cells and pericytes/vSMC [63,70-72]. We further demonstrated that vasculogenesis is essential for the growth of Ewing's sarcoma *in vivo*. This was done by selectively inhibiting vasculogenesis but not angiogenesis, which resulted in small, avascular tumors [62]. The first step in vasculogenesis, migration of BM cells to the tumor, is largely mediated by the chemoattractant properties of $VEGF_{165}$ [70,71]. The molecular signals that contribute to the regulation of BM cell differentiation into pericytes/vSMC are poorly understood. Here, we demonstrated for the first time a critical role for DLL4-Notch signaling in BM cell differentiation into pericytes/vSMC during vasculogenesis in Ewing's sarcoma. The inhibitory role of DLL4-Notch signaling in endothelial cell proliferation and vessel sprouting during angiogenesis is well established. However, we are the first to demonstrate a role for DLL4 in regulating BM-derived pericyte/vSMC formation during vasculogenesis. We are also the first to demonstrate that inhibiting DLL4 inhibits the growth of Ewing's sarcoma *in vivo*, indicating that DLL4 may be a therapeutic target for the treatment of patients with Ewing's sarcoma.

DLL4 expression by BM-derived pericytes/vSMC in Ewing's sarcoma

Previously, DLL4 expression by endothelial cells in blood vessels of developing tissues as well as in several tumor models has been reported. While DLL4 expression during physiologic blood vessel development, for example in the developing retina, is restricted only to endothelial tip cells at the growing vessel front, endothelial cells along the length of the vessel express DLL4 in several tumors, for example, in S180 sarcomas in mice [59,73]. We therefore expected to find DLL4 expression by endothelial cells in

Ewing's sarcoma. Surprisingly, in addition to a few $DLL4^+$ $CD31^+$ endothelial cells, DLL4 was expressed by BM-derived pericytes/vSMC in Ewing's sarcoma vasculature. Several thick layers of $DLL4^+$ cells were observed in two xenograft models of Ewing's sarcoma, TC71 and A4573. We are the first to report expression of DLL4 by perivascular cells in tumor vasculature. We therefore confirmed the DLL4 expression pattern using a second anti-DLL4 antibody.

The relevance of this finding to the human disease was confirmed by immunohistochemistry on human Ewing's sarcoma tumor specimens, where 12 of 14 patient samples had similar $DLL4^+$ perivascular layers. The perivascular location and the histology of the cells on the adjacent hematoxylin and eosin stained sections suggests that the $DLL4^+$ cells are pericytes/vSMC. However, we could not perform dual staining on the patient samples to confirm that $DLL4^+$ cells are pericytes/vSMC due to limitations of immunohistochemical staining on paraffin embedded sections.

We have previously demonstrated that the majority of blood vessels in Ewing's sarcoma are surrounded by thick layers of BM-derived pericytes/vSMC that express PDGFRβ, α-SMA, and desmin [63]. Here, we demonstrated that DLL4 co-localizes with the pericyte/vSMC markers desmin and α-SMA, suggesting that the $DLL4^+$ cells are pericytes/vSMC. In the DLL4 and desmin double-stained tumor sections, the vast majority of $DLL4^+$ cells were also $desmin^+$. However, there were several $desmin^+DLL4^-$ cells present, suggesting that not all $desmin^+$ pericytes/vSMC express DLL4. DLL4 and α-SMA co-localized to a lesser extent than DLL4 and desmin. Several $DLL4^+$α-SMA^- cells were present, and vice versa, several α-SMA^+DLL4^- cells were also present. This suggests that some α-SMA^+ pericytes/vSMC do not express DLL4 and some $DLL4^+$ cells

do not express α-SMA. Taken together, the finding of desmin$^+$ and α-SMA$^+$ cells that do not express DLL4 suggests that there is a pericyte/vSMC population present in Ewing's sarcoma tumors that are DLL4$^-$.

The pericytes/vSMC in Ewing's sarcoma are a mosaic of locally derived and BM-derived cells [33]. We used a GFP BM transplant model to demonstrate that DLL4 expression extensively co-localizes with GFP$^+$ BM-derived cells in Ewing's sarcoma (greater than 90% co-localization). One possible explanation for the near complete co-localization of DLL4 with GFP but only partial co-localization of DLL4 with pericyte/vSMC markers is that DLL4 is expressed by BM-derived pericytes/vSMC but not locally derived pericytes/vSMC. To confirm this, flow cytometry could be performed on homogenized tumors from GFP BM transplanted mice to determine the percentage of GFP$^-$ (non-BM-derived) but desmin$^+$ or α-SMA$^+$ (pericyte/vSMC) and DLL4$^+$ cells present. If non-BM derived pericytes/vSMC do not express DLL4, then we would expect to see few or no pericyte/vSMC that are DLL4$^+$ but GFP$^-$.

Though novel and therefore surprising, our demonstration of DLL4 expression by BM-derived pericytes/vSMC has recently been supported by evidence of DLL4 expression by other non-endothelial cell types. For example, DLL4 is expressed by neoplastic goblet cells in colon cancer, normal endometrial epithelial and stromal cells, thymic epithelium, and regulatory T cells [74-76].

The extensive number of GFP$^+$ BM-derived cells surrounding CD31$^+$ endothelial cells is somewhat unique to Ewing's sarcoma, and suggests that in addition to pericytes/vSMC, BM-derived cells may be contributing to other cell populations within the tumor. While a small portion of the GFP$^+$ BM-derived cells in Ewing's sarcoma are

macrophages and monocytes ($F4/80^+$ or $CD14^+$), the majority are not. The GFP^+ macrophages and monocytes are spread throughout the tumor and do not make up the bulk of perivascular BM-derived cells [30].

Another possibility is that a portion of the perivascular GFP^+ cells are fibroblasts. Fibroblasts can be BM-derived, can be in perivascular locations, and can express several of the same markers as pericytes/vSMC [77]. Immunohistochemistry for the fibroblast marker S100A4 demonstrated that fibroblasts are present in Ewing's sarcoma tumors. However, the fibroblasts are spread throughout the tumor mass. The majority of $CD31^+$ blood vessels had no or very few perivascular fibroblasts surrounding them. Co-staining for GFP, to identify BM-derived cells, and S100A4, to identify fibroblasts, demonstrated that the majority of BM-derived cells within TC71 tumors are not fibroblasts.

The role of Notch in BM cell participation in vasculogenesis

After demonstrating DLL4 expression by BM-derived pericytes/vSMC, we sought to determine what role DLL4-Notch signaling might play in BM cell participation in vasculogenesis. While BM-derived pericytes/vSMC have been observed in several different physiologic and pathologic settings, such as in the retinal and femoral arteries after injury and in the vasculature of glioblastomas, little is known about the molecular signals that direct the formation of BM-derived pericytes/vSMC postnatally [42,78,79]. The expression of DLL4 by BM-derived pericytes/vSMC in Ewing's sarcoma suggests that DLL4-Notch signaling might be involved in this process.

Inhibition of DLL4 causes hyperproliferation of unorganized, non-functional microvessels. These vessels are immature as determined by their lack of pericyte/vSMC coverage and lack of blood perfusion. A correlation between DLL4 expression and α-

SMA^+ cell coverage in bladder cancer and lymphomas has been demonstrated [47,60]. There are several possible explanations for why the loss of the DLL4 signal leads to the proliferation of immature vessels that lack pericyte coverage. One possibility is that the endothelial cells are proliferating so rapidly that pericytes/vSMC can not keep up. In this case, endothelial cells can be imagined in two states: An immature state, where proliferation and sprouting are active and therefore pericyte recruitment signals are downregulated by endothelial cells, and a mature state, where endothelial cell proliferation is stopped and pericytes/vSMC are recruited. In this model, the role of DLL4-Notch signaling is simply to induce a mature, quiescent state of endothelial cells, allowing for pericyte coverage. This model is supported by the role of DLL4-Notch1 in tip vs. stalk cell identity. DLL4 stimulation of Notch1 is necessary for endothelial cells to assume the stalk cell phenotype. When either DLL4 or Notch1 is inhibited, endothelial cells proliferate excessively *in vitro* and extend filopodia (indicating tip cell phenotype) *in vivo* [52,53]. This indicates that the loss of DLL4 causes endothelial cells to enter into a proliferative state where pericytes/vSMC are not recruited to the vessel.

Another possibility is that in addition to the need for endothelial cells to be in a quiescent, mature state, Notch signaling directly informs immature pericyte precursor cells to adhere to sites of developing vasculature, proliferate, and/or differentiate into pericytes/vSMC. This model is supported by the phenotype of Notch3 knockout mice. The arteries in these mice are enlarged and have reduced pericyte/vSMC coverage, but do not display increased branching or sprouting [45]. This indicates defective pericyte/vSMC formation without hyperproliferation of endothelial cells. Regulation of pericyte/vSMC coverage independent of endothelial cell proliferation is suggested by this phenotype. It is

important to note that these two possible models are not mutually exclusive; a reduction in pericyte/vSMC coverage of vessels in the absence of DLL4 could be due in part to a prolonged immature, hyperproliferative state of endothelial cells and in part to a direct role for Notch signaling in BM cell differentiation into pericytes/vSMC. Little is understood about which of these two models, if either, DLL4-Notch signaling regulates.

After determining that DLL4 is expressed by BM-derived pericytes/vSMC in Ewing's sarcoma, and with both of the above mentioned models in mind, we hypothesized that the DLL4 expressed by BM cells activates Notch receptors on surrounding BM cells during the process of maturation from immature BM cell to pericyte/vSMC. This hypothesis assumes that DLL4-Notch signaling is involved in pericyte/vSMC differentiation or maturation independently of the endothelial cell proliferative state. In support of this hypothesis, immunohistochemical evaluation of TC71 tumors from mice that had received GFP BM transplants revealed similar patterns of GFP, DLL4, and NICD1 on adjacent tumor sections. Additionally, GFP^+ BM-derived cells isolated from TC71 tumors expressed DLL4 and the Notch effector Hes1, Hey1, and Hey2 mRNA, as demonstrated by RT-PCR and real time PCR. Expression of these Notch effectors indicates active Notch signaling. Together, these data indicate that Notch receptors are active in BM-derived cells within Ewing's sarcoma tumors.

MigR1-GFP/DNMAM was used to inhibit Notch signaling in BM cells, and BM transplants were performed. Tumors from mice with MigR1-GFP/DNMAM BM had dramatically reduced perivascular BM cells compared to control. This indicates that without the ability to receive Notch signals, BM cell adherence to developing vessels and/or differentiation into pericytes/vSMC is severely inhibited. Another possibility is

that the expression of DNMAM in BM cells was toxic and reduced the number of viable BM-derived pericyte precursor cells prior to the cells reaching the tumor. Mice received MigR1-GFP/DNMAM BM transplants one month prior to injection of tumor cells, and no toxicity was observed. Mice remained healthy and active throughout the duration of the experiment. If extensive BM cell toxicity had occurred due to expression of DNMAM, we would expect to have seen some indication in the health of the mice. However, to definitely disprove the possibility of BM cell death prior to reaching the tumor due to DNMAM, extensive evaluation of the whole mouse BM would need to be performed at the end of the experiment.

Recently, Doi et al. reported high expression of Notch3 and Jagged1 by BM-derived α-SMA$^+$ vSMC in the neointima of the femoral artery after wire injury in mice [42]. However, they did not examine whether this high expression of Notch3 plays a functional role in vSMC formation. Our demonstration of reduced numbers of perivascular BM-derived cells in tumors from mice that had received DNMAM BM transplants suggests that the expression of Notch receptors and the ability of BM cells to receive the Notch signal is functionally important for BM-derived pericyte/vSMC formation.

A role for DLL4 in BM-derived pericyte/vSMC formation *in vivo*

DLL4 inhibition in several tumor models, including breast, colon, and lung cancer, correlated with a decrease in α-SMA$^+$ cell coverage and decreased vessel functionality, ultimately inhibiting tumor growth. However, this decreased vessel functionality has previously been attributed to excessive angiogenic sprouting of endothelial cells. The role of DLL4 in vasculogenesis specifically has not been studied. Due to the high number of BM-derived pericytes/vSMC and the essential role of

vasculogenesis in Ewing's sarcoma tumor growth, Ewing's sarcoma is a unique model for the study of the role of DLL4 in blood vessel formation by the process of vasculogenesis. Studies of the role of DLL4 in vascular formation and tumor growth in Ewing's sarcoma have not been previously reported.

We used two different methods to inhibit DLL4 signaling, shDLL4 and YW152F, to confirm and expand upon findings in other tumor models. While a reduction in α-SMA$^+$ cells after DLL4 inhibition has been reported, evaluation of other pericyte/vSMC markers after DLL4 inhibition has not been previously evaluated. To our knowledge, we are the first to extensively evaluate the effects of DLL4 inhibition on BM-derived cell participation in vascular development and pericytes/vSMC formation using multiple pericyte/vSMC markers. Inhibition of DLL4 using either shDLL4 or YW152F significantly decreased the number of BM-derived pericytes/vSMC in Ewing's sarcoma tumors. This was demonstrated by immunohistochemical evaluation of GFP (to identify BM-derived cells), desmin, NG2, and α-SMA (to identify pericytes/vSMC). GFP$^+$ BM-derived cells and expression of all three pericyte/vSMC markers were significantly decreased in YW152F treated tumors. In shDLL4 treated tumors, GFP expression was not quantified although the reduction was visually apparent. Desmin and α-SMA were significantly decreased, and the reduction in NG2 bordered significance. The greater reduction in BM-derived pericytes/vSMC by treatment with YW152F compared to shDLL4 is probably due to the more complete suppression of DLL4 signaling afforded by systemic delivery of YW152F. In the shDLL4 model, DLL4 expression was not equally downregulated throughout treated tumors; regions of each tumor still had some

DLL4$^+$ cells. In the vessels where DLL4 remained, so did the BM-derived pericytes/vSMC.

In addition to a reduction in BM-derived pericyte/vSMC coverage, the CD31$^+$ vessel morphology was altered in tumors of YW152F treated mice. Blood vessels in control tumors were elongated, well-organized, and often had visible lumens. CD31$^+$ structures in YW152F treated tumors, however, were often small, punctate, and non-lumen bearing. This observation is in agreement with prior observations by several labs, including Scehnet et al., who demonstrated that treatment of HT29 colon carcinoma xenografts with soluble DLL4 (dominant negative DLL4) leads to "decreased or absent vascular lumen"[59]. We further demonstrated that the change in vascular morphology correlates with a decrease in blood vessel functionality. Hypoxia was significantly increased in shDLL4 and YW152F treated tumors compared to controls. Presumably, increased hypoxia is due to reduced delivery of oxygenated blood to tumor cells and is representative of decreased vessel functionality.

Most importantly, the change in vessel morphology and reduced vessel functionality due to inhibition of DLL4 by YW152F correlated with a significant inhibition of tumor growth in both TC71 and A4573 xenograft models. This inhibition was not due to a direct effect of the antibody on tumor cell viability or proliferation; YW152F did not affect TC71 or A4573 viability or proliferation *in vitro*. Taken together, these studies indicate that the inhibition of DLL4 leads to a reduction in the number of BM-derived pericytes/vSMC and fewer large lumen-bearing vessels, which impairs blood vessel functionality and ultimately inhibits tumor growth in Ewing's sarcoma.

We have previously demonstrated that inhibition of vasculogenesis in Ewing's sarcoma inhibits tumor growth [62]. However, this was done by genetic manipulation of BM cells to prevent their migration to the tumor and therefore did not represent a therapeutically relevant method of inhibiting vasculogenesis. Our demonstration of tumor growth inhibition by treatment with YW152F indicates that DLL4 could be a therapeutic target for the treatment of patients with Ewing's sarcoma.

DLL4-Notch: Role in BM cell differentiation into pericytes/vSMC during vasculogenesis

Our *in vivo* data does not clearly distinguish which step of the vasculogenesis process DLL4-Notch signaling is important for: BM cell adhesion to the endothelial cells of developing vasculature, migration to the extra-luminal side of vessels, proliferation, or differentiation into pericytes/vSMC. Caiado et al. recently demonstrated a role for Notch in BM cell adhesion at sites of developing vasculature. $Lin^{-}Sca1^{+}$ BM cells treated with γ-secretase inhibitor displayed a reduced ability to bind to extracellular matrix components *in vitro*, and a decreased capacity to participate in wound healing *in vivo*[80].

Interestingly, in our work, many of the vessels in YW152F treated tumors had a very thin layer of GFP^{+} BM-derived pericytes/vSMC. This seems to indicate that incoming BM-cells are able to adhere to the vessel wall, extravasate and even begin expressing pericyte/vSMC markers, but at a significantly reduced rate compared to control tumors. One explanation for this is that even when DLL4 is inhibited by YW152F other Notch ligands, possibly DLL1, expressed by endothelial cells, or Jagged1, expressed by endothelial and vSMC, are able to partially compensate for the loss of DLL4. In that case, our data can be reconciled with Caiado's demonstration of reduced

BM cell adhesion by treatment with a γ-secretase inhibitor because the reduced adhesion may be due to inhibition of signaling by another Notch ligand [49,80,81].

In support of a role for DLL4 in the stimulation of immature BM-derived cells to begin differentiating toward a pericyte/vSMC fate, YW152F dramatically reduced expression of RGS5 and desmin mRNA by BM cells in co-culture *in vitro*. Treatment with DAPT, a γ-secretase inhibitor and pan Notch inhibitor, more completely reduced mRNA levels of RGS5 and desmin. Further, the Notch effector Hey2 mRNA was reduced roughly 50% by YW152F but greater than 95% by DAPT. Hey2 is a downstream target of active Notch signaling and is a surrogate marker for Notch pathway activation. The remaining Hey2 after YW152F treatment indicates that another Notch ligand is stimulating Notch receptors in the absence of DLL4 stimulation, and this stimulation is inhibited further by pan Notch inhibition with a γ-secretase inhibitor.

Inhibiting DLL4 or Notch receptor activation in BM cells in co-culture reduced pericyte/vSMC marker expression. To compare the effects of Notch inhibition to stimulation of the Notch pathway, we introduced DNMAM, NICD1, or Hes1 into 10T1/2 mesenchymal precursor cells. While DNMAM reduced RGS5 mRNA, NICD1 increased desmin, RGS5, and PDGFR-β mRNA expression. This demonstrates a stimulatory effect of Notch signaling for pericyte/vSMC differentiation. Our data is supported by evidence from Jin et al demonstrating that both NICD1 and NICD3 induce PDGFR-β upregulation by vSMC *in vitro* [82].

Interestingly, while NICD1 increased RGS5, desmin and PDGFR-β in 10T1/2 cells, Hes1 only increased desmin mRNA. This implies that either Notch directly induces desmin and PDGFR-β expression (by binding directly to the gene's promoter and

bypassing Notch effectors), or other Notch effectors are involved. Jin et al demonstrated binding of NICD1 to the PDGFR-β promoter, indicating direct regulation of PDGFR-β by Notch1 [82]. However, the mechanism by which Notch stimulates RGS5 and desmin upregulation is unknown. We demonstrated increased Hey1 and Hey2 expression in 10T1/2 cells following transfection with NICD1 and DLL4 plasmids. Hey1 or Hey2 may therefore be intermediate mediators of Notch regulation of RGS5 and desmin expression.

We are the first to demonstrate increased RGS5 and desmin expression by NICD1 and to confirm NICD1 upregulation of PDGFR-β in 10T1/2 cells. Previously, Notch3 stimulation of pericyte/vSMC maturation has been indicated by the demonstration that Notch3 upregulates α-SMA expression [83]. However, to our knowledge, an examination of the activity of all four Notch receptors during pericyte/vSMC differentiation and/or maturation in the same model system has not been reported. Transfection of 10T1/2 cells with each of the four active Notch receptors, NICD1-4, increased expression of RGS5 and desmin. It is important to note that the relative potency of one receptor compared to another cannot be evaluated in this assay because the transfection efficiency of each MigR1-GFP/NICD plasmid into the 10T1/2 cells was not equal. This assay is therefore qualitative, and demonstrates that each of the four Notch receptors has the capacity to induce increased mRNA expression of RGS5 and desmin in 10T1/2 cells.

Conclusion

DLL4-Notch signaling is critical for the formation of BM-derived pericytes/vSMC. Due to this critical role of DLL4, DLL4 is essential to the process of vasculogenesis and the formation of functional vasculature in Ewing's sarcoma, and is thus essential for Ewing's sarcoma tumor growth.

We have demonstrated:

1. DLL4 is expressed by BM-derived pericytes/vSMC in Ewing's sarcoma.

This was demonstrated in 12 out of 14 patient samples and in TC71 and A4573 xenograft models.

2. DLL4 is critical for the formation of BM-derived pericytes/vSMC in Ewing's sarcoma.

This was demonstrated by inhibition of DLL4 using shDLL4 and YW152F in both T7C1 and A4573 models. Pericytes/vSMC were identified by using immunohistochemistry for α-SMA, NG2, and desmin.

3. DLL4 is a valid therapeutic target for the treatment of Ewing's sarcoma.

This was demonstrated by treating TC71 or A4573 tumor bearing mice with YW152F or IgG control. YW152F significantly inhibited the growth of both tumor models.

4. Notch signaling regulates the expression of the pericyte/vSMC markers RGS5, desmin, and PDGFR-β *in vitro*.

This was demonstrated by co-culturing whole BM cells with SC9-19 cells in the presence of YW152F or IgG. It was further demonstrated by transfecting the

Notch intracellular domains into 10T1/2 cells and measuring the expression of pericyte/vSMC markers.

FUTURE DIRECTIONS

Determining how Notch regulates pericyte/vSMC marker expression

We have demonstrated that the Notch effectors Hes1, Hey1, and Hey2 are present in GFP^+ BM cells isolated from TC71 tumors. We also demonstrated that each of the NICDs can induce expression of the pericyte/vSMC markers RGS5 and desmin in 10T1/2 mesenchymal precursor cells. However, the mechanism by which NICD induces this increase in pericyte/vSMC marker expression is largely unknown. In the canonical Notch signaling pathway, Notch receptor activation can lead to expression of multiple Notch effectors, including Hes and Hey family members, which may then directly or indirectly regulate RGS5 and desmin expression. A role for Hes1 and HeyL, for example, is suggested by work Liu et al, demonstrating that co-culture of endothelial cells and human smooth muscle cells led to increased expression of Hes1 and HeyL in smooth muscle cells [83]. The authors did not determine the functional effect of Hes1 or HeyL upregulation. To determine whether a Hes or Hey transcription factor is involved in Notch regulation of desmin and RGS5 expression, transfection of 10T1/2 cells with MigR1/Hes or MigR1/Hey constructs could be used. Individual MigR1/Hes (Hes 1,2,4,5) or MigR1/Hey(1,2,L) would be transfected into 10T1/2 cells. Forty-eight hours later, RNA would be collected and analyzed by RT-PCR for changes in expression levels of RGS5, PDFR-β and desmin. If the amount of RGS5, PDGFR-β or desmin increases after transfection with one of the Notch effectors, that indicates a potential role for that effector as a specific intermediate in the stimulation of pericyte/vSMC maturation by Notch. If there is no change in the expression of pericyte/vSMC markers after

transfection with a particular Hes or Hey, then that Hes or Hey is probably not an intermediate in the pericyte/vSMC regulatory pathway by Notch.

Other non-canonical mechanisms may also mediate Notch regulation of pericyte/vSMC differentiation. For example, NICD can directly bind to gene promoters to induce transcription. In human aortic smooth muscle cells, the NICD1-RBP-Jk complex can directly bind to the α-SMA promoter and induce gene expression *in vivo*, and in vSMC, NICD1 can bind to the PDGFR-β promoter [82,84]. To determine whether a NICD is able to directly bind to the promoter of RGS5 or desmin, ChIP assays could be employed using antibodies for each of the individual Notch intracellular domains and primers specific for the promoter regions of RGS5 or desmin. 10T1/2 cells could be transfected with either MigR1 control or MigR1/NICD1,2,3, or 4. Forty eight hours later, ChIP assay would be performed to determine whether any of the NICDs are bound to the promoters of RGS5 or desmin. If an NICD is bound to the promoter of either RGS5 or desmin, that indicates that regulation of the gene by Notch signaling may be directly through the Notch receptor without intermediate Notch effectors.

Translational Applications of DLL4 inhibition

We have demonstrated that DLL4 inhibition by either shDLL4 or the monoclonal antibody YW152F significantly inhibits Ewing's sarcoma growth *in vivo*. This suggests that DLL4 may be a valid therapeutic target for the treatment of Ewing's sarcoma. A monoclonal anti-DLL4 antibody, REGN421, has been developed by Regeneron Pharmaceuticals. A multiple-ascending-dose phase I trial to determine the safety and tolerability of REGN421 is currently underway. Adult patients with advanced solid malignancies are included in the patient population that can participate in the study, with

specific eligibility criteria. Plans for a pediatric trial of REGN421 at St. Jude Children's Hospital (Memphis, TN) are currently being developed. The phase I testing of REGN421 in conjunction with our demonstration of the efficacy of the DLL4 neutralizing antibody YW152F against Ewing's sarcoma is exciting. However, there are several factors to be considered and further experimentation is needed to determine whether anti-DLL4 therapy is appropriate for the treatment of pediatric patients with Ewing's sarcoma.

Post-YW152F effects

In both the shDLL4 and YW152F treatment schemas presented in this dissertation, treatment was begun five days after tumor inoculation and mice were sacrificed within three days of the final treatment. We have demonstrated that during a three or four week period where shDLL4 or YW152F is administered regularly, tumor growth is significantly inhibited. However, particularly when a therapy is to be used in a pediatric population, the long term effects after cessation of therapy must be understood. It is therefore important to understand both immediate effects after cessation of therapy and what, if any, permanent toxicity is associated with anti-DLL4 therapy.

The most pertinent concern about immediate effects after cessation of anti-DLL4 therapy is the possibility of a rebound in tumor growth. To determine whether Ewing's sarcomas are likely to rebound rapidly after cessation of anti-DLL4 therapy, an experimental schema similar to the one used in chapter five could be utilized. Tumor bearing mice would be treated twice weekly with i.v. YW152F or IgG for several weeks. After the final treatment, mice would be allowed to live until the tumor burden is too great for the animal. Tumor volume would be followed throughout the duration of the experiment, from first treatment until sacrifice. The tumor volume growth curves would

then be analyzed to determine whether the tumor growth rate decreased, stayed the same, or increased after cessation of YW152F treatment.

In addition to the possibility of immediate tumor rebound, the possibility of long term toxic effects of YW152F therapy must also be considered. Initially, DLL4 was believed to be expressed only by endothelial tip cells in actively sprouting vessels of growing tissues or tumors, and was therefore expected to be a relatively tumor specific target. However, DLL4 is now known to be expressed in the thymus and important for T cell maturation. This indicates a potential risk for a severely compromised immune system when DLL4 is systemically inhibited in patients. Further, Yan et al recently demonstrated pathologic changes in the livers of mice, rats, and monkeys after 8 or 12 weeks of YW152F therapy. Long term YW152F treatment caused dilation of centrilobular hepatic sinusoids, bile ductular proliferation, and atrophy of centrilobular hepatic cords. No lethality occurred due to these changes; the animals were sacrificed after 12 weeks in the experimental design[85]. Whether the observed liver toxicity is permanent or reversible after cessation of therapy remains to be determined.

The observed liver pathology serves as a warning of possible unforeseen toxicity using anti-DLL4 therapy. However, the method of inhibiting DLL4 may affect the toxicity caused; inhibition of DLL4 with YW152F may have greater toxicity, for example, than DLL4 inhibition by REGN421, the DLL4 targeting antibody currently in Phase I trials. One purpose of a Phase I trial is to determine toxicity of the therapy. Careful attention should be given to any reports of adverse side effects generated by use of REGN421 in the adult population before anti-DLL4 therapy is tested in pediatric patients.

Targeting VEGF and DLL4 in Combination Studies

VEGF and DLL4 are key regulators of vessel development during both physiologic and pathologic conditions. The essential role of both molecules is demonstrated by the fact that VEGF and DLL4 are the only two known proteins involved in vascular development for which haploinsufficiency is embryonically lethal [61]. VEGF stimulates endothelial cell proliferation and sprouting; DLL4 inhibits these processes. VEGF can be imagined as the gas that increases vascular growth while DLL4 is the brake that stops vessel branching and growth. A precise balance between VEGF and DLL4 is needed for the development of a properly organized, mature vasculature. It makes sense, then, that the two to regulate each other in a feedback loop. VEGF-A induces DLL4 expression in cultured human endothelial cells [53,56,86]. DLL4 then activates Notch, and Notch signaling inhibits VEGFR2 expression, effectively removing the receptor target of VEGF on endothelial cells, and preventing further sprouting [53].

The relationship between VEGF and DLL4 has also been demonstrated in vivo, in both developing mouse retinas and tumor models. Intravitreal injection of $VEGF_{165}$ led to increased DLL4 expression in mouse retinal vasculature within 24 hours of treatment [73] . Conversely, inhibition of VEGF using VEGF Trap led to a nearly 80% reduction in DLL4 mRNA expression in rat C6 gliomas, as assessed by microarray analysis [58].

The essential roles of both DLL4 and VEGF in tumor vascular development imply that DLL4 may be an alternative therapeutic target for vascular inhibition in tumors that are resistant to anti-VEGF therapy. This is supported by data from several tumor models that are resistant to VEGF inhibition, including HT1080-RM (the resistant subline of HT1080 fibrosarcoma cells), mouse mammary tumors, and PC3 tumors.

Growth of each of these tumor models continues during anti-VEGF therapy but is significantly inhibited by systemic delivery of soluble DLL4 [58,87]. Additionally, mouse WEHI3 tumors, which are resistant to treatment with a monoclonal antibody against VEGF, were susceptible to growth inhibition by treatment with YW152F, the same DLL4 neutralizing antibody used in our studies[56]. This suggests that inhibition of DLL4 may be an effective therapy even in tumors that are not sensitive to VEGF inhibition, or in tumors that progress after an initial period of sensitivity to anti-VEGF therapy.

In addition to use as a single agent, anti-DLL4 therapy may be most effective in combination with anti-VEGF therapy. The synergistic effect of anti-VEGF (avastin) and anti-DLL4 (YW152F) therapies has already been demonstrated in MV522 lung carcinoma xenografts, which are only moderately sensitive to either alone. The combination of both VEGF and DLL4 neutralizing antibodies together yielded significantly more growth inhibition than either single agent[56].

Currently, the sensitivity of Ewing's sarcoma to anti-VEGF therapy (bevacizumab) in combination with chemotherapy is being evaluated in a phase 2 trial by the Children's Oncology Group (COG). We have previously demonstrated that DC101, a VEGF receptor 2 inhibiting antibody, significantly inhibits the growth of Ewing's sarcoma in mice, indicating that a positive outcome of the COG trial is likely [88]. Our previous demonstration of Ewing's sarcoma growth inhibition by DC101 combined with the synergistic effects of YW152F and avastin in the treatment of lung carcinoma in mice indicates that targeting DLL4 and VEGF together may be an effective therapy for the treatment of Ewing's sarcoma. Studies combining inhibitors of DLL4 and VEGF to treat Ewing's sarcoma tumor bearing mice are merited.

DLL4 as a therapeutic target for metastatic disease

While the five year survival rate for patients with non-metastatic Ewing's sarcoma is nearly 70%, it remains at less than 25% for the majority of patients, those with meatastatic disease [1]. Thus, there is a need for identifying therapeutic targets that may be important for the growth of metastatic lesions. DLL4 may be involved in vasculogenesis in metastatic lesions as well as primary tumors. We evaluated 14 patient samples for DLL4 expression. Of these, 6 were metastatic lesions. DLL4 was expressed in a perivascular pattern in metastatic tumors similar to the pattern observed in primary tumors and xenograft models. Additionally, BM-derived cells participate in vasculogenesis in TC71 cell lung metastases in mice (unpublished data, Zichao Zhou). We have therefore confirmed that DLL4 is present around blood vessels in metastases and that BM-derived cells are also present. Further studies are needed to determine whether DLL4 inhibition would significantly impact vasculogenesis in metastases and metastatic growth.

Recently, Wang et al reported the development of an orthotopic xenograft model of Ewing's sarcoma, TC-W, in which 54% of mice developed pulmonary metastases [89]. This model could be utilized to study the potential effects of inhibiting DLL4 on metastatic development. Two interesting questions that should be addressed are: 1. Can DLL4 inhibition be used before the appearance of detectable metastatic disease to prevent formation of macrometastases? 2. Is DLL4 inhibition therapy effective against substantial metastatic disease?

To determine whether anti-DLL4 therapy such as YW152F can prevent formation of metastatic lesions, TC-W cells could be labeled with luciferase, injected into the rib

bone and allowed to form tumors. Lungs can then be monitored for tumor cells using bioluminescence imaging. Prior to the formation of detectable metastases, bi-weekly treatment with YW152F or IgG control would be administered. The experiment would be allowed to continue until mice must be sacrificed due to metastatic tumor burden, at which time the number and size of metastatic lesions between treatment and control groups would be compared.

To determine whether anti-DLL4 therapy would be effective against substantial metastatic disease, TC-W cells could again be labeled with luciferase and injected into mice rib bones. Again, the lungs would be monitored using bioluminescent imaging. In this experimental schema, treatment with YW152F or IgG would not be started until after significant detectable disease is present in the lungs. Treatment with YW152F or IgG would then be begun to determine whether the growth rate of the metastatic lesions is affected by DLL4 inhibition.

Chapter 8

Materials and Methods

A4573 and TC71 Ewing's Sarcoma cell culture and mouse models

A4573 and TC71 cells were grown in Dulbecco's Modified Eagle Medium (company) supplemented with 10% fetal bovine serum, 2 mmol/L L-glutamine, 1 mmol/L nonessential amino acids, 1 mmol/L penicillin-streptomycin, and a two-fold vitamin solution (Life Technologies, Inc., Grand Island, NY). Cells were used between passage 3 and 7.

All animal experiments were approved by the Institutional Animal Care and Use Committee at The University of Texas M.D. Anderson Cancer Center. For GFP BM transplant experiments, donor mice were purchased from the M.D. Anderson Cancer Center Genetic Mouse Engineering Facility (Jackson Laboratory Strain 003115). The mice express enhanced GFP under control of the CMV-enhanced chicken β-actin promoter. This strain of mice was used for all experiments where mice were treated with shRNA. When these GFP mice were no longer available for purchase, GFP transgenic mice were purchased from Jackson laboratories (Strain C57BL/6-Tg(UBC-GFP)30Scha/J). These mice express enhanced GFP under control of the human ubiquitin C promoter. This strain of GFP mice was used for all experiments where mice were treated with YW152F. Recipient mice were athymic nu/nu nude mice. Nude mice were purchased at six weeks old from either the National Cancer Institute (strain 01B70) or Charles River (strain nu/nu 088).

GFP BM Transplant

For all experiments where mice received bone marrow transplants, the following standard procedure was followed. BM was collected from GFP transgenic mice. Femurs were collected, bone ends were clipped with scissors, and flushed with PBS using a

sterile syringe and 30 gauge needle. Cells collected by flushing were pelleted and then resuspended in PBS. Nude mice were given 900 rads whole body irradiation using a Cesium irradiator (^{137}Cs Mark 1 Irradiator; J. L. Shepherd & Associates, Glendale, CA). This dose is sufficient to eradicate endogenous BM. Irradiated mice were then rescued by i.v. injection of previously collected GFP^+ BM cells. Each mouse received 1 x 10^6 GFP^+ BM cells in 100 ul PBS. After transplant, four to six weeks was allowed for BM cell engraftment before injection of tumor cells. At the end of each experiment, bone marrow was collected from at least three representative mice to confirm GFP expression. Greater than 90% of BM cells were GFP^+ by flow cytometry (BD FACSAria, BD Biosciences).

shRNA vector and polyethylenimine (PEI). shRNA targeting mouse DLL4 (shDLL4) was made by annealing the DNA oligomer 5'-GATCCAGTCACTTGGGTGCAGTGTTTCAAGAGAACACTGCACCCAAGTGACTTTTTTTGGAAA-3' to its complimentary sequence. This double stranded oligomer was then annealed into pSilencer 2.1-U6 hygro (Ambion, Austin, TX) shRNA vector between the BamHI and HindIII sites. pSilencer 2.1-U6 hygro containing a sequence with minimal homology to the mouse genome was used for the sh^- control.

shRNA was delivered to tumors in PEI (M_r 25,000, branched form; Aldrich Chemical, Milwaukee, WI). A stock solution of PEI (pH 7.0 – 7.5) was prepared at a concentration of 4.3 mg/ml (0.1 M nitrogen) in PBS. PEI:shRNA complexes were prepared at a PEI nitrogen:DNA phosphate ratio of 10:1 and a PEI:DNA ratio of 1.29:1 (w/w). DNA and PEI were diluted in H_2O so that the final volumes were the same for each solution. DNA was then added dropwise to PEI while vortexing, for a final concentration of 0.4 μg DNA per 1 μl PEI/DNA mixture.

shRNA treatment in vivo

Nude mice that had previously received a GFP BM transplant (described above) were injected subcutaneously with 2 x 10^6 TC71 cells on both right and left flanks. Five days later, tumors were palpable and intratumor injections were begun. Left side tumors were injected with PEI/sh$^-$ control while right side tumors were injected with PEI/shDLL4. Each tumor received a total of 50 μl PEI/DNA mixture (20 μg DNA) per treatment. Twenty-four days later (12 total treatments), final tumor volumes were recorded, mice were sacrificed and tumors were harvested for examination by immunohistochemistry. This experiment was repeated three times (n = 6, n = 8, and n =13). In the third experiment, mice were injected with hypoxyprobe 2.5 hours prior to sacrifice and Hoescht 33342 one minute prior to sacrifice, as described below.

Hoescht 33342 in vivo

For experiments where Hoescht 33342 was used to label functional vessels prior to sacrifice, Hoescht 33342 was resuspended in sterile H2O at a concentration of 12mg/mL. Mice received i.v. injection of 100μl (1.2mg) of Hoescht33342 solution at varying time points (1-5 minutes) prior to sacrifice. Mice were sacrificed by cervical dislocation and tumors were harvested immediately after sacrifice.

Hypoxyprobe (pimonidazole HCl)

Hypoxyprobe-1 (HPI, inc, Burlington, MA) was reconstituted in PBS at a final concentration of 7mg/mL. Two hours and thirty minutes prior to sacrifice, mice received i.v. injections of 200 μl of hypoxyprobe/PBS solution (total 1.4mg hypoxyprobe). Pimonidazole adducts (hypoxic cells) were detected by immunohistochemistry. Slides were first incubated with mouse Fab fragment (Jackson Immunoresearch) diluted 1:10 in

4% fish gel blocking solution overnight. Slides were then washed with PBS and incubated with mouse anti-mouse monoclonal anti-hypoxyprobe antibody, diluted 1:800 in 4% fish gel for 3 hours. Slides were again washed with PBS, then incubated with anti-mouse Cy5, diluted 1:1000 in 4% fish gel for 1 hour. Images were captured by confocal microscopy as described in the microscopy section of materials and methods.

YW152F *in vivo* experiments

Experiments using YW152F DLL4-neutralizing antibody were performed with either TC71 or A4573 xenograft models. For all experiments, a GFP BM transplant was performed and at least four weeks were allowed for BM cell engraftment before tumor inoculation. After this period, mice were injected subcutaneously with either 2×10^6 TC71 or 6×10^6 A4573 cells. Five days later, mice were randomly divided into either treatment or control groups. Mice were treated twice weekly by i.v. injection of either YW152F (1.3mg YW152F in 100μl PBS), IgG (1 mg human IgG in PBS, Southern Biotech, Birmingham, AL), or 100 μl PBS. TC71 cells were allowed to grow for a total of 21 days (5 treatments), and A4573 for 24 days (6 treatments). Tumor volumes were measured using calipers twice weekly and on the day of sacrifice. Mice were sacrificed by euthanasia or cervical dislocation and tumors were harvested and frozen for immunohistochemistry.

Experiments treating mice with TC71 tumors were done three times. In the first experiment, n = 9 for YW152F and n= 8 for PBS. In the second, n = 9 for YW152F, n = 9 for IgG, and n = 7 for PBS. In the third, n = 6 for YW152F and n = 7 for IgG. In the third experiment, mice were injected with hypoxyprobe 2.5 hours prior to sacrifice and biotin was delivered by cardiac perfusion immediately following sacrifice.

Experiments treating mice with A4573 tumors were performed twice. Both times, n = 9 for YW152F and n =8 for IgG treated groups.

Biotin perfusion

For vessel perfusion studies using biotin, mice were sacrificed by cervical dislocation and a 23 gauge needle was inserted into the left ventricle of the heart. 10 mL of PBS was perfused through each animal to flush the circulation, followed by perfusion with 8 mL of EZ Link Sulfo-NHS-Biotin in PBS (0.5mg/ml, Pierce Chemicals, Rockford, IL). Immediately following perfusion, tumors were harvested and frozen for immunohistochemistry.

YW152F *in vitro*

1.33×10^5 TC71 or A4573 cells per well were plated in 6 well dishes in complete DMEM growth media. One day after seeding, YW152F or IgG was added to the media. Two doses, 2.8μg/ml and 5μg/ml, were tested. Media was changed and fresh YW152F or IgG was added daily. Total cell number and viability were counted at 48 and 72 hours by automated trypan blue assay and ViCell (Beckman Coulter, Brea,CA). Experiments were done two times in triplicate each time.

MigR1/mDLL4 plasmid

The retroviral MigR1 plasmid containing mouse DLL4 was constructed by excising the full length mouse DLL4 gene out of pCR2.1/mDLL4 vector kindly provided by Amgen (Thousand Oaks, CA) using EcoR1 restriction enzyme, and isolating the DLL4 portion using agarose gel purification. MigR1 was then cut using EcoR1 restriction enzyme in the presence of alkaline phosphatase per manufacturers instructions (New England Biosciences, Ipwich, MA). The mouse DLL4 DNA was then ligated into the

EcoR1 restriction enzyme site of cut MigR1 using T4 DNA ligase (New England Bioscienes).

MigR1 control, MigR1/DNMAM, MigR1/NICD1, MigR1/NICD2, MigR1/NICD3, MigR1/NICD4 plasmids

All MigR1 plasmids except those containing human or mouse DLL4 were the kind gift of Dr. Patrick Zweidler-McKay (The University of Texas M.D. Anderson Cancer Center, Houston,TX). The intracellular domains of each of the Notch receptors were cloned between the EcoRI and BglI cloning sites under control of the MSCV LTR retroviral promoter. There is an internal ribosome entry site (IRES) between the Notch intracellular domain and enhanced GFP, so that the two are not expressed as a fusion protein. For MigR1/DNMAM, a 61 amino acid portion of mastermind like 1 is directly fused to enhanced GFP.

10T1/2 transfected with MigR1/ NICD1, MigR1/ NICD2, MigR1/ NICD3, MigR1/ NICD4, MigR1/DLL4

10T1/2 cells were purchased from ATCC (cell line C3H/10T1/2, Clone 8) and were cultured in complete DMEM media as described above for TC71 and A4573 cells. Transfection of 10T1/2 cells with MigR1 plasmids was done using Fugene 6 transfection reagent (Roche, San Fransisco, CA) per manufacturer's instructions. 2 μg of DNA was used for each transfection in a six well dish. 48 hours after transfection, efficiency was checked visually by looking for GFP expression. RNA was then collected using trizol (Invitrogen, Carlsbad, CA) per manufacturer's instructions.

Immunohistochemistry

Xenograft Models Frozen slides were permeabalized by submersion in acetone for 10 minutes followed by incubation in PBS. Slides were then blocked in 4% fish gelatin for 20 minutes. For mouse anti-mouse primary antibodies, slides were then incubated overnight in mouse Fab fragment blocking solution (mouse Fab diluted 1:10 in 4% fish gel). Primary antibodies were diluted as indicated in 4% fish gel (table 1). Tissues were incubated with primary antibodies for 3 hours or overnight. Slides were then washed in PBS and incubated with 4% fish gel for ten minutes before addition of secondary fluorescent antibodies. All secondary antibodies were diluted 1:1000 in 4% fish gel and left on the tissue sections for one hour before slides were again washed with PBS. Nuclei were stained with either Hoescht 33342 for 3 minutes or Sytox Green for 10 minutes.

Patient Samples Fourteen paraffin embedded Ewing's sarcoma patient samples were obtained from the tumor bank at M.D. Anderson Cancer Center. These samples represent both primary and metastatic lesions from a total of ten different patients. The Institutional Review Board at M.D. Anderson approved the use of human specimens for this study. Deparaffinization and rehydration was performed by sequential submersion in xylene for 4 minutes, fresh xylem for 3 minutes, absolute ethanol for 2 minutes, fresh absolute ethanol for 2 minutes, 95% ethanol for 1 minute, fresh 95% ethanol for 1 minute, 80% ethanol for 1 minute, and PBS for 3 minutes. Antigen retrieval was performed by incubation with pepsin at 37°C for thirty minutes, and endogenous peroxidase was blocked with 3% H_2O_2. To detect DLL4, slides were then blocked with normal horse serum and normal goat serum for ten minutes followed by incubation with rabbit anti-DLL4 (Abcam) diluted 1:750 in normal horse serum and normal goat serum for three

hours. Slides were then washed with PBS, and incubated with peroxidase labeled biotinylated goat anti-rabbit secondary antibody (Jackson Immunoresearch). $DLL4^{+}$ cells were detected with 3,3'-diaminobenzidine (DAB; Open Biosystems, Huntsville, AL) which turns brown on positive cells, and counterstained with Gill's hematoxylin (Sigma-Aldrich). Tumors were scored in a qualitative manner as either DLL4 positive or DLL4 negative.

	Dilution Factor	company
Primary Antibodies		
rabbit anti-mouse/human DLL4	1000	Abcam, Cambridge, MA
rabbit anti-human DLL4	1000	Cell Signaling Technology, Danvers, MA
anti-mouse-a-SMA-Cy3	200	Sigma-Aldrich, St. Louis, MO
mouse anti-mouse a-SMA	100	Abcam, Cambridge, MA
rabbit anti-mouse desmin	400	Abcam, Cambridge, MA
rabbit anti-GFP	1000	Santa Cruz Biotechnology, Santa Cruz, CA
chicken anti-GFP	400	Abcam, Cambridge, MA
rabbit anti-mouse NG2	500	Millipore, Billerica, MA
rabbit anti-mouse S100A4	1000	Abcam, Cambridge, MA
rat anti-mouse CD31	1000	BD Biosciences, Franklin Lakes, NJ
rabbit anti-human/mouse NICD1	1000	Cell Signaling Technology, Danvers, MA
rabbit anti-human Notch1	1000	Abcam, Cambridge, MA
mouse anti-mouse hypoxyprobe-1	800	HPI, inc., Burlington, MA
Secondary Antibodies		
Alexa Flour 488 (anti-rat, anti- rabbit)	1000	Molecular Probes, Eugene, OR
Alexa Flour 594 (anti-rabbit)	1000	Molecular Probes, Eugene, OR
Cy3 (anti-rat, anti-rabbit, anti-mouse)	1000	Jackson Immunoresearch, West Grove, PA
Cy5 (anti-rat, anti-mouse, anti-rabbit)	1000	Jackson Immunoresearch, West Grove, PA

Table 2. Immunohistochemistry antibodies used on frozen sections. Antibodies used for immunohistochemistry are listed. Antibodies were diluted in 4% fish gelatin in PBS by the dilution factor listed.

Microscopy

For non-confocal fluorescent microscopy, Images were captured using using a Zeiss Axioplan fluorescence microscope (Carl Zeiss, Inc., Thornwood, NY) equipped with a 100-W Hg lamp and narrow bandpass excitation filters. Representative images were obtained using a cooled charge-coupled device Hamamatsu C5810 camera (Hamamatsu Photonics, Bridgewater, NJ) and Optimas imaging software (Media Cybernetics, Bethesda, MD). For confocal microscopy, images were collected using a Zeiss Laser Confocal Microscope, and LSM software (Carl Zeiss MicroImaging, Inc., Thornwood, NY).

Immunohistochemistry Quantification

Five random 10x-magnification fields were captured on each slide. A minimum and maximum fluorescent intensity was set for positive staining for each antibody. Positive areas for each marker were measured using Simple PCI software (Hamamatsu, Sewickley, PA). For each of the five fields per slide, we measured the mean pixel area of positive fluorescence for the protein of interest as well as the mean pixel area for nuclei and a mean positive pixel:nuclei ratio was calculated.

Tumor homogenization and collection of GFP^+ BM-derived cells

GFP BM transplants were performed on nude mice. One month later, 2×10^6 TC71 cells were implanted subcutaneously. Tumors were allowed to grow until they reached $2cm^3$. Mice were then sacrificed, tumors were harvested, and minced using a razor blade. Tumor pieces were then passaged through progressively smaller needles and incubated with collagenasese 1 (2mg/mL) in DMEM at 37 degrees Celsius while rotating for 45 minutes. Tumor homogenate was then passaged through a filter with 100μm pores,

until a single cell suspension was achieved. GFP^+ (BM-derived) cells were then collected from the cell suspension using FACS, and RNA was collected from these GFP^+ cells.

PCR primers

DLL4 Forward: 5'actcaccactctccgtgcaagaat Reverse: 5'tgtgtaacagccggttcactcctt

Hes1 Forward: 5'caacacgacaccggacaaaccaaa Reverse: 5' ttccggaggtgcttcacagtcatt

Hey1 Forward: 5' tcagatgcgcagctttactggaga Reverse: 5' tttcagactccgatcgtctacgca

Hey2 Forward: 5' acttgaaagcagcacaccaacgtc Reverse: 5' tggaggcttcggtggaattgctta

RGS5 Forward: 5' tcaagttgaggatctaagccgcca Reverse:5' ttctcacaggcaacccagaactca

Desmin Forward: 5' tcgtattgacctggagcgcagaat Reverse:5' atgttcttagccgcgatggtctca

PDGFR-β Forward: 5'aaacacaccttcttgcagcgacac Reverse: 5'attaaggtggcgcgataggtcctt

Real-time Hes1 Forward: 5' gctgctaccccagccagtgt Reverse: 5' gcccttcgcctcttctccat

Real-time Hey1 Forward: 5' tggcctgcttggcttttctc Reverse: 5' gccaagtgcaggcaaggtct

Real-time Hey2 Forward: 5' accactgggcagctgctttc Reverse: 5' atgggcaaacgttgctgtga

Real-time RGS5 Forward: 5' taagccgccagccaaaatgt Reverse: 5' gtgtgccttggcaggcttct

Real-time desmin Forward: 5' gagccaggcctactcgtcca Reverse: 5' tgaactcgaggagcccttgg

Chapter 9.

Appendix

Greater than 90% of BM cells are GFP$^+$ after GFP BM transplant in nude mice

At the end of all *in vivo* experiments, bone marrow is collected from three random representative mice and is examined by flow cytometry for the presence of GFP$^+$ cells. GFP$^+$ cells consistently made up greater than 90% of the BM in transplanted mice. In a representative experiment, 94.5% of BM cells collected from a nude mouse 51 days after GFP transplant were GFP$^+$ compared to 0.19% in a non-transplanted nude mouse control (Figure A1).

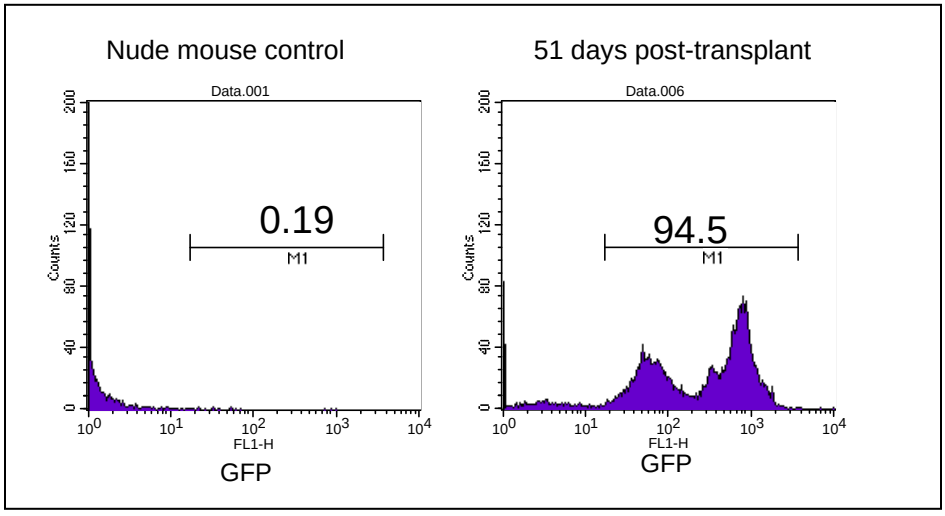

Figure A1. After GFP BM transplant, greater than 90% of BM cells are GFP$^+$. Whole BM was collected from the femurs of nude mice that had not received any bone marrow transplant, or from nude mice 51 days after GFP BM transplant. Flow cytometry was performed to measure the percent of cells that are GFP$^+$. Representative data from one mouse in each group is presented. 0.19% of BM cells from the nude mouse control were GFP compared to 94.5% of BM cells from the mouse that had received a GFP BM transplant.

Hoescht 33342 *in vivo* perfusion studies were inconclusive

As explained in Chapter 4, we attempted to measure blood vessel perfusion in tumors using tail vein injections of Hoescht33342 sixty seconds prior to sacrifice. Due to the excessive labeling of nuclei throughout the tumor, it was difficult to determine which vessels had blood flow and which did not. Representative images of tumors after Hoescht33342 perfusion are shown in figure A2.

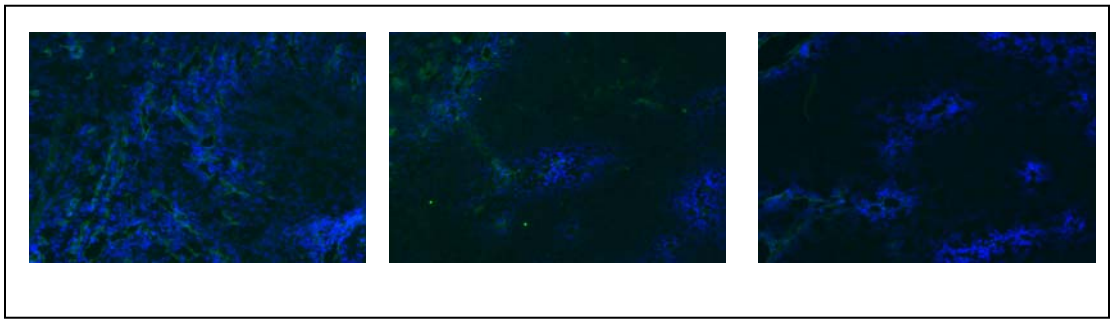

Figure A2. Hoescht33342 perfusion studies were inconclusive. Mice bearing bilateral tumors received tail vein injections of Hoescht33342 in H_2O sixty seconds prior to sacrifice. After sacrifice, tumors were harvested and immunohistochemistry was performed for CD31 (green, to identify endothelial cells). Nuclei labeled by the leaking of Hoescht33342 out of functional vasculature are blue.

MigR1/DLL4 increases mouse DLL4 expression and shDLL4 inhibits mouse DLL4 expression in vitro

I constructed the retroviral MigR1/DLL4 plasmid by PCR amplification of the mouse DLL4 gene and insertion of this gene into the multiple cloning site of the MigR1 retroviral vector (see materials and methods). Therefore, prior to using this plasmid as a tool in my research, it was important to demonstrate that DLL4 was, in fact, overexpressed in cells transfected with MigR1/DLL4. Human 293T cells were transfected with MigR1/DLL4. Forty eight hours later, protein lysates were made and a

western blot was run to probe for DLL4. DLL4 expression was increased in cells transfected with MigR1/DLL4 but not with MigR1 control (Figure A3).

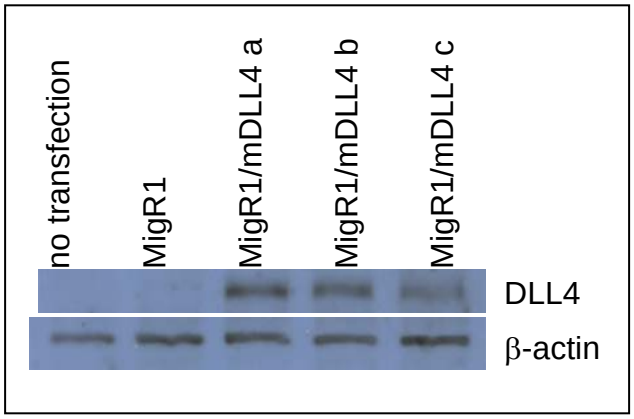

Figure A3. MigR1/DLL4 increases expression of mouse DLL4 in 293T cells. Human 293T cells were transfected with MigR1 or MigR1/DLL4 plasmid isolated from three different bacterial clones (a,b,c). Forty eight hours later, western blot was performed to probe for DLL4. Clone A was used in all experiments hereafter.

In addition to MigR1/DLL4, I constructed shDLL4 to inhibit mouse DLL4 expression by ligating two different sequences targeting DLL4 into a pSilencer2.0 hygro plasmid (shDLL4-a and shDLL4-b). Prior to use in experiments, the efficacy of each shDLL4 plasmid was demonstrated by transfecting SC9-19 mouse stromal cells, which express DLL4, with shDLL4-a or shDLL4-b. Twenty-four hours later, RNA was collected and RT-PCR for DLL4 was performed. Both shDLL4 plasmids inhibited DLL4 expression (Figure A4). Inhibition of DLL4 expression by shDLL4-a was most efficient, and this plasmid was used for all in vivo experiments described in this thesis.

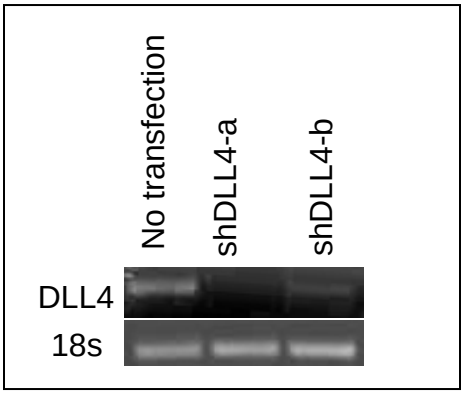

Figure A4. shDLL4-a inhibits DLL4 mRNA expression in mouse SC9-19 cells. SC9-19 cells were transfected with shDLL4-a or shDLL4-b. Twenty-four hours later, RNA was collected and RT-PCR was performed to examine DLL4 RNA levels.

Bibliography

1.Vivek Subbiah PA, Alexander Lazar, Emily Burdett, Kevin Raymond, Joseph Ludwig. Ewing's Sarcoma: Standard and Experimental Treatment Options. Current Treatment Opinions in Oncology. 2009;10:126-140.

2. Nicolo Riggi, Ivan Stamenkovic. The biology of Ewing sarcoma. Cancer Letters. 2007;254:1-10.

3. Patrick Leavey, Anderson Collier. Ewing sarcoma: prognostic criteria, outcomes, and future treatment. Expert Reviews Anticancer Therapeutics. 2008;8:617-624.

4. Pete Anderson, Lisa Kopp, Nicholas Anderson, Kathleen Cornelius, Cynthia Herzog, Dennis Hughes, Winston Huh. Novel bone cancer drugs: investigational agents and control paradigms for primary bone sarcomas (Ewing's sarcoma and osteosarcoma). Expert Opinion Investigational Drugs. 2008;17:1703-1715.

5. L. Diaz-Flores RG, J.F. Madrid, H. Varela, F. Valladares, E. Acosta, P. Martin-Vasallo, L. Diaz-Flores Jr. Pericytes. Morphofunction, interactions and pathology in quiescent and activated mesenchymal cell niche. Histology and Histopathology. 2009;24:909-969.

6. Annika Armulik, Alexandra Abramsson, Christer Betsholz. Endothelial/Pericyte Interactions. Circulation Research. 2005;97:512-523.

7. Gittenberger-de-Groot AC, DeRuiter MC, Bergwerff M, Poelmann RE. Smooth Muscle Cell Origin and Its Relation to Heterogeneity in Development and Disease. Arterioscler Thromb Vasc Biol. 1999;19:1589-1594.

8. Rensen SS, Doevendans PA, van Eys GJ. Regulation and characteristics of vascular smooth muscle cell phenotypic diversity. Netherlands Heart Journal 2007 15:100-108.

9. Sennino B, Falcon BL, McCauley D, Le D, McCauley T, Kurz T, Haskell J, Epstein A, McDonald D, Sequential Loss of Tumor Vessel Pericytes and Endothelial Cells after Inhibition of Platelet-Derived Growth Factor B by Selective Aptamer AX102. Cancer Res. 2007;67:7358-7367.

10. Karen Hirschi SR, Patricia D'Amore. PDGF, TGF-b, and Heterotypic Cell-Cell Interactions Mediate Endothelial Cell-induced Recruitment of 10T1/2 Cells and Their Differentiation to a Smooth Muscle Fate. The Journal of Cell Biology. 1998;141:805-814.

11. von Tell D, Armulik A, Betsholtz C. Pericytes and vascular stability. Experimental Cell Research. 2006;312:623-629.

12. Chan-Ling T, Page MP, Gardiner T, Baxter L, Rosinova E, Hughes S. Desmin Ensheathment Ratio as an Indicator of Vessel Stability: Evidence in Normal Development and in Retinopathy of Prematurity. Am J Pathol. 2004;165:1301-1313.

13. Forbes MS, Rennels ML, Nelson E. Ultrastructure of pericytes in mouse heart. American Journal of Anatomy. 1977;149:47-70.

14. Gabriele Bergers, Steven Song . The role of pericytes in blood-vessel formation and maintenance. Neuro-Oncology. 2005;7:452-464.

15. Parmacek MS. MicroRNA-modulated targeting of vascular smooth muscle cells. The Journal of Clinical Investigation. 2009;119:2526-2528.

16. Owens GK, Kumar MS, Wamhoff BR. Molecular Regulation of Vascular Smooth Muscle Cell Differentiation in Development and Disease. Physiol Rev. 2004;84:767-801.

17. Benjamin LE, Hemo I, Keshet E. A plasticity window for blood vessel remodelling is defined by pericyte coverage of the preformed endothelial network and is regulated by PDGF-B and VEGF. Development. 1998;125:1591-1598.

18. Ribatti D, Vacca A, Nico B, Roncali L, Dammacco F. Postnatal vasculogenesis. Mechanisms of Development. 2001;100:157-163.

19. Goldie LC, Nix NM, Hirschi KK. Embryonic vasculogenesis and hematopoietic spefication. Organogenesis 2008;4:257-263.

20. Masahiro Shin HN, Guojun Sheng. Notch mediates Wnt and BMP signals in the early separation of smooth muscle progenitors and blood/endothelial common progenitors. Development. 2009;136:595-603.

21. Takayuki Asahara, Haruchika Masuda, Tomono Takahashi, Christoph Kalka, Christopher Pastore, Marcy Silver, Marianne Kearne, Meredith Magner, Jeffrey Isner. Bone Marrow Origin of Endothelial Progenitor Cells Responsible for Postnatal Vasculogenesis in Physiological and Pathological Neovascularization. Circulation Research. 1999;85:221-228.

22. Asahara T, Takahashi T, Masuda H, Kalka C, Chen D, Iwaguro H, Inai Y, Silver M, Isner J. VEGF contributes to postnatal neovascularization by mobilizing bone marrow-derived endothelial progenitor cells. EMBO J. 1999;18:3964-3972.

23. Kalka C, Masuda H, Takahashi T, Kalka-Moll W, Silver M, Kearney M, Li T, Isner J, Asahara T. Transplantation of ex vivo expanded endothelial progenitor cells for therapeutic neovascularization. Proceedings of the National Academy of Sciences of the United States of America. 2000;97:3422-3427.

24. Au P, Tam J, Fukumura D, Jain RK. Bone marrow-derived mesenchymal stem cells facilitate engineering of long-lasting functional vasculature. Blood. 2008;111:4551-4558.

25. Yokoi H, Yamada H, Tsubakimoto Y, Takata H, Kawahito H, Kishida S, Kato T, Matsui A, Hirai H, Ashihara E, Maekawa T, Iwai M, Horiuchi M, Ikeda K, Takahashi T, Okigaki M, Matsubara H Bone Marrow AT1 Augments Neointima Formation by Promoting Mobilization of Smooth Muscle Progenitors via Platelet-Derived SDF-1{alpha}. Arterioscler Thromb Vasc Biol;30:60-67.

26. Iiro Rajantie MI, Agne Alminaite, Ugur Ozerdem, Kari Alitalo, and Petri Salven. Adult bone marrow-derived cells recruited during angiogenesis comprise precursors for periendothelial vascular mural cells. Blood. 2004;104:2084-2086.

27. Du R, Lu K, Petritsch C,Liu P, Ganss R, Passegué E,Song H,VandenBerg S, Johnson R, Werb Z, Bergers G. HIF1-a Induces the Recruitment of Bone Marrow-Derived Vascular Modulatory Cells to Regulate Tumor Angiogenesis and Invasion. 2008;13:206-220.

28. Bolontrade MF ZR, Kleinerman ES. Vasculogenesis Plays a Role in the Growth of Ewing's Sarcoma in Vivo. Clinical Cancer Research. 2002;8:3622-3627.

29. Krishna Reddy, Zichao Zhou, Keri Schadler, Shu-Fang Jia and Eugenie S. Kleinerman. . Bone Marrow Subsets Differentiate Into Endothelial Cells and Pericytes Contributing to Ewing's Tumor Vessels *Molecular Cancer Research*. 2008;6:929-936.

30. Krishna Reddy, Ying Cao, Zichao Zhou, Shu-fang Jia, Eugenie Kleinerman. $VEGF_{165}$ expression in the tumor microenvironment influences the differentiation of bone marrow-derived pericytes that contribute to the Ewing’s sarcoma vasculature. Angiogenesis. 2008;11:257-267.

31. Keri Schadler, Patrick Zweidler-McKay, Hui Guan, Eugenie Kleinerman. Clinical Cancer Research. 2010.

32. Zhou Z, Reddy K, Guan H, Kleinerman ES. VEGF165, but not VEGF189, Stimulates Vasculogenesis and Bone Marrow Cell Migration into Ewing's Sarcoma Tumors In vivo. Vol. 5; 2007:1125-1132.

33. Reddy K, Zhou Z, Jia S-F, Tim Lee, Jaime Morales-Arias, Ying Cao, Eugenie S Kleinerman. Stromal cell-derived factor-1 stimulates vasculogenesis and enhances Ewing's sarcoma tumor growth in the absence of vascular endothelial growth factor. International Journal of Cancer. 2008;123:831-837.

34. Lee TH, Bolontrade M, Worth LL, Guan H, Ellis LM, Kleinerman ES. Production of VEGF165 by Ewing's sarcoma cells induces vasculogenesis and the incorporation of CD34+ stem cells into the expanding tumor vasculature. International Journal of Cancer. 2006;119:839-846.

35. Ulla-Maj Fiuza AMA. Cell and Molecular Biology of Notch. Journal of Endocrinology. 2007;194:459-474.

36. Maillard I, Sandy A. Notch signaling in the hematopoietic system. Expert Opinion in Biologic Therapeutics. 2009;9:1383-1398.

37. Fortini ME. Notch Signaling: The Core Pathway and Its Posttranslational Regulation. 2009;16:633-647.

38. Gridley T. Notch signaling in vascular development and physiology. Development. 2007;134:2709-2718.

39. Kume T. Novel insights into the differential functions of Notch ligands in vascular formation. Journal of Angiogenesis Research. 2009;1:8.

40. Krebs LT, XueY, Norton CR, Shutter JR, Maguire M, Sundberg JP, Gallahan D, Closson V, Kitajewski J, Callahan R, Smith GH, Stark KL, Gridley T. Notch signaling is essential for vascular morphogenesis in mice. Genes Dev 2000;14:1343-1352.

41. Xue Y, Gao X, Lindsell C, Norton CR, Chang B, Hicks C, Gendron-Maguire M, Rand EB, Weinmaster G, Gridley, T. Embryonic lethality and vascular defects in mice lacking the Notch ligand Jagged1. Hum Mol Genet. 1999;8:723-730.

42. Doi H, Iso T, Shiba Y. Notch signaling regulates the differentiation of bone marrow-derived cells into smooth muscle-like cells during arterial lesion formation. Biochemical and Biophysical Research Communications. 2009;381:654-659.

43. Henrik Lovschall TM, Knud Poulsen, Kristina Jensen, Annette Kjeldsen. Coexpression of Notch3 and Rgs5 in the pericyte-vascular smooth muscle cell axis in response to pulp injury. International Journal of Developmental Biology. 2007;51:715-721.

44. Li Y, Takeshita K, Liu P-Y, Satoh M, Oyama N, Mukai Y, Chin M, Krebs L, Kotlikoff M, Radtke F, Gridley T, Liao J. Smooth Muscle Notch1 Mediates Neointimal Formation After Vascular Injury. Circulation. 2009;119:2686-2692.

45. Morrow D, Guha S, Sweeney C, Birney Y, Walshe T, O'Brien C, Walls D, Redmond EM, Cahill PA. Notch and Vascular Smooth Muscle Cell Phenotype. Circ Res. 2008;103:1370-1382.

46. Frances A High MZ, Aaron Proweller, Lili Tu, Michael S. Parmacek, Warren S. Pear, Jonathan A. Epstein. An essential role for Notch in neural crest during cardiovascular development and smooth muscle differentiation. The Journal of Clinical Investigation. 2007;117:353-363.

47. John Ridgway, Zhang G, Wu Y, Scott Stawicki, Wei-Ching Liang, Yvan Chanthery, Joe Kowalski, Ryan J. Watts, Christopher Callahan, Ian Kasman, Mallika Singh, May Chien, Christine Tan, Jo-Anne S. Hongo, Fred de Sauvage, Greg Plowman, Minhong Yan. Inhibition of Dll4 signalling inhibits tumour growth by deregulating angiogenesis. Nature. 2006;444:1083-1087.

48. Frances A. High MML, Warren S. Pear, Kathleen M. Loomes, Klaus H. Kaestner, and Jonathan A. Epstein Endothelial expression of the Notch ligand Jagged1 is required for vascular smooth muscle development Proceedings of the National Academy of Science. 2008;105:1955-1959.

49. Limbourg A, Ploom M, Elligsen D, Sorensen I, Ziegelhoeffer T, Gossler A, Drexler H, Florian P. Notch Ligand Delta-Like 1 Is Essential for Postnatal Arteriogenesis. Circ Res. 2007;100:363-371.

50. Gale NW DM, Noguera I, Pan L, Hughes V, Valenzuela DM, Murphy AJ, Adams NC, Lin HC, Holash J, Thurston G, Yancopoulos GD. Haploinsufficiency of delta-like 4 ligand results in embryonic lethality due to major defects in arterial and vascular development. Proc Natl Acad Sci U S A. 2004;101:15949-15954.

51. Antonio Duarte RB, Alexandre Trindale, Patricia Diniz, Eugenia Bekman, Luis Costa, Domingos Henrique, Janet Rossant. Dosage-sensitive requirement for DLL4 in mouse artery development. Genes and Development. 2004;18:2474-2478.

52. Mats Hellstrom L-KP, Jennifer J. Hofmann, Elisabet Wallgard, Leigh Coultas, Per Lindblom, Jackelyn Alva, Ann-Katrin Nilsson, Linda Karlsson, Nicholas Gaiano Keejung Yoon, Janet Rossant, M. Luisa Iruela-Arispe, Mattias Kalen, Holger Gerhardt,

Christer Betsholz. DLL4 signalling through Notch1 regulates formation of tip cells during angiogenesis. Nature. 2007:1-5.

53. Suchting S FC, le Noble F, Benedito R, Breant C, Duarte A, Eichmann A. The Notch ligand Delta-like 4 negatively regulates endothelial tip cell formation and vessel branching Proc Natl Acad Sci U S A. 2007;104:3225-3230.

54. Hanahan D, Weinberg RA. The Hallmarks of Cancer. Cell. 2000;100:57-70.

55. Carolina Mailhos JL, David Ish-Horowicz, Ute Modlich, Adrian Harris, Roy Bicknell Delta4, an endothelial specific Notch ligand expressed at sites of physiological and tumor angiogenesis. Differentiation. 2001;69 135-144.

56. John Ridgway GZ, Yan Wu, Scott Stawicki, Wei-Ching Liang, Yvan Chanthery, Joe Kowalski, Ryan J. Watts, Christopher Callahan, Ian Kasman, Mallika Singh, May Chien, Christine Tan, Jo-Anne S. Hongo, Fred de Sauvage, Greg Plowman, Minhong Yan. Inihibition of DLL4 signalling inhibits tumor growth by deregulating angiogenesis. Nature. 2006;444:1083-1087.

57. Hoey T, Yen W-C, Axelrod F, et al. DLL4 Blockade Inhibits Tumor Growth and Reduces Tumor-Initiating Cell Frequency. Cell Stem Cell. 2009;5:168-177.

58. Irene Noguera-Troise CD, Nicholas J. Papadopoulos, Sanda Coetzee, Pat Boland, Nicholas W. Gale, Hsin Chieh Lin, George D. Yancopoulos, Gavin Thurston. Blockade of DLL4 inhibits tumour growth by promoting non-productive angiogenesis. Nature. 2006;444:1032-1037.

59. Jeffrey S. Scehnet WJ, S. Ram Kumar, Valery Krasnoperov, Alexandre Trindade, Rui Benedito, Dusan Djokovic, Cristina Borges, Eric J. Ley, Antonio Duarte, Parkash S. Gill.

Inhibition of DLL4 mediated signaling induces proliferation of immature vessels and results in poor tissue perfusion. Blood. 2007.

60. Nilay S. Patel MSD, Mark Rochester, Graham Steers, Richard Poulsom, Karena Le Monnier, David Cranston, Ji-Liang Li, Adrian Harris. Up-Regulation of Endothelial Delta-like 4 Expression Correlates with Vessel Maturation in Bladder Cancer. Clinical Cancer Research. 2006;12:4836-4844.

61. Thurston G KJ. VEGF and Delta-Notch: interacting signaling pathways in tumor angiogenesis. British Journal of Cancer. 2008;99:1204-1209.

62. Yu L, Su B, Hollomon M, Deng Y, Facchinetti V, Kleinerman ES. Vasculogenesis Driven by Bone Marrow-Derived Cells Is Essential for Growth of Ewing's Sarcomas. Cancer Res. 2010;70:1334-1343.

63. Reddy K, Zhou Z, Schadler K, Jia S-F, Kleinerman ES. Bone Marrow Subsets Differentiate into Endothelial Cells and Pericytes Contributing to Ewing's Tumor Vessels. Molecular Cancer Research. 2008;6:929-936.

64. Li J-L, Sainson RC, Shi W, Leek R, Harrington LS, Preusser M, Biswas S, Turley H, Heikamp E, Hainfellner JA, Harris AL. Delta-like 4 Notch Ligand Regulates Tumor Angiogenesis, Improves Tumor Vascular Function, and Promotes Tumor Growth In vivo. Cancer Res. 2007;67:11244-11253.

65. Jeffery Scehnet, Weidong Jiang, S. Ram Kumar, Valery Krasnoperov, Alexandre Trindade, Rui Benedito, Dusan Djokovic, Cristina Borges, Eric J. Ley, Antonio Duarte, Parkash S. Gill, et al. Inhibition of Dll4-mediated signaling induces proliferation of immature vessels and results in poor tissue perfusion. Blood. 2007;109:4753-4760.

66. Schadler KL, Zweidler-McKay PA, Guan H, Kleinerman ES. Delta-Like Ligand 4 Plays a Critical Role in Pericyte/Vascular Smooth Muscle Cell Formation during Vasculogenesis and Tumor Vessel Expansion in Ewing's Sarcoma. Clinical Cancer Research;16:848-856.

67. Ennulat D, Steffens WL, Brown SA. Desmin Expression in Mesangial Cells and Fibroblasts in vitro. In Vitro Cellular & Developmental Biology Animal. 1998;34:450-454.

68. Hirschi KK, Rohovsky SA, D'Amore PA. PDGF, TGF-{beta}, and Heterotypic Cell-Cell Interactions Mediate Endothelial Cell-induced Recruitment of 10T1/2 Cells and Their Differentiation to a Smooth Muscle Fate. J Cell Biol. 1998;141:805-814.

69. Doi H, Iso T, Sato H, Yamazaki M, Matsui H, Tanaka T, Manabe I, Arai M, Nagai R, Kurabayashi M.Jagged1-selective Notch Signaling Induces Smooth Muscle Differentiation via a RBP-JÎº-dependent Pathway. Journal of Biological Chemistry. 2006;281:28555-28564.

70. Zhou Z, Reddy K, Guan H, Kleinerman ES. VEGF165, but not VEGF189, Stimulates Vasculogenesis and Bone Marrow Cell Migration into Ewing's Sarcoma Tumors In vivo. Molecular Cancer Research. 2007;5:1125-1132.

71. Lee TH, Bolontrade MF, Worth LL, Guan H, Ellis LM, Kleinerman ES. Production of VEGF165 by Ewing's sarcoma cells induces vasculogenesis and the incorporation of CD34+ stem cells into the expanding tumor vasculature. International Journal of Cancer. 2006;119:839-846.

72. Bolontrade MF, Zhou R-R, Kleinerman ES. Vasculogenesis Plays a Role in the Growth of Ewing's Sarcoma in Vivo. Clinical Cancer Research. 2002;8:3622-3627.

73. I. B. Lobov RAR, N. Papadopoulos, N. W. Gale, G. Thurston, G. D. Yancopoulos, S. J. Wiegand. Delta-like ligand 4 (DLL4) is induced by VEGF as a negative regulator of angiogenic sprouting. Proc Natl Acad Sci U S A. 2007;104:3219-3224.

74. Jubb AM, Turley H, Moeller HC, Turley, H, Steers G, Han C, Li JL, Leek R, Tan EY, Singh B, Mortensen NJ, Noguera-Troise I, Pezzella F, Gatter KC, Thurston G, Fox SB, Harris AL. Expression of delta-like ligand 4 (Dll4) and markers of hypoxia in colon cancer. Br J Cancer. 2009;101:1749-1757.

75. Huang M-T, Dai Y-S, Chou Y-B, Juan Y-H, Wang C-C, Chiang B-L. Regulatory T Cells Negatively Regulate Neovasculature of Airway Remodeling via DLL4-Notch Signaling. J Immunol. 2009;183:4745-4754.

76. Mikhailik A, Mazella J, Liang S, Tseng L. Notch ligand-dependent gene expression in human endometrial stromal cells. Biochemical and Biophysical Research Communications. 2009;388:479-482.

77. Paunescu V, Bojin FM, Tatu CA, Gavriliuc O, Rosca A, Gruia A, Tanasie G, Bunu C, Crisnic D, Gherghiceanu M, Tatu F, Tatu C, Vermesan S. Tumor-associated fibroblasts and mesenchymal stem cells: more similarities than differences. Journal of Cellular and Molecular Medicine;9999.

78. Du R, Lu K, Petritsch C,Liu P, Ganss R, Passegué E,Song H,VandenBerg S, Johnson R, Werb Z, Bergers G. HIF1[alpha] Induces the Recruitment of Bone Marrow-Derived Vascular Modulatory Cells to Regulate Tumor Angiogenesis and Invasion. Cancer Cell. 2008;13:206-220.

79. Wang H-C, Brown J, Alayon H, Stuck BE. Transplantation of quantum dot-labelled bone marrow-derived stem cells into the vitreous of mice with laser-induced retinal

injury: Survival, integration and differentiation. Vision Research;In Press, Corrected Proof.

80. Caiado F, Real C, Carvalho Tn, Dias Sr. Notch Pathway Modulation on Bone Marrow-Derived Vascular Precursor Cells Regulates Their Angiogenic and Wound Healing Potential. PLoS ONE. 2008;3:e3752.

81. Liu H, Kennard S, Lilly B. NOTCH3 Expression Is Induced in Mural Cells Through an Autoregulatory Loop That Requires Endothelial-Expressed JAGGED1. Circ Res. 2009;104:466-475.

82. Jin S, Hansson EM, Tikka S, Lanner F, Sahlgren C, Farnebo F, Baumann M, Kalimo H, Lendahl U. Notch Signaling Regulates Platelet-Derived Growth Factor Receptor-{beta} Expression in Vascular Smooth Muscle Cells. Circ Res. 2008;102:1483-1491.

83. Liu H, Kennard S, Lilly B. NOTCH3 Expression Is Induced in Mural Cells Through an Autoregulatory Loop That Requires Endothelial-Expressed JAGGED1. Vol. 104; 2009:466-475.

84. Tang Y, Urs S, Liaw L. Hairy-Related Transcription Factors Inhibit Notch-Induced Smooth Muscle {alpha}-Actin Expression by Interfering With Notch Intracellular Domain/CBF-1 Complex Interaction With the CBF-1-Binding Site. Circ Res. 2008;102:661-668.

85. Minhong Yan CC, Joseph Beyer, Krishna Allamneni, Gu Zhang, John Brady Ridgway, Kyle Niessen, Greg Plowman. Chronic DLL4 blockade induces vascular neoplasms. Nature. 2010;463:E6-E7.

86. Patel NS, Li J-L, Generali D, Poulsom R, Cranston DW, Harris AL. Up-regulation of Delta-like 4 Ligand in Human Tumor Vasculature and the Role of Basal Expression in Endothelial Cell Function. Cancer Res. 2005;65:8690-8697.

87. Li JL SR, Shi W, Leek R, Harrington LS, Preusser M, Biswas S, Turley H, Heikamp E, Hainfellner JA, Harris AL. Delta-like 4 Notch ligand regulates tumor angiogenesis, improves tumor vascular function, and promotes tumor growth in vivo. Cancer Research. 2007 67:11244-11253.

88. Zichao Zhou MB, Krishna Reddy, Xiaoping Duan, Hui Guan, Ling Yu, Daniel Hicklin, Eugenie Kleinerman. Suppression of Ewing's Sarcoma Tumor Growth, Tumor Vessel Formation, and Vasculogenesis Following Anti–Vascular Endothelial Growth Factor Receptor-2 Therapy Clinical Cancer Research. 2007;13:4867-4873.

89. Wang YX, Mandal D, WangS, Hughes D, Pollock R, Lev D, Kleinerman E, Hayes-Jordan A. Inhibiting Platelet-derived Growth Factor Î² Reduces Ewing's Sarcoma Growth and Metastasis in a Novel Orthotopic Human Xenograft Model. In Vivo. 2009;23:903-909.

VITA

Keri Schadler was born in Austin, Texas on March 20, 1982. She received her Bachelor of Science degree in molecular and cell biology, with honors, from Texas A&M University in College Station, Texas in 2004. Keri entered The University of Texas Health Science Center at Houston Graduate School of Biomedical Sciences in August 2005, and completed rotations in the laboratories of Michelle Barton, PhD, Douglas Boyd, PhD, and Eugenie S Kleinerman, M.D. In the summer of 2006, Keri joined the Kleinerman laboratory to carry out her dissertation research. Keri was awarded the Graduate School of Biomedical Sciences Faculty and Alumni Merit Award in 2005, and it was renewed yearly for the duration of her time in graduate school. Keri was also awarded an NIH Center for Clinical and Translational Sciences T32 Trainee Fellowship in April 2008, renewed in April 2009. Keri's research thus far on the role of DLL4 in bone marrow cell differentiation into pericytes/vSMC in Ewing's sarcoma has led to the following publication: Schadler, K.L., Zweidler-McKay, P.A., Guan, H, and Kleinerman, E.S. *Delta-Like Ligand 4 Plays a Critical Role in Pericyte/Vascular Smooth Muscle Cell Formation during Vasculogenesis and Tumor Vessel Expansion in Ewing's Sarcoma.* Clinical Cancer Research. **16**(3): p. 848-856.